1-1-1970

Pressure effects in the capillary flow of newtonian and shear-thinning polymers.

Richard Carlton Penwell
University of Massachusetts Amherst

PRESSURE EFFECTS IN THE CAPILLARY FLOW OF NEWTONIAN AND SHEAR-THINNING POLYMERS

A Dissertation Presented

By

Richard C. Penwell

Submitted to the Graduate School of the
University of Massachusetts in
partial fulfillment of the requirements for the degree of

DOCTOR OF PHILOSOPHY

August 1970

Major Subject - Polymer Science and Engineering

PRESSURE EFFECTS IN THE CAPILLARY FLOW OF NEWTONIAN AND SHEAR-THINNING POLYMERS

A Dissertation

By

Richard C. Penwell

Approved as to style and content by:

Roger S. Porter
(Chairman of Committee)

Roger S. Porter
(Head of Department)

W. Dan Drake
(Member)

Arthur E. Reinhart
(Member)

August 1970

Dedicated to Patricia and Melissa

ACKNOWLEDGMENT

I would like to express my appreciation to those who helped make this research and thesis possible.

Sincere gratitude is extended to my thesis advisor, Professor R.S. Porter. His continued enthusiasm and encouragement throughout the research were constant sources of inspiration.

I have greatly appreciated discussions concerning this work with other students and professors. Particularly, I enjoyed discussions with Professor R. Lawrence and working with Professor S. Middleman.

Thanks is extended to the secretarial staff for their effort in preparing the manuscripts.

Research support is gratefully acknowledged during my Ph.D. candidacy from the University of Massachusetts, Owens Illinois Glass Company and the Paint Research Institute.

PREFACE

This thesis consists of four manuscripts which are interrelated and are generally concerned with the effect of pressure in capillary flow. The manuscripts are presented as submitted for publication. Additional comments and figures, not in the original manuscripts, are given in the appendices.

Chapter I and Appendix A introduce the problem of a viscosity increase with increasing shear rate. The phenomenon is related to possible shifts in the glass transition, T_g. The WLF and Tammann-Hesse equations are used to correlate viscosity changes with shifts in T_g. The initial parameters considered which possibly affect T_g are frequency, shear rate and pressure.

Chapter II and Appendix B consider a more critical view of the WLF model used in Chapter I. Further justification for its use in describing the pressure dependence of viscosity is discussed. It is applied as a potential means of accounting for the nonlinearities encountered in Bagley plots of low melt temperature capillary data of polystyrene.

In Chapter III and Appendix C general expressions describing the effect of pressure on the isothermal, Newtonian and shear-thinning flow of fluids are derived. The pressure-viscosity model used is derived from the WLF equation and a general method for determining the pressure coefficient is presented. The derived expressions are applied to low and high molecular weight polystyrene data.

Chapter IV and Appendix D apply information obtained from Chapters I-III to another amorphous system, poly(methyl methacrylate). A pressure correction is applied to viscosity-shear rate data, based on the results from Chapter III. An expression is derived which predicts the observed increase in activation energy with increasing stress.

Chapter V contains suggestions for future consideration, originating from the work done in this thesis and from many helpful discussions. In particular cases, a representative literature search is presented to possibly initiate further work.

TABLE OF CONTENTS

C H A P T E R I

VISCOSITY OF POLYSTYRENE NEAR THE GLASS TRANSITION

Richard C. Penwell and Roger S. Porter
Polymer Science and Engineering Program
University of Massachusetts
Amherst, Massachusetts 01002

SYNOPSIS

A quantitative explanation is given for the apparent viscosity increase with increasing capillary shear rate for polystyrene at temperatures approaching the glass transition, T_g. Possible shifts in T_g as a function of the parameters shear rate, frequency and pressure are interrelated to possible viscosity changes. Experimentally, the Instron Capillary Rheometer and the Weissenberg Rheogoniometer provided a means for uncoupling the variables for individual consideration. Calculated and experimental data for the apparent viscosity as a function of the given parameters are presented and discussed. The explanation of the apparent viscosity increase in capillary flow can be quantitatively explained through the pressure dependence of T_g. Brief mention is made of the pressure effects on the Bagley and Rabinowitsch corrections normally made in capillary measurements.

INTRODUCTION

Anomalous viscosity increases with increasing shear have been reported for both amorphous and crystalline polymer systems[1,2]. This

behavior has been reasonably explained for crystalline polymers. No quantitative interpretation has been given, however, for the viscosity increase of amorphous polymers other than an exponential dependence of viscosity on pressure[3,4]. This study considers possible explanations for this anamalous behavior by measurements made on high and low molecular weight polystyrenes of narrow distribution.

The viscosity increase, as presented by Ballman[1] for a high molecular weight polystyrene, was most noticeable at temperatures approaching T_g, down to 136°C, and disappeared at high temperatures, around 200°C. The glass transition appeared, therefore, to be a region of prime importance. Its potential shift with the interdependent variables pressure, frequency, and shear rate was considered as a possible cause for the viscosity increase. This explanation can involve representing a change in T_g as a change in viscosity.

The parameters pressure, shear rate, and frequency were separated by the use of different viscometers, and temperatures of measurement for both the low and high molecular weight polystyrenes approached their respective glass transition regions. Experimental and calculated data of viscosity as a function of frequency, shear rate and pressure are discussed.

Shifts of T_g with pressure were converted to a viscosity change using available P-V-T data and the well known WLF and Tammann-Hesse equations. The calculated change in viscosity was combined with the zero shear viscosity values for the polystyrenes with a molecular weight below M_c, the critical entanglement molecular weight. For polystyrene tested with a molecular weight above M_c, a suitable power law expression for shear thinning was combined with the pressure effect. This provided a direct comparison between calculated and experimental data.

EXPERIMENTAL

Samples

Narrow distribution samples of low (19.6K, 20.4K) and high (670K) molecular weight polystyrene were obtained from Pressure Chemicals. The low molecular weight polystyrenes had a $M_w/M_n \leq 1.06$ and the 670K sample had a $M_w/M_n \leq 1.10$. Sufficient material was available to limit the use of each aliquot to one pass, thus minimizing the effects of degradation which could occur in successive passes of the same sample.

Cone-Plate Viscometer

The Weissenberg Rheogoniometer (Model No. 17) provided the means to separate the variables shear rate and frequency from pressure. Dynamic measurements on the 19.6K sample were made with a cone and plate diameter of 2.54 centimeters and a four degree cone angle. A cone and plate diameter of 5.03 centimeters with a two degree cone angle was used for steady state viscosity measurements of the 20.4K and 670K samples. Steady state measurements were made in both directions of rotation and data taken only within the region where heat generation was not significant. At successively higher shear rates, a sufficient time was allotted between measurements to allow the system to thermally equilibrate. Nitrogen gas was used to thermostat and to minimize degradation which might occur at higher temperatures and shear rates. The samples were inserted in the instrument in a way which virtually eliminated air voids.

Capillary Viscometer

The effects of pressure were studied using an Instron Capillary Rheometer with a main barrel diameter of .375 inches. Several capillaries

were used. These include in units of inches, .060 diameter and .257 length (L/D ≈ 50/1) and .030 diameter and 3.00 length (L/D ≈ 100). All capillaries had an entrance angle of 90°. Data points were rechecked on successive days and the reproducibility was continually verified. Possible heating effects at higher shear rates were checked by reducing the shear rate and comparing the stress to that originally obtained without shear heating, by waiting a sufficient time between measurements and by observing any decrease in load with time. The total stress capacity of the instrument was usually reached, especially at the lower temperature, long before shear heating became appreciable.

A number of possible capillary corrections were considered. The kinetic energy correction was negligible for the conditions used here. Both the elastic energy or Bagley correction[5] and the Rabinowitsch[6] or non-parabolic flow correction were considered. The Rabinowitsch correction is not required for Newtonian flow, and, for simple power law non-Newtonian behavior, is reasonably straightforward to apply as is the Bagley correction in the absence of pressure effects. However, as will be seen, deviations from Newtonian and power law behavior occur under the influence of pressure. It thus becomes impossible to justify either of these corrections for pressure dependent viscosities. Under these conditions shear stress is observed to increase markedly with little increase in shear rate to a level which rapidly exceeds the load capacity of the capillary instrument. This effect becomes ever more noticeable as the test temperature is decreased. The Bagley correction, based on a linear extrapolation of pressure versus L/D, becomes non-linear at sufficiently high L/D ratios.

The exact L/D ratio at which it becomes non-linear is apparently a function of the temperature and shear rate. The lower the temperature and higher the shear rate, the lower the L/D at which the non-linearity appears. Additional comments on the application of capillary corrections will be mentioned in a later section.

RESULTS AND DISCUSSION

An increase in viscosity for the amorphous polymer, polystyrene, with increasing shear rate has been reported previously[1,2]. It has been independently suggested that this increase is exponentially dependent on pressure[3]. It is of interest to examine this phenomenon more closely and to ascribe, if possible, a quantitative explanation to the anomalous viscosity increase with increasing shear. From Ballman's data[1], it is apparent that the viscosity increase becomes ever more noticeable as the temperature is decreased towards the glass transition temperature, T_g. At T_g the viscosity is known to be $\geq 10^{10}$ poise, a range quite inaccessible by steady flow measurements made with instruments such as the Instron Rheometer and Weissenberg Rheogoniometer. What is interesting to note, however, is that both the previous data and these new results show a sharp increase in viscosity with increasing shear rate at 30°C and more above the nominal glass transition which is near 100°C for the high molecular weight polystyrene. By extrapolation to yet higher shear rates, it is possible to visualize viscosities corresponding to the glass transition temperature. By restricting molecular motions of an amorphous polymer to those associated with the glass transition region, one can effectively cause a marked shift in the glass transition temperature. It is this possible shift in T_g and its relationship to viscosity which is

discussed in terms of the measureable parameters shear rate, frequency, and pressure.

Assuming the relationship of T_g with a given parameter to be known, the WLF equation may be used to calculate the anticipated viscosity change. Consider the WLF equation where C_1 and C_2 have been tabulated for different polymers including polystyrene[6].

$$\log \eta/\eta_g = \frac{-C_1 (T - T_g)}{C_2 + T - T_g} \qquad (I\text{-}1)$$

Knowing η_g and holding T, the test temperature, constant, a change in η can be found by inserting the various values of T_g calculated from the response to a given parameter. This change in viscosity can then be combined with η_o for a polystyrene exhibiting Newtonian flow or with a power law expression for the non-Newtonian (high molecular weight) polystyrenes. If there is no change in T_g with a given parameter, no viscosity change will be predicted.

The first consideration will be to see how a change in shear rate (at constant pressure) or a change in frequency might affect a change in viscosi through a shift in the glass transition temperature. Lewis has collected data on the dynamic glass transition measured at several frequencies for many polymers[7]. Rearranging his semi-empirical equation gives the following equation for the frequency dependent T_g, called T_d.

$$T_d = \Delta H_a/[-(\log \nu_d/\nu_c)\ 4.57 + T_c\ \Delta H_a] \qquad (I\text{-}2)$$

where

ΔH_a = activation energy for the glass transition

ν_d = frequency of measurement

T_d = dynamic glass transition

ν_c, T_c = constants for a given polymer

ΔH_a, ν_c and T_c were evaluated for polystyrene using data given by Lewis. A considerable shift in T_d of 30°C and more was predicted for an experimentally accessible range of frequencies (See Appendix A, Figure 1). The same correlations were used for steady shear measurement comparisons with Weissenberg data by using a factor of 2π. The justification for this rests on past favorable comparisons of dynamic and steady state data in the onset region for non-Newtonian flow and the dimensional consistency of frequency and shear rate. This conversion is made with the recognition of possible fallibility due to different mechanisms occurring in dynamic and steady state deformations.

Figure 1 compares experimental data from the Weissenberg viscometer with viscosities calculated using the combined Lewis and WLF equations as described above. An increase in shear rate was converted to a shift in T_g using the Lewis equation. This shift was used in the WLF equation to calculate the increase in viscosity. The calculated viscosity increase was combined with η_o, superimposing the curves at the lowest shear rate measured. The results in Figure 1 clearly indicate that the calculated curves diverge from the experimental points, predicting an increase at high shear where in fact none occurs in the data. Similar results were obtained in comparisons of dynamic viscosity measurements on the high and low molecular weight polystyrenes and for steady state measurements of the high molecular weight polystyrene (See Appendix A, Figures 2 and 3).

The reason why an increase in viscosity with frequency is predicted where none occurs experimentally is not entirely clear in view of the large change in T_d with frequency presented by Lewis[7]. The change in T_g with frequency likely occurs but this is not reflected in a viscosity

increase. The discrepancy in the steady state measurements might also be in the inappropriate application of dynamic glass transition data to the steady state flow. It can be clearly concluded from the Weissenberg data that no viscosity increase occurs in dynamic or steady state data for high or low molecular weight polystyrenes, at least in the temperature and shear ranges studied.

Pressure effects on viscosity were independently studied in this work using an Instron Capillary Rheometer. Varying the shear rates and temperature give an indication of how the variable pressure affects the viscosity, in that increasing the shear rate is effectively the same as increasing pressure. It is possible to use an exponential pressure dependence of viscosity and with experimental data to calculate the exponential and pre-exponential constants[3,4]. However a more quantitative approach to the prediction of viscosity under pressure in a capillary has been considered here.

In the glass transition region molecular motions are limited to those involving a distribution of short chain segments[8]. Any external influence which reduces the motion of polymer subsegments to those corresponding to the glassy state will effectively shift the glass transition. Pressure is an external influence which can operate by reducing free volume and long-range coordinated molecular motions. With a shift in the glass transition to a higher temperature, the observation of higher viscosities can be expected. It appears of interest, then, to consider how pressure affects the free volume and T_g and how these features influence the apparent viscosity.

Considerable P-V-T data is available for polystyrene[9,10] from which the shift in the glass transition can be evaluated using, for example,

the Tait equation[11,12,13]

$$V_o - V = V_o C \ln [1 + P/B] \qquad (I\text{-}3)$$

where V = volume at pressure P, V_o = volume at zero pressure, and B = (bars) temperature dependent parameter (constant under isothermal conditions).

The Tait equation originally was used in studying the P-V relationships of sea water[11]. It was subsequently found to be applicable to polystyrene[12,13]. Differentiating the Tait equation with respect to pressure and temperature results in expressions for the compressibility and coefficient of expansion, respectively, which were used by Gee and Miller in their T_g versus pressure calculations[12,14]. Gee evaluated the Tait equation constants and used it to calculate the volume which he then subtracted from the measured volume. Plotting this difference (at several temperatures) as a function of pressure and extrapolating to zero difference in volume, Gee obtained a linear relationship between pressure and the glass transition as given by the following equation (See Appendix A, Figure 4).

$$T_g = T_{go} + .028P \text{ (bars)} \qquad (I\text{-}4)$$

The data of Gee is apparently for a low molecular weight polystyrene as indicated by his value of T_{go} at atmospheric pressure of 90°C. By changing the value of T_{go} to 100°C, this same relationship was used here for flow data on high molecular weight polystyrene.

Miller approached the pressure dependence of T_g somewhat differently but with essentially the same result[14]. Considering the viscosity to depend on P, V and T and assuming T_g to be an iso-viscous state, he arrived at the following relationship, where α_ℓ (thermal expansion coefficient) and

β_ℓ (compressibility coefficient) are calculated using Gee's expressions derived from the Tait equation:

$$\frac{dT_g}{dP} = \frac{\beta_\ell}{1/v_g\,(dv_g/dT - \alpha_\ell)} \qquad \text{(I-5)}$$

Miller's expression (Equation 5) can be used to calculate the desired T_g - pressure relationship if sufficient P-V-T data is available. What remains to be done is to combine this shift in T_g with a suitable expression for calculation of possible viscosity changes with pressure.

The WLF equation was used previously to calculate the viscosity increase and is also applied here. A second means of determining the exponential dependence of viscosity on pressure was also considered based on correlations made by Miller[14]. Using Williams' "free volume" expression[15] of the melt viscosity for a series of polystyrene fractions (measured by Fox and Flory[9]), Miller correlated the free volume parameters with those given in the Tammann-Hesse equation:[16]

$$\log \eta = \log A + B/(T - T_o) \qquad \text{(I-6)}$$

The parameters A, B and T_o were then evaluated by Miller using the available data for the polystyrenes. By assuming that a change in T_o is equivalent to a change in T_g as Miller did, a second means of calculating the pressure dependence of viscosity is available.

Figure 2 is a comparison, for high molecular weight polystyrene, of results obtained experimentally and viscosities calculated independently using the WLF and the Tammann-Hesse equations. The viscosity increase was combined with a power law expression to produce the calculated results. At 200°C, all points superimpose with very little deviation from power law behavior. At 180°C, appreciable power law deviation occurs and significantly

is predicted reasonably well by either the WLF or the Tammann-Hesse equations. As the test temperature is lowered, the increase in capillary pressure necessary to obtain a given shear rate increases the viscosity, apparently through a shift in the glass transition temperature. This effect becomes ever larger as the test temperature is decreased, as shown in Figure 3. It may be noted that the viscosity increase observed in the pressure capillary is also predicted quite well by either of the two methods of calculation at both 165 and 150°C. The pressure required for flow at 150°C in the shear rate range of 10 sec^{-1}, according to the data of Gee[11], is equivalent to shifting the glass transition 45° or more. Assuming the glass transition to be approximately 100°C for this polystyrene at atmospheric pressure, a glass transition in the region of 145°C is then predicted at the higher pressures. This would certainly seem to account, then, for the very rapid rise in viscosity with shear rate at 150°C.

Viscosity data, comparable to that in Figure 3, is presented for a low molecular weight polystyrene in Figure 4. Recall that for essentially Newtonian behavior the calculated viscosity change with pressure is simply added to the zero shear viscosity. At 180°C, the behavior is Newtonian as predicted by calculation and verified experimentally by both the Weissenberg and Instron Capillary instruments. As the test temperature is decreased, the pressure effect becomes more noticeable and is predicted well at all test temperatures which were performed down to 120°C. The behavior in the Weissenberg viscometer is Newtonian at all temperatures and shear rates studied indicating that in the absence of increasing pressure no viscosity increase or decrease occurs. The pressure required in the capillary

at the highest shear rates, both at 120 and 140°C, was sufficient to cause an apparent shift in the glass transition temperature towards the test temperatures in a manner which can account for the viscosity increases observed.

Problems in applying the Bagley and Rabinowitsch capillary corrections have been mentioned previously and will be only briefly reconsidered. For the high molecular weight polystyrene, both corrections are difficult to apply in the region where the viscosity increases with increasing shear rate. The Bagley plot is non-linear which makes a linear extrapolation impossible. Also, it is not clear what deviations from parabolic flow may occur at high pressures, thus making a Rabinowitsch correction untenable. A possible solution to these difficulties might evolve from a consideration of Figure 5. In Figure 4 the experimental curve was duplicated semi-quantitatively by calculating a viscosity increase and combining it with a suitable power law expression. An alternate approach would be to subtract the calculated viscosity increase from the experimental curve giving the corrected curve in Figure 5. The resultant curve, which represents a pressure corrected version of the experimental data, can be described by a power law expression over the entire range and the Rabinowitsch correction can nominally now be applied. Ballman's data and the data presented here would superimpose over the entire shear rate range if the pressure correction was made. This same pressure correction applied to the low molecular weight polystyrenes returns the experimental data to Newtonian behavior. Although this was not done, it seems reasonable to suggest that this same pressure correction applied to a non-linear Bagley plot would result in linear curves. This would eliminate the difficulty imposed by a non-linear plot and would make the correction possible for both the high

and low molecular weight polystyrenes.

The study of variable capillary pressure has provided a quantitative explanation for the increase in apparent viscosity with shear rate from considerations of changes in free volume. Calculations, using independently the Tammann-Hesse and WLF equations coupled with Gee's pressure versus T_g relationship, agree well with experimental data on both high and low molecular weight polystyrenes. Comparisons with the Weissenberg data also supported the idea that pressure reduces the free volume which apparently shifts the glass transition 30° and more. This shift in T_g can account for the apparent viscosity increase with increasing shear rate. In the absence of pressure effects the low molecular weight polystyrene is Newtonian throughout the measurable shear rate range and the high molecular weight polystyrene obeys the power law at the higher rates of shear.

REFERENCES

I-1. R.L. Ballman, Nature 202, 288 (1964).

I-2. A.K. Van der Vegt and P.P.A. Smit, S.C.I. Monograph No. 26,313.

I-3. P. Meares, Polymers: Structure and Bulk Properties, pg. 315, D. Van Nostrand, New York, 1965.

I-4. J.D. Ferry, Viscoelastic Properties of Polymers, pg. 231, Wiley, New York, 1961.

I-5. E.B. Bagley, J. Appl. Phys. 28, 624 (1957).

I-6. S. Middleman, The Flow of High Polymers, pg. 15, Interscience, New York, 1968.

I-7. A.F. Lewis, J. Polymer Sci. B-1, 649 (1963).

I-8. G. Adam and J.H. Gibbs, J. Chem. Phys. 43, 139 (1965).

I-9. T.G. Fox and P.J. Flory, J. Appl. Phys. 21, 581 (1950).

I-10. K.H. Hellwege, W. Knappe and P. Lehmann, Kolloid-Z. 183, 110 (1962).

I-11. P.G. Tait, Physics and Chemistry of the Voyage of H.M.S. Challenger, University Press, Cambridge, Volume II, Part IV, 1900.

I-12. G. Gee, Polymer 7, 177 (1966).

I-13. L.A. Wood, J. Polymer Sci. B-2, 703 (1964).

I-14. A.A. Miller, J. Polymer Sci. A-2, 6, 1161 (1968).

I-15. M.L. Williams, J. Appl. Phys. 29, 1395 (1958).

I-16. G. Tammann and W. Hesse, Z. anorg. allgem. chem. 156, 245 (1926).

CAPTIONS FOR FIGURES

I-1. Comparison of experimental data from Weissenberg Rheogoniometer and calculated apparent viscosities for narrow distribution low molecular weight polystyrene.

I-2. Capillary flow data compared with calculated apparent viscosities for narrow distribution high molecular weight polystyrene at 180 and 200°C.

I-3. Capillary flow data compared with calculated apparent viscosities for narrow distribution high molecular weight polystyrene at 150 and 165°C.

I-4. Comparison of Weissenberg Rheogoniometer and capillary flow data with calculated results for narrow distribution low molecular weight polystyrene.

I-5. Pressure correction of the apparent viscosity of the narrow distribution high molecular weight polystyrene.

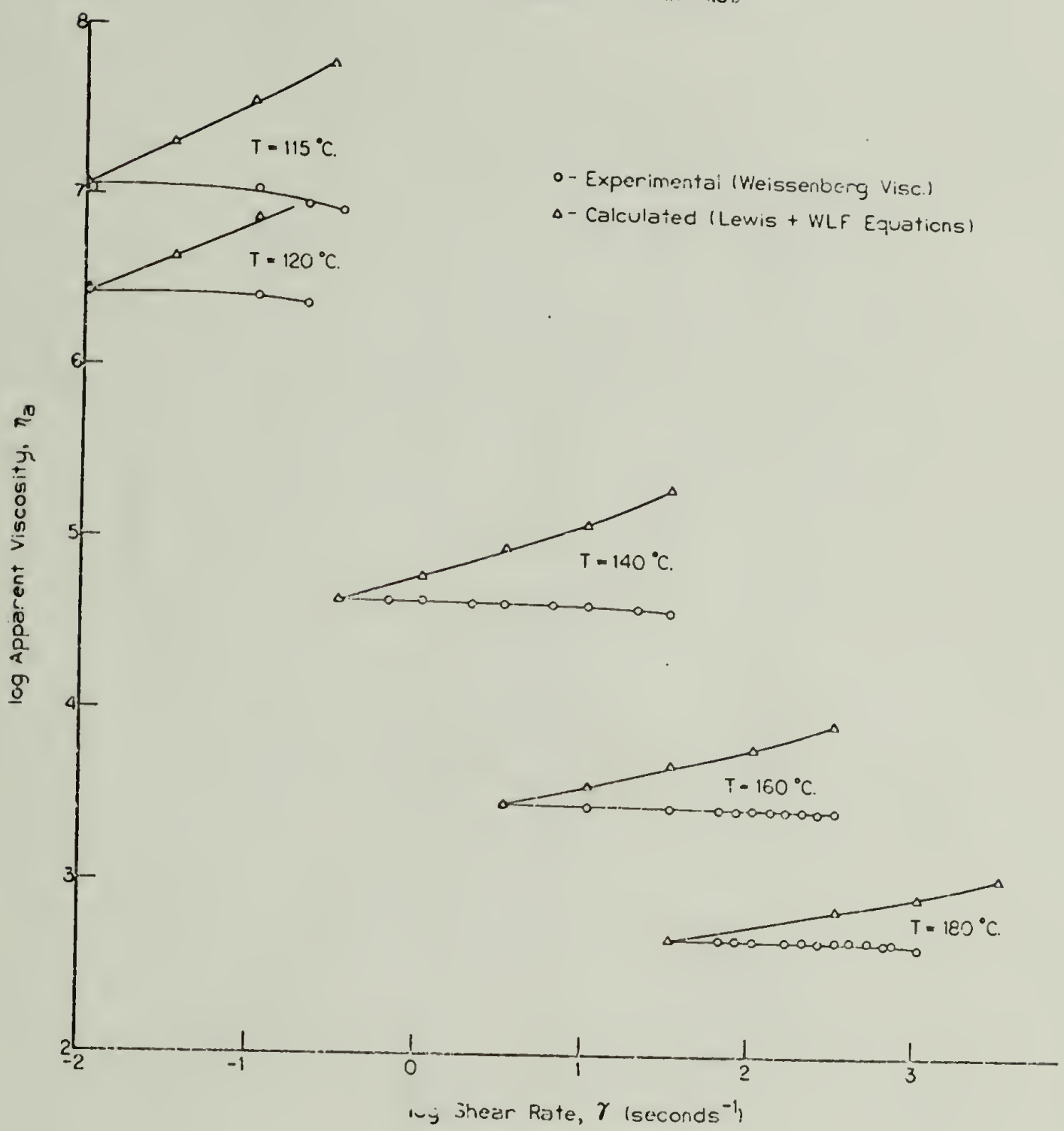
Narrow Distribution Polystyrene
Mw = 20,400 Mw/Mn = 1.06
o - Experimental (Weissenberg Visc.)
Δ - Calculated (Lewis + WLF Equations)
T = 115 °C.
T = 120 °C.
T = 140 °C.
T = 160 °C.
T = 180 °C.
log Apparent Viscosity, η_a
log Shear Rate, γ (seconds^{-1})
8
7
6
5
4
3
2
-2
-1
0
1
2
3

FIGURE I-1

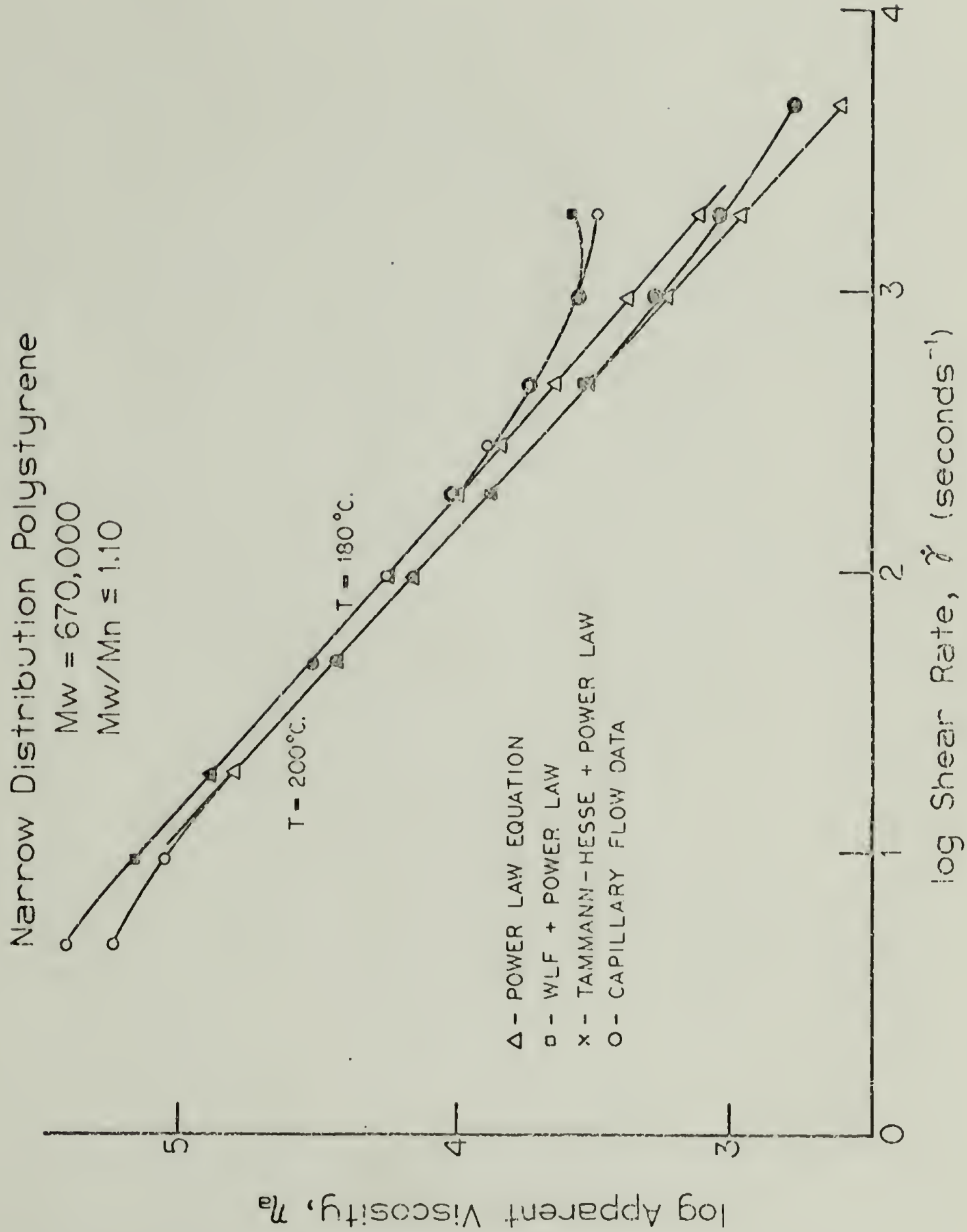
Narrow Distribution Polystyrene
Mw = 670,000
Mw/Mn = 1.10
T = 200°C.
T = 180°C.
Δ - POWER LAW EQUATION
□ - WLF + POWER LAW
x - TAMMANN-HESSE + POWER LAW
O - CAPILLARY FLOW DATA
log Apparent Viscosity, η_a
log Shear Rate, $\dot{\gamma}$ (seconds^{-1})
5
4
3
0
1
2
3
4

FIGURE I-2

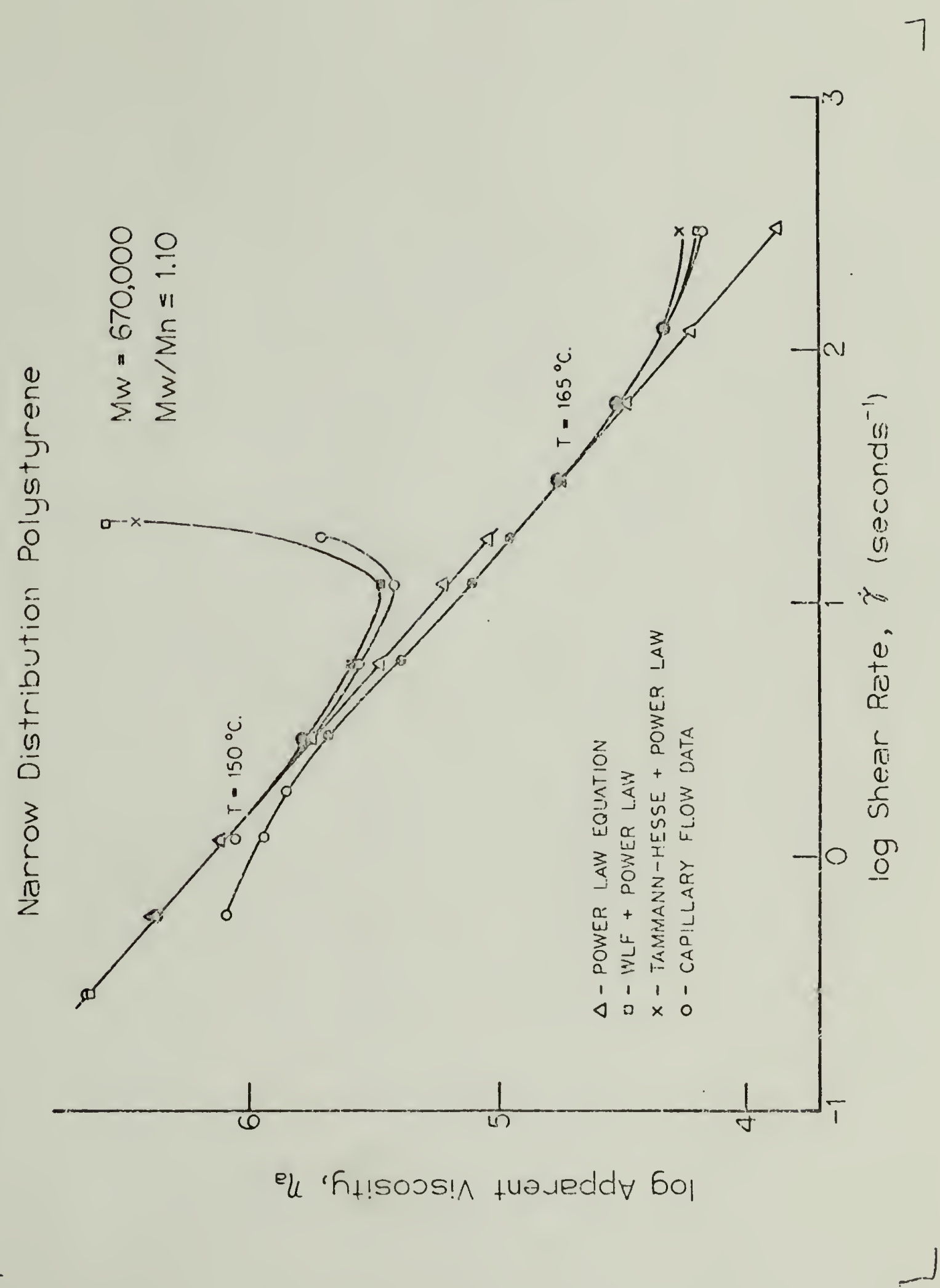
Narrow Distribution Polystyrene
Mw = 670,000
Mw/Mn = 1.10
T = 165 °C.
T = 150 °C.
Δ - POWER LAW EQUATION
□ - WLF + POWER LAW
x - TAMMANN-HESSE + POWER LAW
o - CAPILLARY FLOW DATA
log Apparent Viscosity, η_a
log Shear Rate, $\dot{\gamma}$ (seconds^{-1})
6
5
4
-1
0
1
2
3

FIGURE I-3

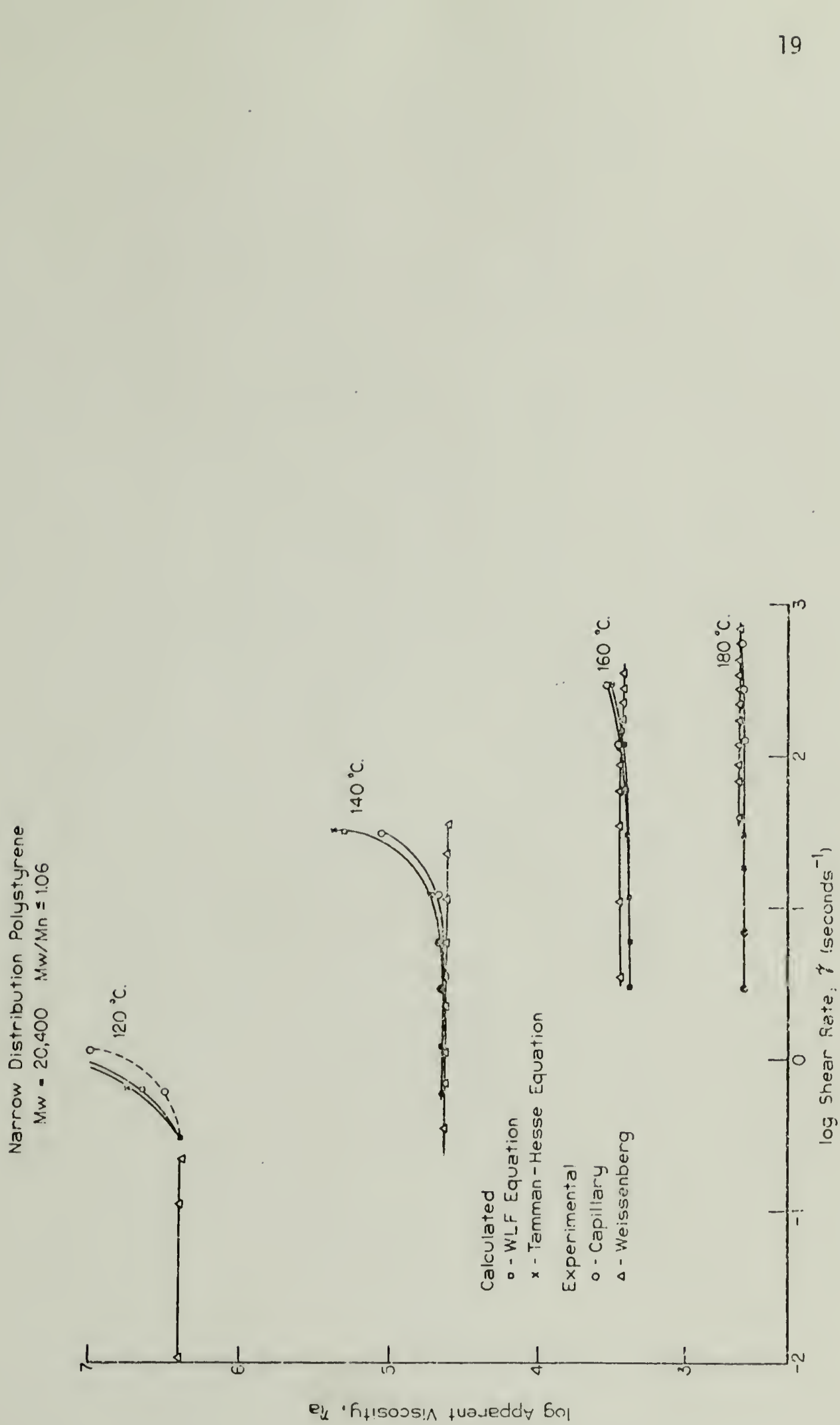
Narrow Distribution Polystyrene
Mw = 20,400 Mw/Mn = 1.06
120 °C.
140 °C.
160 °C.
180 °C.
Calculated
o - WLF Equation
x - Tamman-Hesse Equation
Experimental
o - Capillary
Δ - Weissenberg
log Apparent Viscosity, ηa
log Shear Rate, γ (seconds⁻¹)
7
6
5
4
3
-2
-1
0
1
2
3

FIGURE I-4

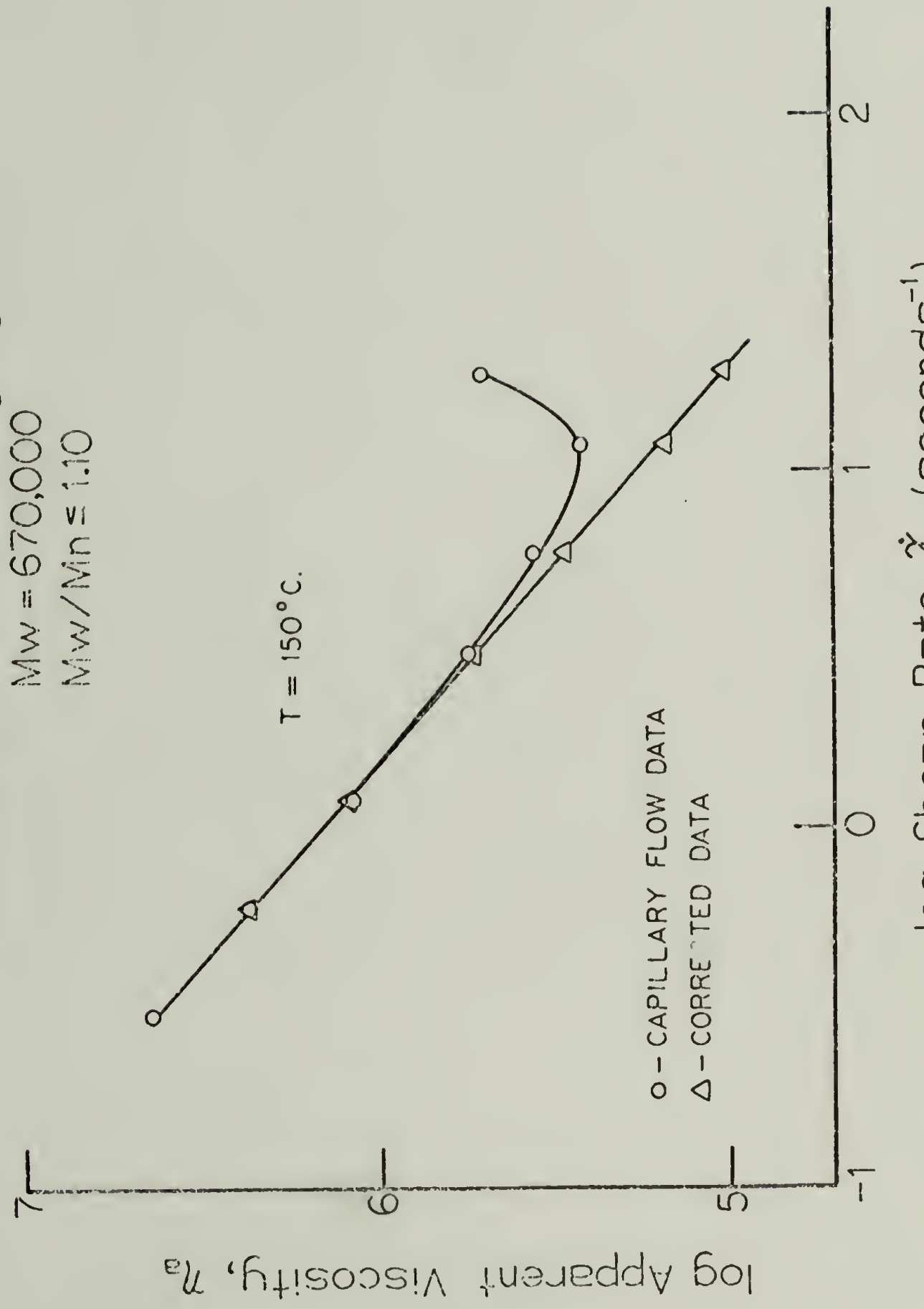
Narrow Distribution Polystyrene
Mw = 670,000
Mw/Mn = 1.10
T = 150°c.
o – CAPILLARY FLOW DATA
Δ – CORRECTED DATA
log Apparent Viscosity, η_a
log Shear Rate, $\dot{\gamma}$ (seconds^{-1})
7
6
5
-1
0
1
2

FIGURE I-5

C H A P T E R I I

THE EFFECT OF PRESSURE IN CAPILLARY FLOW OF POLYSTYRENE

Richard C. Penwell and Roger S. Porter
Polymer Science and Engineering
University of Massachusetts
Amherst, Massachusetts 01002

SYNOPSIS

Several corrections possibly required for capillary flow are based on the existence of a linear relationship between the pressure drop along the capillaries and their length to diameter ratios at a given temperature and shear rate. Recently, the appearance of non-linearities in this relationship has created some concern as to the cause of this behavior. The occurrence and an explanation of the non-linearities for polystyrene form the basis of this study. A narrow distribution, low molecular weight (20.4K) polystyrene is tested in eight capillaries at temperatures of 140 and 160°C to initiate the discussion of the non-linearity in a ΔP (pressure) versus L/D (length/diameter of capillary) plot. The sample exhibits negligible extrudate swelling at all pressures which reinforces the idea that pressure is influencing the flow. The pressure dependence of viscosity is determined using the equivalent expression of the WLF equation derived from free volume theory. Justification for its use is presented. A pressure correction, representing the increased shear stress necessary for flow of the higher viscosity material, is found to linearize the ΔP versus L/D data.

A narrow distribution, high molecular weight polystyrene (670K) is subjected to a similar analysis at 165°C using nine capillaries. The

situation is quite different as the high molecular weight sample is not nearly as ideal as the low molecular weight sample.

INTRODUCTION

In a previous work[1] (Chapter I) a possible pressure effect on polymer viscosity in capillary flow was considered. Narrow distribution samples of low (20.4K) and high (670K) molecular weight polystyrene were studied. Pressure was thought to decrease the free volume available for flow and thereby increase the glass transition temperature, T_g. Variations in the viscosity resulting from a shift in the glass transition were calculated using the WLF equation. A more critical view of the use of the WLF equation for this purpose, based on its derivation from Doolittle's free volume expression, is discussed in the present work.

Non-linearities occurring in pressure versus L/D (length to diameter ratio of a capillary) plots, frequently called Bagley plots,[17] for polystyrenes have consistently been reported in the literature.[1-4] The non-linear data was disregarded in one case[2] while another suggested, without analysis, the possibility of hydrostatic pressure affecting the results.[4] Although McLuckie and Rogers have chosen to analyze their non-linear pressure - L/D plots as due to elastic energy effects,[3] there is much evidence to suggest that the non-linearities could very well be due to the pressure dependence of the apparent viscosity.[1,3-15]

The present work is concerned with an attempt to clarify the cause for the non-linearities appearing in Bagley plots for polystyrene which have appeared and been mentioned many times recently. A low molecular weight (20.4K) polystyrene of narrow distribution was selected for initial

study as it represents a model system in many respects. The apparent viscosity exhibits Newtonian behavior in the absence of pressure effects,[1] it gives no indication of elastic energy storage and it is comparitively stable to shear and thermal degradation for the conditions used. The influence of pressure is evaluated for any non-linearities appearing in Bagley plots utilizing the WLF equation.

Conclusions drawn from the study of the low molecular weight polystyrene are applied to the analysis of the non-linearities appearing in Bagley plots for a high (670K) molecular weight polystyrene of narrow distribution. This represents a more complicated system as it is highly susceptible to thermal and shear degradation.[16] It is also a power law fluid and exhibits appreciable elastic energy effects. The total entrance correction is of such magnitude that it must be accounted for before a pressure correction can be applied. Pressure corrected capillary data is presented and compared with data from a cone and plate viscometer.

EXPERIMENTAL

The low and high molecular weight polystyrene standards used in the tests were obtained from Pressure Chemical Company, Pittsburgh, Pennsylvania. The 20.4K sample has a $M_w/M_n \leq 1.06$ and the 670K sample has a $M_w/M_n \leq 1.10$. Sufficient material of each molecular weight was available so its reuse was unnecessary, thus minimizing any thermal or shear oxidation effects.

All flow measurements were made through tungsten carbide capillaries in an Instron capillary rheometer, Instron Corporation. Several capillaries, necessary to obtain data for the Bagley plots, were used and are listed in

Table I. The various capillaries gave a span of length to diameter ratios from approximately 4 to 100. The temperature uncertainty along their lengths was estimated to be within 1°C.

It is desirable to eliminate voids in samples packed in the capillary reservoir. This was accomplished by careful packing of the polymer powder and flakes. The test temperatures were 140°C and 160°C for the low molecular weight polystyrene and 165°C for the high molecular weight polystyrene. Inside the rheometer, thermal degradation at these temperatures was negligible.[16] This was important as the time required for stress equilibrium was large compared to the time required for thermal equilibrium. The limitation in most of the tests was the maximum recommended load that the instrument would sustain, 1900 kg/cm^2. Data points were rechecked at various times within the same run and on different runs, resulting in a reproducibility of approximately 5%.

Several corrections possibly required for capillary flow measurements were considered. Pressure losses in the barrel region were measured, using the barrel as a capillary, for all crosshead speeds and were found to be negligible except for the lowest L/D capillary. This matter is discussed in a later section. The kinetic energy correction was assumed to be negligible for the conditions of these tests. In the absence of pressure effects, the end correction obtained from a linear extrapolation of a Bagley plot[17] and the Rabinowitsch correction[18] are easily obtained. However, as found earlier, [1] deviations from Newtonian and power law behavior caused by pressure effects make both corrections fatuous. The possibility of making the Bagley corrections under conditions of pressure effects forms the basis for this work.

A Weissenberg Rheogoniometer (Model No. 17) was used to measure the apparent viscosity of the 670K polystyrene sample for comparison with the corrected capillary data. To insure the removal of all air voids, the powder was placed on the plate of the rheometer and was maintained at 185°C in a nitrogen atmosphere for several hours. Upon establishing thermal equilibrium at 165°C, measurements were made using a 5.0 centimeter plate and a 2° angle cone. The viscosity values calculated, by comparison with the literature,[19] were for a polystyrene with a molecular weight of 67K. The sample had thermally degraded reducing the molecular weight by a decade, which agrees with the work of Arisawa and Porter.[16] The thermal degradation problem was circumvented by pre-forming the test sample in a press at 165°C until all voids were eliminated. The time required for thermal equilibrium at 165°C has little effect on the degradation of the sample while in the rheometer.[16]

DISCUSSION

Free Volume Model

The pressure dependence of the apparent viscosity and related properties for amorphous polymers has received considerable attention recently.[1,3,5-15,14-23] A discussion appropriate to the present work can be initiated by considering Doolittle's viscosity-free volume relationship.[24] Doolittle found a linear relationship existed when ln η was plotted as a function of v_o/v_f. He originally defined η as the coefficient of viscosity and v_f/v_o as the relative free volume. He suggested that changes in the relative free volume could result from changes in pressure and temperature. This appeared to be a very convenient means of relating viscosity to free volume rather than temperature.

Williams,[25] using an equivalent form of Doolittle's equation given below,

$$\log \eta = \log A + B/2.303\left[\frac{v_g - v_o}{v_o} + \frac{1}{v_o}\frac{dv}{dT}(T - T_g)\right] \qquad (II\text{-}1)$$

$$= \log A + B/2.303\ f$$

where f = relative free volume

A and B may be considered constants

v_g = the volume at the glass transition temperature, T_g

calculated the free volume parameters from the data of Fox and Flory on polystyrene fractions.[26] Since $\log a_T \cong \log \eta_T - \log \eta_{T_g}$, as mentioned by Williams,[25] the following equilvalent form of the WLF equation results:

$$\log a_T = -\frac{(B/2.303\ f_g)(T - T_g)}{f_g/\alpha + T - T_g} \qquad (II\text{-}2)$$

where the glass transition temperature T_g is a reference temperature, α is the thermal expansion coefficient and f_g is the relative free volume at T_g.

Ferry and Stratton subsequently attempted to include the pressure dependence of viscosity by using the following modified form for the relative free volume[21]:

$$f = f_g + \alpha(T - T_g) - \beta P \qquad (II\text{-}3)$$

where, in their development, α and β are considered as constants.

Haward has considered the compressibility of polymers as being the sum of a free volume compressibility and a molecular compressibility,[5] noting that molecular compressibility occurs only at high pressures

(> 3000 bars). He uses his modified van der Waals equation to calculate compressibility coefficients.

Martynyuk and Semenchenko studied the temperature dependence of compressibility of amorphous polymers, defining three regions;[6] a region of low compressibility ($T < T_g$), a region in which β changes rapidly with T($T \cong T_g$) and a region of high compressibility ($T > T_g$) in which the compressibility is a linear function of T. They used x-ray techniques to verify that the polymers were amorphous at various pressures.

Matheson has used his modified free volume approach to show that the pressure dependence of viscosity for liquids can be calculated from free volume theory.[10] He suggests that the viscous flow must be determined by the probability of sufficient free volume being available to the flow molecule rather than the probability of a molecular jump which predominates at higher temperatures.

Ito, using a Westover type extrusion rheometer, reported the effect of hydrostatic pressure on viscosity for several polymers.[9] At 190°C, the viscosity of polystyrene showed an increase by approximately a factor of 10 when subjected to a hydrostatic pressure of 500 kg/cm^2.

Holliday ran tension tests on polystyrene under hydrostatic pressure and noted a change from brittle to ductile failure as the pressure was increased.[15] He concluded that the increase in the maximum load with pressure was caused by hydrostatic pressure increasing the glass transition temperature. Mears, Pae and Sauer also noted an increase in the modulus and ductility with pressure.[14] They also concluded that high pressure can decrease the free volume and shift the glass transition temperature.

Matsuoka and Maxwell have made extensive measurements of the compressibility of polystyrene.[13] They observed that the shift in the glass transition, or identically the transition from a rubber to glass, depends on the rate of pressure application. They found no indication of crystallization occurring.

Previously, the suggestion was made that the apparent viscosity of narrow distribution polystyrenes, measured in a capillary viscometer, was strongly pressure dependent.[1] Considering the conditions of the tests in the earlier study, the free volume approach to explain the pressure dependence of viscosity seemed to be generally valid. The WLF equation was used as given in equation 2 where the relative free volume is:

$$f = f_g + \alpha(T - T_g) \qquad \text{(II-4)}$$

with α (thermal expansion coefficient), T_g (glass transition temperature) and β (compressibility coefficient) being pressure dependent. The pressure functions for the above parameters for polystyrene have been given by Gee and appear to be based on sound analysis.[20] He has used the Tait equation to describe the compression of polystyrene in the form:

$$V_o - V = V_o\, C\, \ell n[1 + P/B] \qquad \text{(II-5)}$$

where V = volume at pressure P, V_o = volume at zero pressure, C = constant and B = (bars) temperature dependent parameter (constant under isothermal conditions).

Differentiation of the Tait equation with respect to temperature and pressure gives the following expressions for the coefficient of expansion and the compressibility coefficient:[20]

$$\alpha_\ell = \alpha_{o\ell} + P\, \beta_\ell (d\, \ell n\, B_L/dT) \qquad \text{(II-6)}$$

$$\beta = V_o C/V(P + B) \qquad \text{(II-7)}$$

where $\alpha_{o\ell} = 5.34 \times 10^{-4}$ deg^{-1} (subscript ℓ refers to values above T_g) and the other parameters are as defined previously. The pressure dependence of the glass transition is presented graphically by Gee[20] and in equation form by Miller.[27] Sasabe and Saito have recently used the Tait equation to successfully calculate the pressure dependence of v_ℓ, v_g and α for polyvinyl chloride and polymethylmethacrylate.[8]

With the relationships for the pressure dependence of the free volume parameters available,[20] equations 3 and 4 may now be compared as shown in Table II. The value of f_g selected is for a polystyrene fraction with a molecular weight of 19,300.[25] The value is comparable to the widely accepted value of 0.025 and certainly in agreement with the work of Bondi[28] and Plazek.[29] Gee[20] and Miller[27] present values of approximately 0.927 for v_g at a temperature of 140°C. For the values of α and β selected (same as Gee's values[20]) calculations of the relative free volume were made at a temperature of 140°C. The pressure was increased until the volume was reduced to v_g. The value of the relative free volume, F_2, is 0.025 at $v = 0.925$ using equation 4. With α and β having constant values at $P = 0$, the relative free volume F_1, given by equation 3, decreases much toorapidly. The resulting values of F_1 and F_2 as the pressure is increased reinforce the use of equation 2 to describe the pressure dependence of viscosity.

The relative free volume is most dependent on the initial values of α and β selected. The different values for these two parameters found in the literature for polystyrene[5,6,11,12,20,27-31] cause some change in the computed relative free volume. Equation 4, nonetheless,

gave the better results in all cases. Slight variations in v_o, v_ℓ, $\partial T_g/\partial P$ and v_{go} found in the literature affects the values of the relative free volume very little. Considering all the parameters involved, the work of Gee[20] and Miller[27] appears to be the most consistent and was used in the calculations presented in Table II.

Considering the results of Table II, the derived WLF expression as represented by equation 2 appears valid for determining the pressure dependence of viscosity for polystyrene. For temperature shifts of viscosity data, C_1 ($=B/2.303f_g$) and C_2 ($=f_g/\alpha$) are constants for a given system. However, since α is pressure dependent, C_2 will vary somewhat with pressure. In the average pressure ranges encountered in the present study ($P_{ave.} < 300$ bars), C_2 changes very little and was assigned a fixed value. The variation in C_2 with the pressure ranges encountered was less than the variation in using the different values of α in the literature.

Table III lists the values of C_1 and C_2 used in the calculations involving the low and high narrow distribution molecular weight polystyrenes. The procedure for obtaining C_1 and C_2 has been described elsewhere.[32] The necessary zero shear viscosity data to obtain C_1 and C_2 for the low molecular weight sample was presented earlier.[1] Zero shear viscosity data was not available for the 670K sample. Plazek,[33] Ballman and Simon[19] have obtained sufficient zero shear viscosity data for a polystyrene of molecular weight 600K to enable a precise calculation of C_1 and C_2. These values of C_1 and C_2, evaluated in the immediate range of the test temperature, were used in the calculations involving the 670K sample. The values of the constants C_1 and C_2 derived from free volume parameters selected from the data of Williams[25] and Gee[20] are included in Table III.

CAPILLARY VISCOMETRY

Capillary extrusion studies of polymers are of continuing interest as normally the measurements are comparitively simple to make and the data straightforward to analyze. However, several possible problems arise when pressure losses at the entrance of the capillaries become appreciable. Bagley[17] first suggested a means of eliminating the entrance loss from capillary data by extrapolation of the linear relationship between pressure and length to diameter ratio of many capillaries. Middleman[18] suggests an alternate approach to the problem which involves plotting the flow rate of the polymer versus the pressure drop for same diameter but different length capillaries. The latter method has the advantage of requiring less data for determination of the end correction. Philippoff and Gaskins[34] have suggested a means of determining elastic energy losses incurred in capillary flow of viscoelastic fluids. The several methods for considering the entrance losses in tubular flow all involve the necessity of a linear relationship existing between the pressure drop and L/D ratio at given shear rates and temperatures. Complications arise when the relationship is no longer linear.

Sakiadis[22] has derived equations for determining the shear stress and two normal stress differences in the equilibrium flow of a general fluid through a cylindrical tube. He presents a measurement of the axial pressure distribution in a tube in which the pressure drop is non-linear. He also states that the residual pressure cannot be used directly to measure normal pressures. Arai, Suzuki and Akino[23] have measured the pressure distribution along the die axis for a commercial grade polystyrene.

The pressure drops at a given shear rate (12 sec.$^{-1}$) and three temperatures (170, 180, 200°C) are non-linear and all indicate a residual pressure at the exit. The residual pressure at the exit and its relationship to extrudate swelling are discussed.

Toelcke, Gogos and Biesenberger,[2] in their study of the effects of molecular weight distribution on the flow properties of polystyrene, obtained non-linear pressure versus L/D curves using three capillaries. They chose to ignore the highest L/D capillary data in their analysis which eliminated the non-linear problem. Thomas and Hagan,[4] in their discussion of the effects of molecular weight distribution on the flow properties of polystyrene, also encountered the non-linear pressure versus L/D curves. Without detailed analysis, they suggested the effect might be due to hydrostatic pressure. McLuckie and Rogers[3] discuss the non-linearity of pressure versus L/D curves as due to elastic back pressure. They state that the relaxation of the polymer creates an elastic back pressure which results in the non-linear behavior as the L/D ratio increases.

RESULTS

The situation in which pressure may be affecting the apparent viscosity has been discussed and an appropriate model which predicts the pressure dependence of viscosity analyzed. The problem is best represented by the non-linearities appearing in capillary data plotted in the form of a Bagley plot. To initiate the study of this problem, a narrow distribution polystyrene of molecular weight 20,400 was selected. The molecular weight of this sample is below the critical entanglement molecular weight for polystyrene. Shear oxidative and thermal degradation are negligible for the test conditions used.[16] In the absence of pressure

effects, the sample is Newtonian and exhibits insignificant extrudate swelling.

The average pressure attainable in these tests rarely exceeded 300 bars. According to Table II, this results in a maximum volume change of less than 2%. This is in agreement with Figures 1 and 2 which represent a comparison of the calculated and measured flow rates, Q(gm/hr.). The points represent measured flow rates and the solid lines the calculated values. In Figure 1, the calculated curve for the L/D = 39.1 capillary extends beyond the measured point as an additional point lies off scale. Within experimental error, it is impossible to detect any difference between the measured and calculated flow rates at the two temperatures indicated and for the several capillaries used. This might lead to the false conclusion that the material is incompressible. However, as seen in Table II and calculated by equation 2, a small volume change increases the viscosity by a large factor.

Figure 3 is a plot of the pressure drop versus shear rate at a temperature of 160°C for eight capillaries used. Additional data should be obtainable for all the capillaries if the material continued to exhibit Newtonian behavior. However, the next higher point for all the curves exceeded the limit of 1900 kg/cm^2 for the instrument. Similar results were obtained at a temperature of 140°C (See Appendix B, Figure 1).

One of the most obvious manifestations of elastic energy storage in capillary flow is the observation of extrudate swelling on exit from the die[4,23,34,35]. In view of the work by McLuckie and Rogers,[3] the tremendous increases in the pressure with shear rate indicated in Figure 3 should be accompanied by appreciable swelling of the extrudate. However, no

significant die swell was observed or measured at the test temperatures of 140 and 160° for any of the capillaries at any shear rate. Any prominent dependence of the entrance loss on pressure should appear as a slight separation of the pressure data for capillaries with the same L/D ratio but different dimensions. This is not observed in Figure 3 which likely indicates a negligible dependence of the entrance losses on pressure.

Figure 4 illustrates the non-linear Bagley plot for the low molecular weight polystyrene at a temperature of 160°C. The curves are linear at lower shear rates and their extrapolation produces very small end corrections. As the shear rate is increased the curves gradually become non-linear at lower L/D ratios. Importantly, the best linear extrapolation of these curves still indicates a small entrance loss. Data was not taken using the capillary with a L/D ratio of 4.26 as the uncertainties involved are such a large percentage of the total reading.

Figure 5 is a plot similar to Figure 4 but at 140°C. It may be noted that the non-linear effect is more pronounced as the temperature is decreased, first appearing at a shear rate of 2 seconds^{-1}. Tremendous increases in the pressure (or stress) have been observed in Figures 4 and 5 while concurrently the extrudate swelling was negligible and the extrapolated end corrections small. The indication is, therefore, that the increase in pressure above that required for Newtonian flow is needed to generate greater stresses to move the higher viscosity material at the same rate. The procedure for calculating the increased viscosity using the WLF equation has been described elsewhere[1] and is only briefly reconsidered. The pressure dependence of the glass transition temperature

is known[20,27] and is used to calculate the change in T_g with pressure. Any shift in T_g can be inserted into the WLF equation and the resulting change in viscosity determined. The stress necessary to accommodate any viscosity increase can then be calculated and applied as a correction to the non-linear data in Figures 4 and 5.

The average pressure used to calculate a shift in T_g was half the total pressure drop over the entire capillary. This assumes a linear pressure drop down the capillary, which is not the case. This assumption involves little error, as the deviations from a linear pressure drop cited earlier[22,23] are small. Residual pressures reported for capillary flow are negligible compared with the total pressure drop as they are of the magnitude of normal stresses generated by the shear field.[22,23] Having assumed a linear pressure drop, the viscosity was calculated as a function of pressure at several intervals along the capillary. The average viscosity calculated in this manner varied less than 1% from the viscosity calculated using the mean value of the pressure drop over the entire capillary.

Applying the pressure correction described earlier to the data in Figure 3 produces the linear curves of Figure 6. Similar results were obtained for the data at 140°C (See Appendix B, Figure 2). The magnitude of the pressure correction becomes quite apparent when comparisons of Figure 7 and Figure 4 are made. The corrected data in Figure 7 is linear at all the shear rates and L/D ratios given. At 140°C, the linear curves in Figure 8 result from applying the pressure correction to the data of Figure 5. The non-linearities in Figures 4 and 5 have been eliminated and appear, then, to be due to the excess pressure required for flow of the higher viscosity material.

Figures 3-8 and previous work[1] indicate that moderate pressures can definitely influence the capillary flow of low molecular weight polystyrene. The effect of pressure on the flow data can be incorporated into a pressure correction factor. However, the low molecular weight material was ideal in that it was a stable system, sustained small losses in the entrance region of the capillaries and gave no indication of appreciable elastic energy storage as witnessed by negligible swelling of the extrudate. It would be meaningful, to study a high molecular weight polystyrene to see if the same pressure dependence applies in a system of practical processing interest and not nearly as ideal.

The polystyrene sample of molecular weight 670K behaves quite differently than the low molecular weight sample under similar test conditions. From studies of Arisawa and Porter[16] on an identical sample, it was shown to be quite susceptible to shear and thermal degradation. Polystyrenes of similar molecular weights have also demonstrated the ability for considerable elastic energy storage.[4] The entrance losses are expected to be larger than those encountered with the low molecular weight sample. These factors tend to make the analysis of the high molecular weight polystyrene much more difficult.

Figure 9 represents the pressure required for flow of the 670K sample in 9 capillaries as a function of shear rate at 165°C. For all but the lowest L/D capillary, the pressure increases non-linearly as the shear rate is increased. The rapid increase in pressure with increasing shear rate and L/D ratio is more easily seen in Figure 10. The lowest L/D capillary data seemingly deviates considerably from the other data at lower shear rates. The force requirements for this capillary are much

less than the other 8 capillaries and the various losses associated with capillary flow become appreciable. As an example the losses in the barrel represent only a small error for the larger L/D capillaries but can approach 30% and possibly more of the total force for the lowest L/D capillary. At higher shear rates, the pressure losses become a smaller percentage of the total pressure and there is less tendency for curvature parallel to the L/D axis. The present analysis is concerned with the non-linearities appearing in Figure 10 at the higher L/D ratios and therefore the behavior as the L/D ratio approaches zero is of interest only as a total end correction.

The separation of the pressure curves in Figure 9 with L/D ratios of approximately 50 might be an indication that the losses in the barrel and entrance region of a capillary are pressure dependent. In Figure 10, however, this possible pressure dependence of the losses is not as obvious or large as first indicated in Figure 9 and will be neglected for the present.

The calculated pressure correction represents the pressure necessary to generate the shear stress to move the higher viscosity material. The magnitude of the additional shear stress depends on the increase in viscosity which is quite sensitive to pressure. Therefore, an attempt to determine the pressure correction with included entrance losses would result in over correcting the data. To avoid this, the entrance losses must be estimated for each shear rate in Figure 10 and be eliminated from the data. No attempt is made to separate the various components of the entrance loss as the entrance to a capillary is a very complex region. Appreciable extrudate swelling was observed for this polymer which indicates elastic energy storage in addition to Couette losses.

With the exception of the lowest L/D capillary, the lower L/D ratios can be used to approximate the entrance losses. A least squares analysis of as many points as approximated straight lines in Figure 10 gave an estimate of the entrance losses at each shear rate. The approximated end corrections were applied to the curves of Figure 10, shifting them as shown in Figure 11. The apparent viscosity was calculated using the data of Figure 11 and is shown in Figure 12. The separation of the curves in Figure 12 at a shear rate of 1 second^{-1} is small and increases with shear rate. The upturns suggested at the highest shear rates for each capillary are justified by recalling that the next increment in shear rate is inaccessible experimentally as indicated by Figure 9. The capillary ...ving the highest L/D ratio requires the greatest pressure at a given ...ar rate and is the first to exceed the capacity of the Instron Capillary ...ometer. As the L/D ratio decreases, the pressure effect does also as is seen in Figure 12.

The problem in applying the WLF equation to determine the pressure dependence of the high molecular weight polystyrene is that it does not include a shear-thinning contribution. However, it can be used to calculate a relative viscosity increase starting with the experimental points at the lowest shear rates recorded for each capillary. Any relative viscosity increase can then be converted to a pressure correction in a procedure similar to that used for the low molecular weight polystyrene.

Applying the pressure correction to the curves in Figure 11 gives the plots shown in Figure 13. Essentially linear plots are obtained at the lower shear rates but a large over-correction occurs at higher shear rates. As mentioned earlier, the viscosity is very sensitive to the pressures encountered in these tests. Any pressure loss not accounted for will tend

to predict too great an increase in viscosity. This will then result in pressure corrections which are too large. A pressure dependent viscosity suggests the possibility that the entrance losses may also be pressure dependent. This would mean that the Couette loss may not be the same for equal diameter capillaries. Earlier, this possibility was acknowledged but was assumed small compared to the total pressure drops in these tests. Considering the results in Figure 13, this may be a limiting assumption.

The pressure corrected viscosity is compared in Figure 14 to data obtained from the Weissenberg rheometer and to data generated from reduced coordinates. From a plot of the zero shear viscosity versus temperature^{-1} data of Ballman, Simon[19] and Plazek and O'Rourke[33] for a narrow distribution sample of molecular weight 600K, the zero shear viscosity at 165°C can be obtained. Using the reduced coordinates log η/η_0 and log $(\dot{\gamma}\eta_0 M/T)$ as presented by Ballman and Simon[19] for narrow distribution polystyrenes, the apparent viscosity curve in Figure 14 was calculated. This curve was generated for reference only and it is not necessary to discuss the value of the exponent of M in the reduced coordinates since it is not a variable.[36] The over correction of the pressure appears in Figure 14 as a greater decrease in the apparent viscosity with shear rate than would be expected.

CONCLUSIONS

Examination of the equivalent form of the WLF equation derived from Doolittle's viscosity-free volume relationship indicates that it can be used to describe the pressure dependence of viscosity of polystyrene.

In the pressure ranges encountered in these tests (P_{ave} < 300 bars), no modification of the equation is necessary.

It is virtually impossible to detect any difference in the measured and calculated flow rates encountered in this study. The conclusion that the polymer is therefore incompressible is false even though the volume change is less than 2%. The viscosity is quite sensitive to small volume changes at the test temperatures used and varied considerably in this work. However, in considering the equation of continuity, it may be possible to neglect the small change in the density and make the assumption that the system is incompressible.

The low molecular weight (20.4K) polystyrene was ideal for an initial study of the non-linearities appearing in a Bagley plot. The observation of negligible end effects and extrudate swelling, while pressures prematurely exceeded the capacity of the viscometer, supported the idea that pressure was influencing the flow. Pressure corrections, based on the pressure needed to generate the increased stress to move the higher viscosity material, linearized the Bagley plots.

To perform a similar analysis on a high molecular weight polystyrene, it is necessary to first estimate the end effect as its magnitude will significantly affect the results. In doing this, the assumption is made that the pressure dependence of the losses in the entrance region of the capillaries can be neglected. The calculated pressure corrections tended to linearize the Bagley plots and predict power law behavior of the apparent viscosity. There is a tendency to over correct the data, possibly a consequence of the limiting assumption that the entrance losses are constant at a given shear rate and temperature.

The results of both the low and high molecular weight polystyrenes indicate that pressure is definitely influencing the flow. It would be of interest to apply the same approach to other amorphous systems exhibiting similar phenomena. It would also be of interest to further examine the limits of the pressure dependence of viscosity using a free volume model. One would expect this model to fail once the probability of sufficient free volume being available to the flow molecule ceases to be the controlling factor. In view of the pressure dependence of the free volume, this limit may be deceivingly higher than might be expected.

REFERENCES

II-1. R.C. Penwell and R.S. Porter, J. Appl. Polym. Sci., 13, 2427 (1969).

II-2. G.A. Toelcke, C.G. Gogas and J.A. Biesenberger, SPE 13th Antec, 98 (1967).

II-3. C. McLuckie and M.G. Rogers, J. Appl. Polym. Sci., 13, 1049 (1969).

II-4. D.P. Thomas and R.S. Hagan, Polym. Eng. Sci., 9, 164 (1969).

II-5. R.N. Haward, J. Polym. Sci. A-2, 7, 219 (1969).

II-6. M.M. Martynyuk and U.K. Semenchenko, Kolloidyni Zhurnal, 26, 83 (1964).

II-7. I. Duvdevani, SPE 13th Antec, 80 (1967).

II-8. H. Sasabe and S. Saito, Rept. Prog. Polym. Phys. (Japan), 12, 265 (1969).

II-9. K. Ito, Rept. Prog. Polym. Phys. (Japan), 12, 131 (1969).

II-10. A.J. Matheson, J. Chem. Phys. 44, 695 (1966).

II-11. R.N. Haward, H. Bruer and G. Rehage, J. Polym. Sci. B, 4, 375 (1966).

II-12. A.A. Miller, J. Polym. Sci. A-2, 4, 415 (1966).

II-13. S. Matsuoka and B. Maxwell, J. Polym. Sci., 32, 131 (1958).

II-14. D.R. Mears, K.D. Pae and J.A. Sauer, J. Appl. Phys., 40, 4229 (1969).

II-15. L. Holliday, Nature 202, 381 (1964).

II-16. K. Arisawa and R.S. Porter, J. Appl. Polym. Sci., accepted.

II-17. E.B. Bagley, J. Appl. Physics, 28, 624 (1957).

II-18. S. Middleman, The Flow of High Polymers, pg. 15, Interscience, New York, 1968.

II-19. R.L. Ballman and R.H. Simon, J. Polym. Sci., Part A, 2, 3557 (1964).

II-20. G. Gee, Polymer 7, 177 (1966).

II-21. J.D. Ferry and R.A. Stratton, Kolloid-Z., 171, 107 (1960).

II-22. B.C. Sakiadis, A.I.Ch.E. J., 8, 317 (1962).

II-23. T. Arai, I. Suzuki and N. Akino, Proc. Fujihara Memorial Faculty of Engineering, Keio University, Tokyo, Japan, 20, 39 (1967).

II-24. A.K. Doolittle, J. Appl. Physics, 22, 1471 (1951).

II-25. M.L. Williams, J. Appl. Physics, 29, 1395 (1958).

II-26. T.G. Fox and P.J. Flory, J. Appl. Phys., 21, 581 (1950).

II-27. A.A. Miller, J. Polym. Sci. A-2, 6, 1161 (1968).

II-28. A. Bondi, J. Polym. Sci., Part A, 2, 3159 (1964).

II-29. D.J. Plazek, J. Phys. Chem., 69, 3480 (1965).

II-30. T.G. Fox and S. Loshaek, J. Polym. Sci., 15, 371 (1955).

II-31. K. Ueberreiter and G. Kanig, J. Colloid Sci., 7, 569 (1953).

II-32. J.D. Ferry, Viscoelastic Properties of Polymers, pg. 212, Wiley and Sons, Inc., 1961.

II-33. D.J. Plazek, private communication.

II-34. W. Philippoff and F.H. Gaskins, Trans. Soc. Rheology, 2, 263 (1958).

II-35. R.S. Spencer and R.E. Dillon, J. Colloid Sci., 3, 163 (1948).

II-36. R.A. Stratton, J. Coll. Inter. Sci., 22, 517 (1966).

TABLE II-I

CAPILLARY DIMENSIONS - ENTRY ANGLES OF 90°

Diameter (Inches)	Length/Diameter
0.02000	12.20
0.02000	50.32
0.03020	30.53
0.03015	66.57
0.03018	99.67
0.05035	39.01
0.06026	4.26
0.06040	33.11
0.06014	49.88

TABLE II-II

FREE VOLUME PARAMETERS FOR
POLYSTYRENE AT T = 140°C

(1) v_ℓ cc/gm	(2) $\alpha_\ell \times 10^4$ Deg^{-1}	$\beta \times 10^5$ $Bars^{-1}$	Pressure Bars	(3) F_1 Relative Free Volume	(4) F_2 Relative Free Volume
1.000	5.34	6.84	0	0.05120	0.05120
0.993	5.02	6.40	100	0.04436	0.04818
0.982	4.48	5.67	300	0.03068	0.04313
0.971	4.05	5.10	500	0.01700	0.03908
0.962	3.70	4.63	700	0.00332	0.03575
0.953	3.40	4.25	900		0.03294
0.945	3.15	3.93	1100		0.03055
0.938	2.94	3.66	1300		0.02849
0.932	2.75	3.42	1500		0.02670
0.925	2.58	3.21	1700		0.02512

(1) $v_g = 0.927$ (Data of Gee and Miller)

(2) $\alpha_{o\ell} = 5.34 \times 10^{-4}$ (Data of Gee)

(3) $F_1 = f_g + \alpha_{o\ell}(T - T_{g_o}) - \beta P$; $T_{g_o} = 90°C$, $f_g = 0.0245$ (Data of Williams)

(4) $F_2 = f_g + \alpha_\ell(T - T_g)$

TABLE II-III

WLF PARAMETERS FOR
NARROW DISTRIBUTION POLYSTYRENES

Molecular Weight	C_1	C_2	$\frac{B}{2.303\ f_g}$	f_g/α
20,400	14.4	36.2		
600,000	16.6	158.2		
			16.13	41.67

CAPTIONS FOR FIGURES

II-1. Comparison of calculated and measured flow rates for narrow distribution low molecular weight polystyrene at 140°C.

II-2. Comparison of calculated and measured flow rates for narrow distribution low molecular weight polystyrene at 160°C.

II-3. Flow data of several capillaries for narrow distribution low molecular weight polystyrene at 160°C.

II-4. Pressure required for flow at various shear rates versus the length/diameter ratio of several capillaries for narrow distribution low molecular weight polystyrene at 160°C.

II-5. Pressure required for flow at various shear rates versus the length/diameter ratio of several capillaries for narrow distribution low molecular weight polystyrene at 140°C.

II-6. Pressure corrected flow data of several capillaries for narrow distribution low molecular weight polystyrene at 160°C.

II-7. Corrected pressure versus length/diameter ratio of several capillaries for narrow distribution low molecular weight polystyrene at 160°C.

II-8. Corrected pressure versus length/diameter ratio of several capillaries for narrow distribution low molecular weight polystyrene at 140°C.

II-9. Flow data of several capillaries for narrow distribution high molecular weight polystyrene at 165°C.

II-10. Pressure required for flow at various shear rates versus the length/diameter ratio of several capillaries for narrow distribution high molecular weight polystyrene at 165°C.

II-11. Pressure versus length/diameter data shifted by an amount which approximates the end correction for narrow distribution high molecular weight polystyrene at 165°C.

NARROW DISTRIBUTION POLYSTYRENE

Mw = 20,400 Mw/Mn ≤ 1.06

T = 140°C

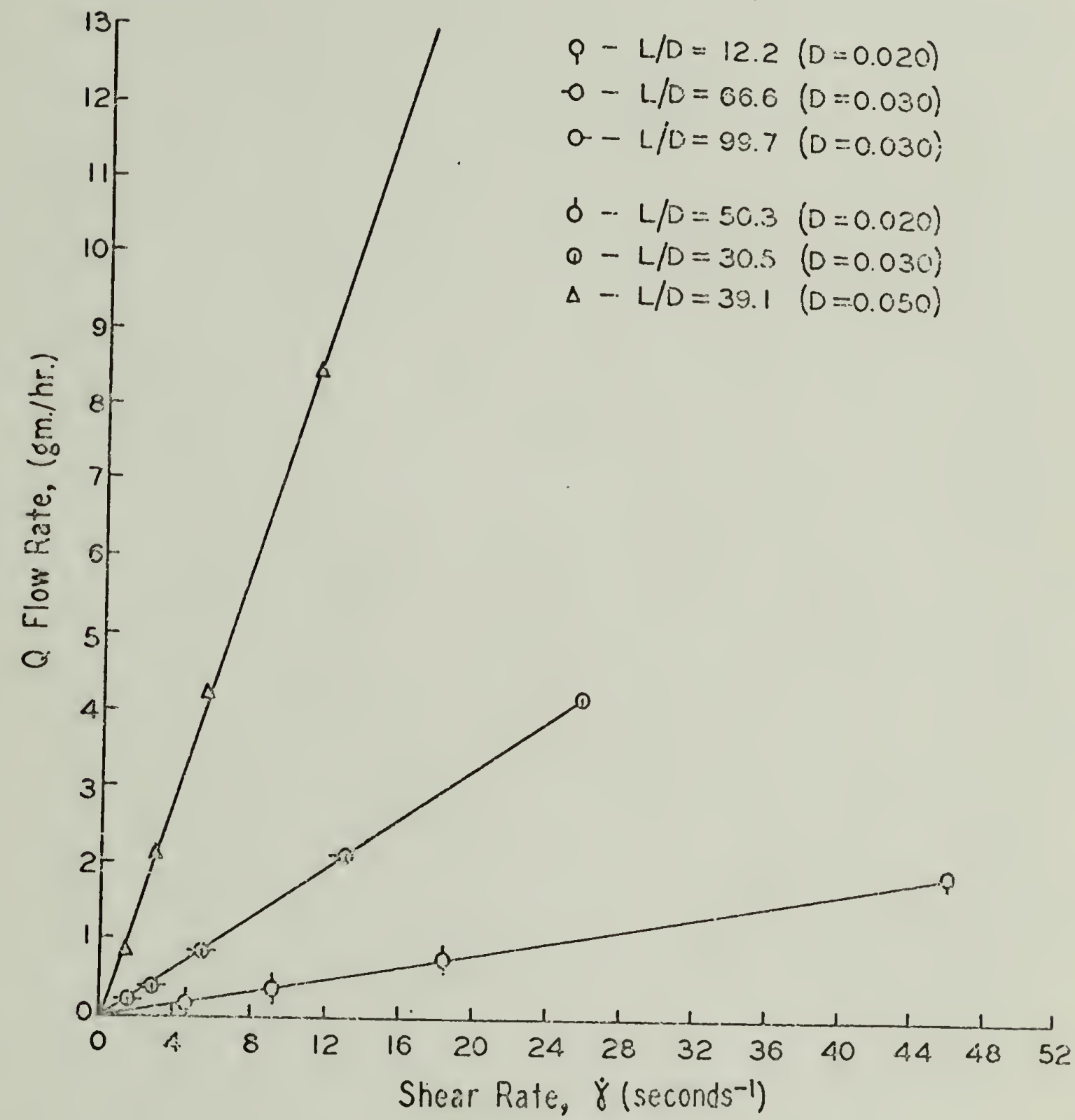

FIGURE II-1

NARROW DISTRIBUTION POLYSTYRENE

Mw = 20,400 Mw/Mn ≤ 1.06

T = 160°C

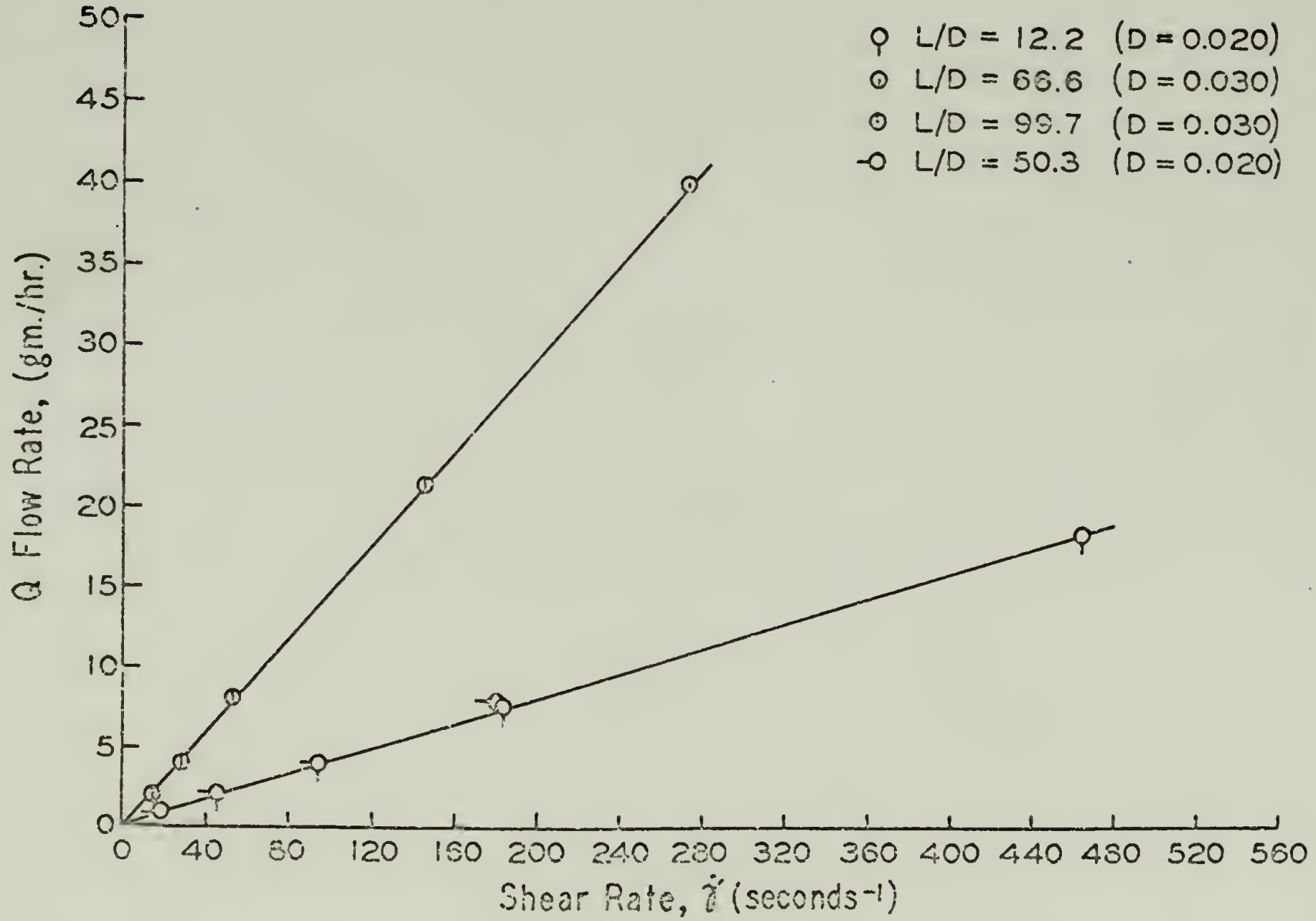

FIGURE II-2

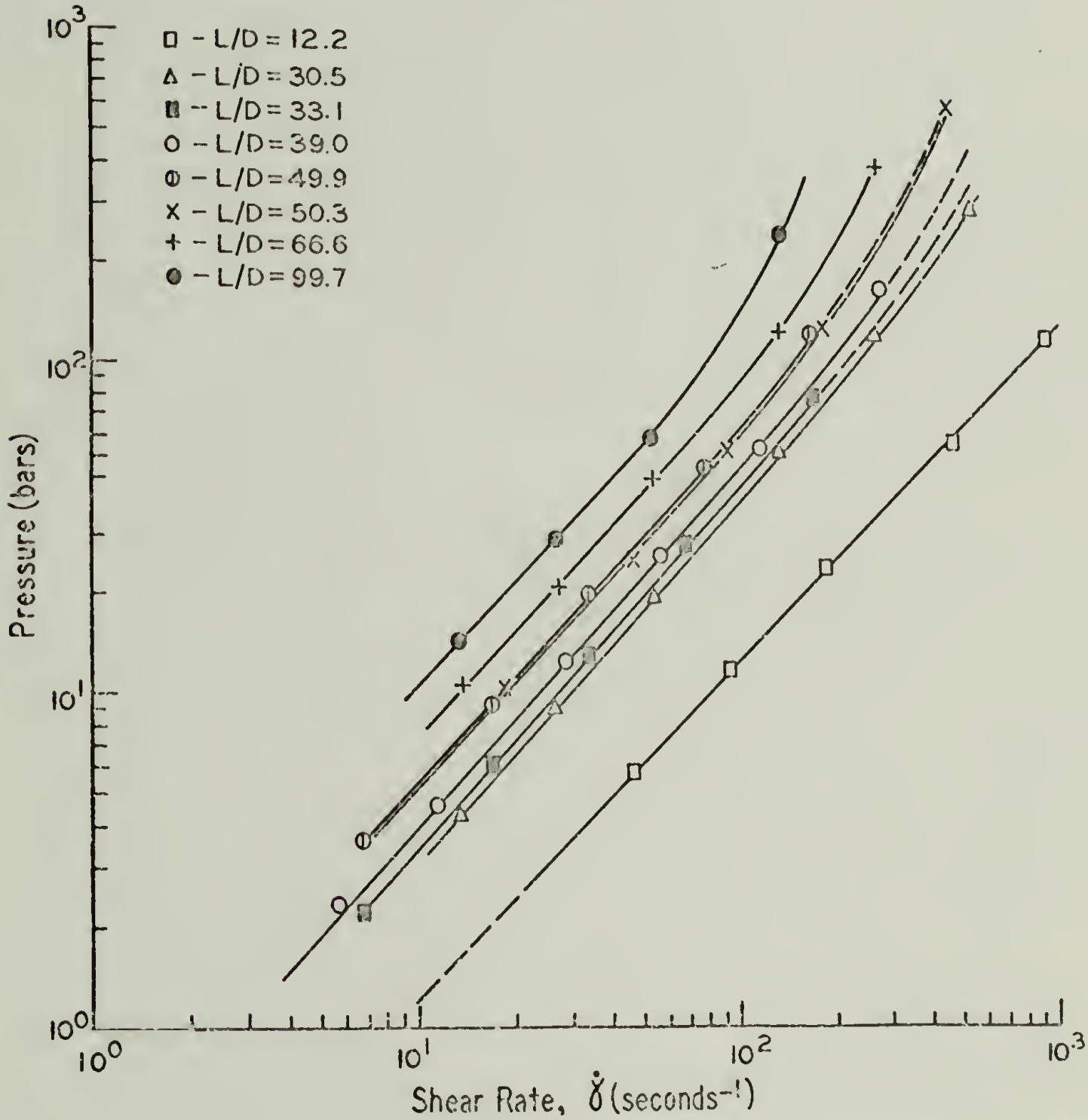
NARROW DISTRIBUTION POLYSTYRENE
Mw = 20,400 Mw/Mn ≤ 1.06
T = 160°C
□ - L/D = 12.2
Δ - L/D = 30.5
■ - L/D = 33.1
○ - L/D = 39.0
◐ - L/D = 49.9
× - L/D = 50.3
+ - L/D = 66.6
● - L/D = 99.7
Pressure (bars)
Shear Rate, γ̇ (seconds⁻¹)
10³
10²
10¹
10⁰
10⁰
10¹
10²
10³

FIGURE II-3

NARROW DISTRIBUTION POLYSTYRENE

Mw = 20,400 Mw/Mn ≤ 1.06

T = 160°C

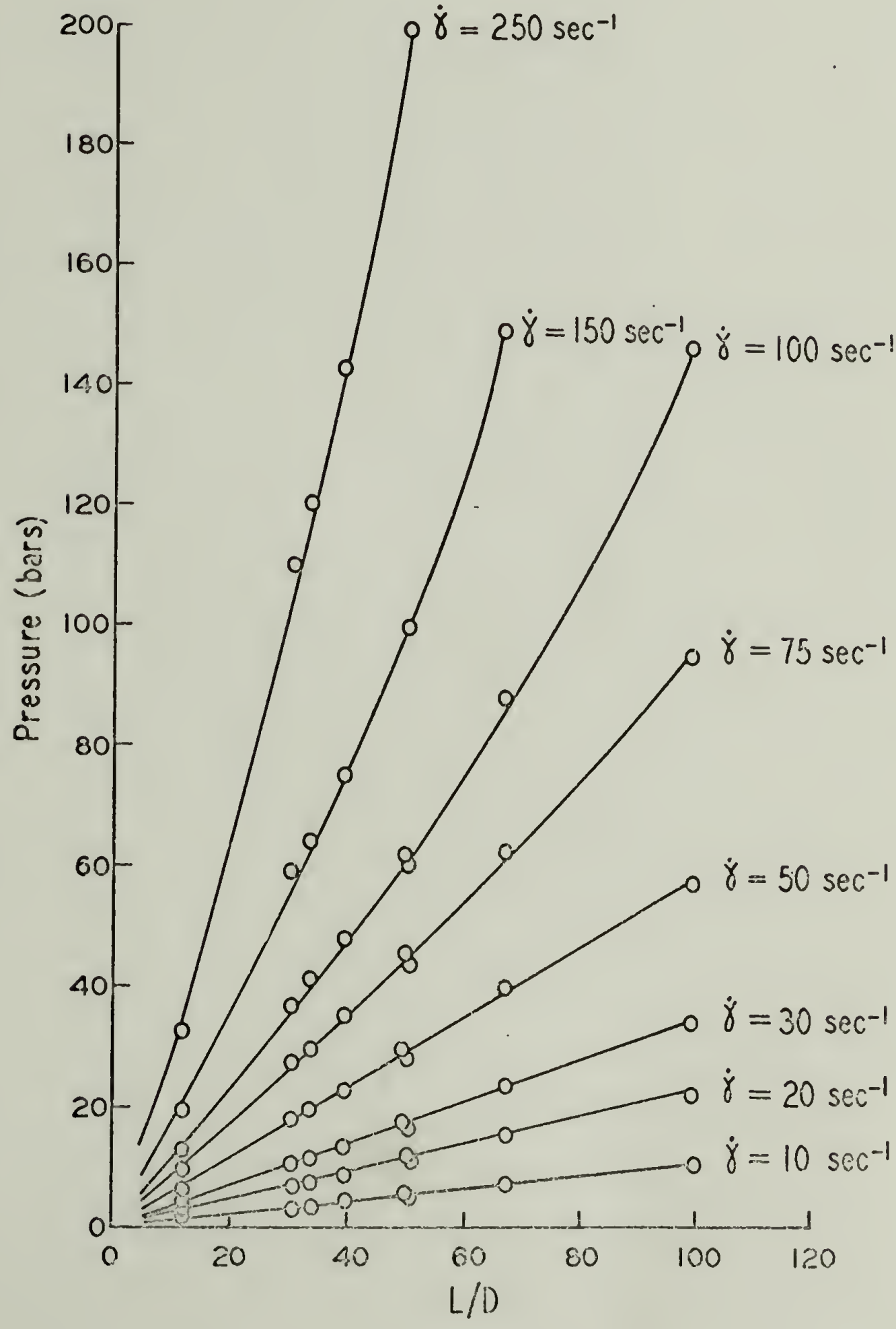

FIGURE II-4

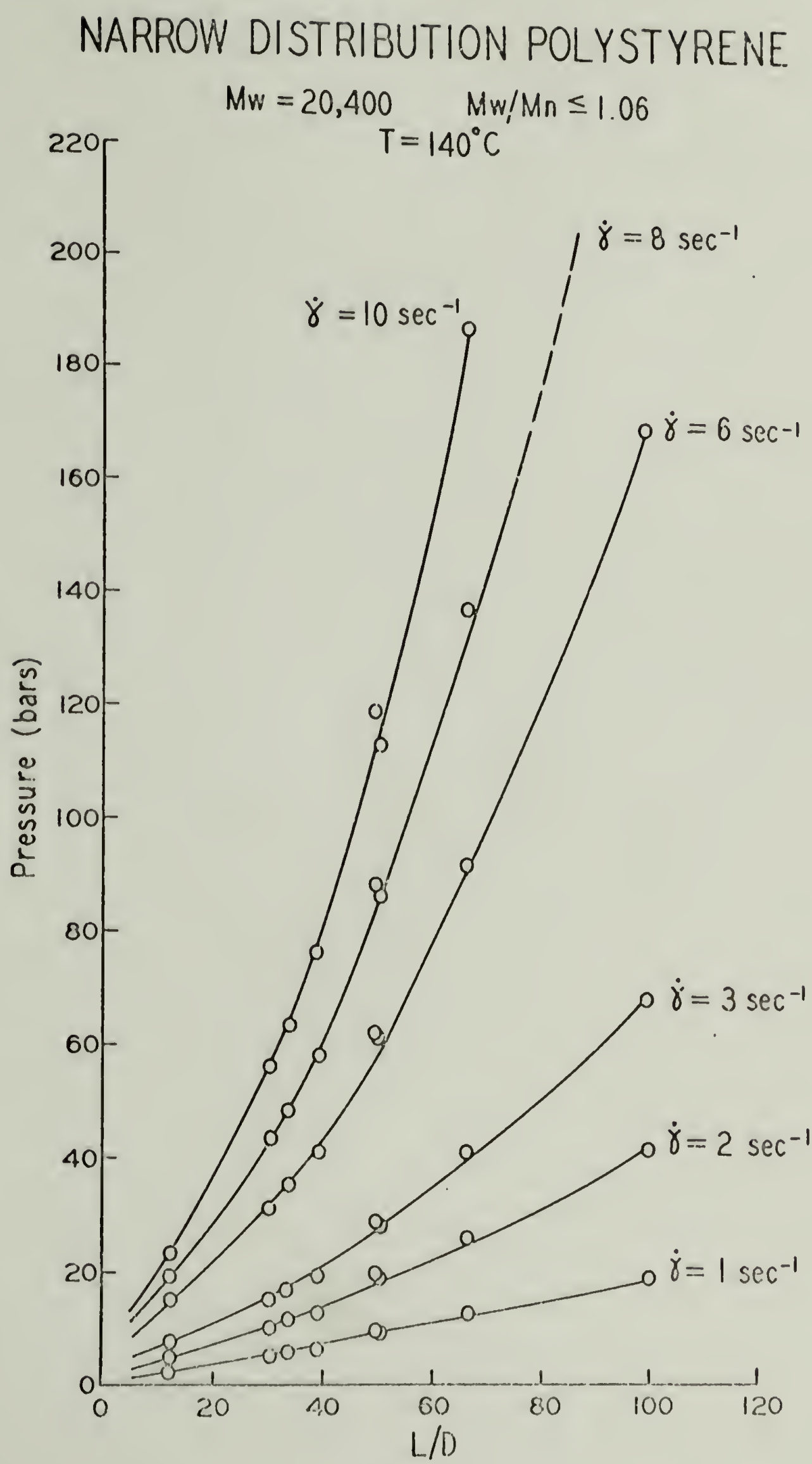
NARROW DISTRIBUTION POLYSTYRENE
Mw = 20,400 Mw/Mn ≤ 1.06
T = 140°C
Pressure (bars)
L/D
$\dot{\gamma}$ = 10 sec^{-1}
$\dot{\gamma}$ = 8 sec^{-1}
$\dot{\gamma}$ = 6 sec^{-1}
$\dot{\gamma}$ = 3 sec^{-1}
$\dot{\gamma}$ = 2 sec^{-1}
$\dot{\gamma}$ = 1 sec^{-1}
0
20
40
60
80
100
120
140
160
180
200
220

FIGURE II-5

NARROW DISTRIBUTION POLYSTYRENE

Mw = 20,400 Mw/Mn ≤ 1.06

T = 160°C

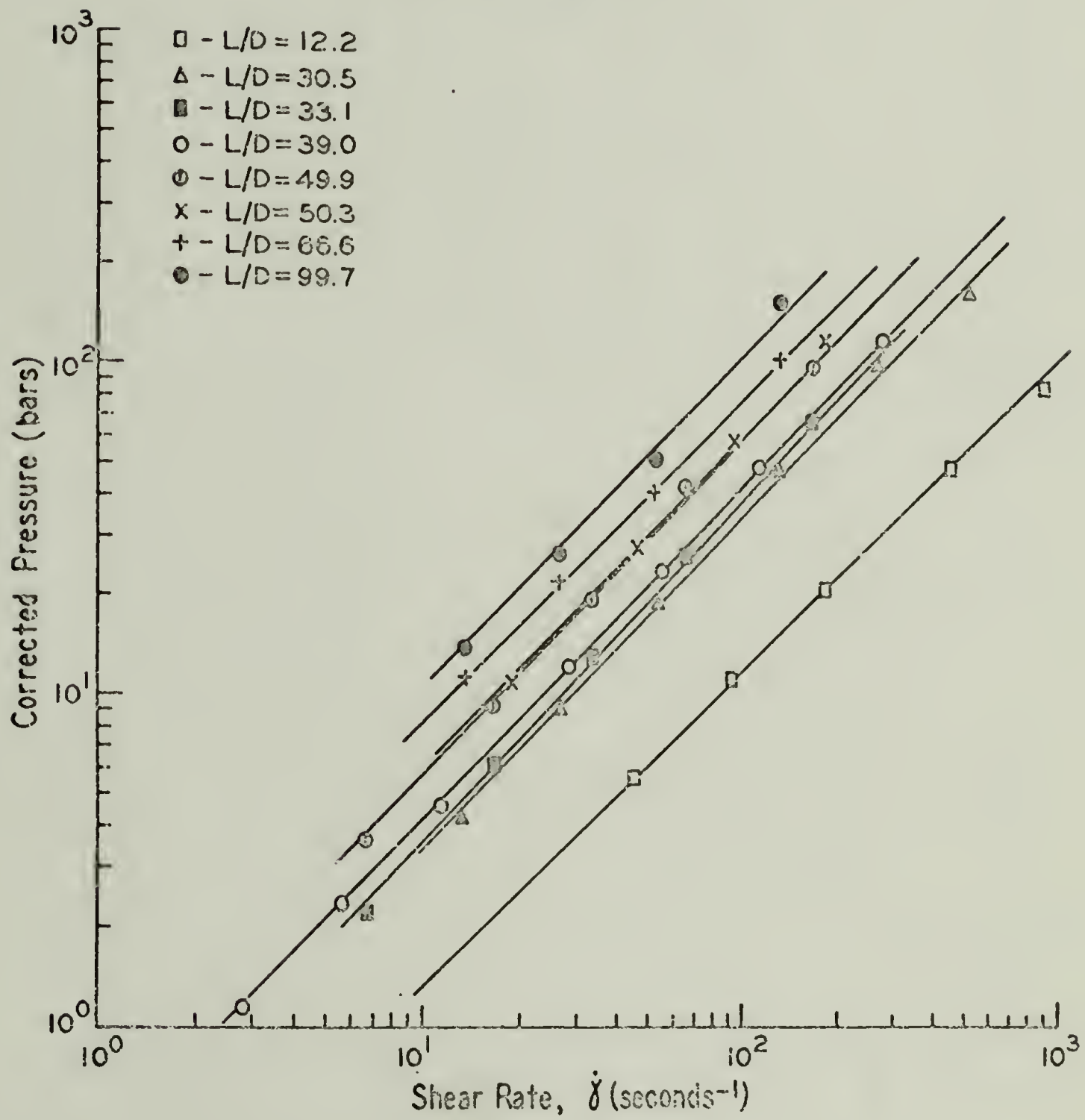

FIGURE II-6

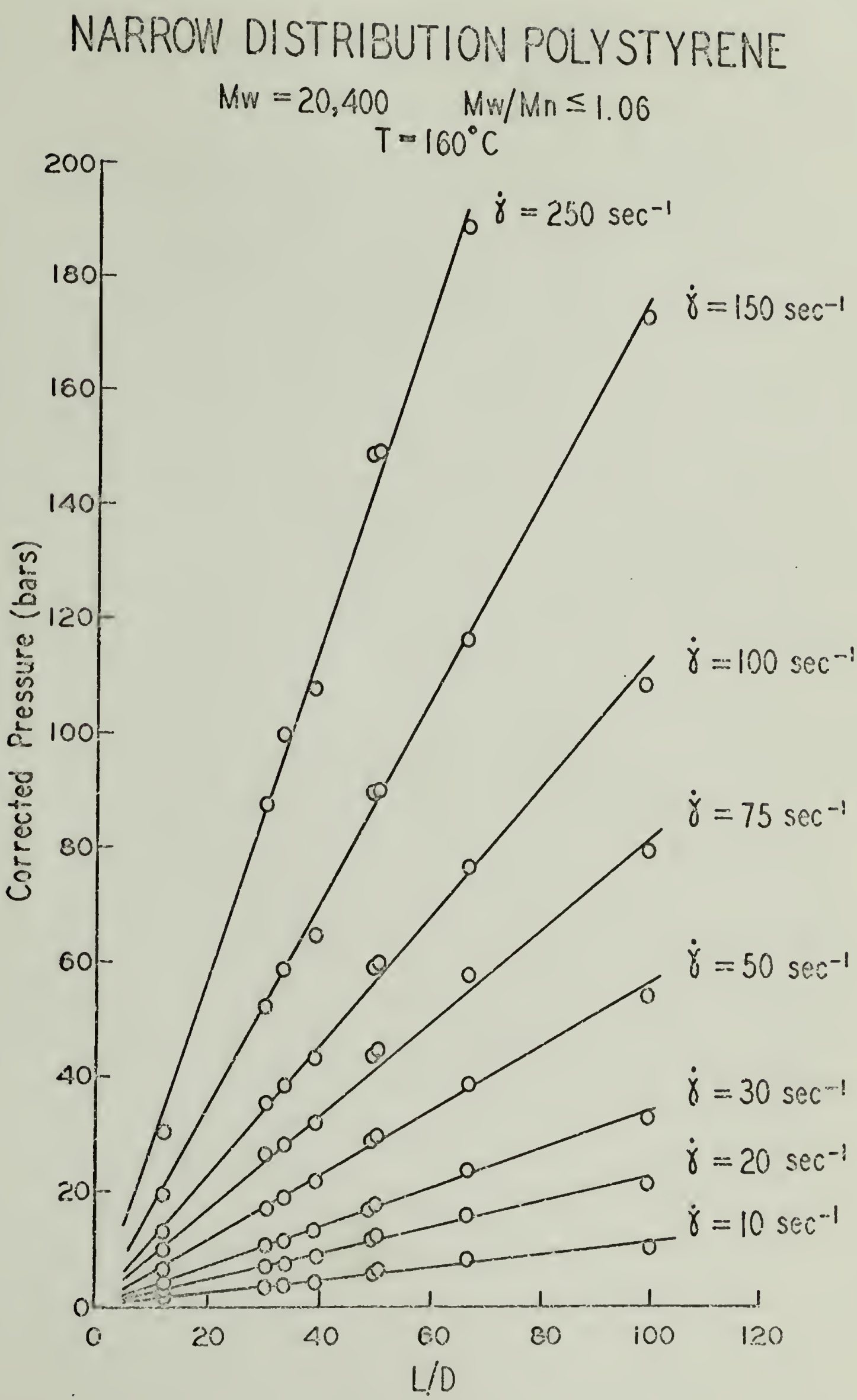
NARROW DISTRIBUTION POLYSTYRENE
Mw = 20,400 Mw/Mn ≤ 1.06
T = 160°C
Corrected Pressure (bars)
200
180
160
140
120
100
80
60
40
20
0
0
20
40
60
80
100
120
L/D
γ̇ = 250 sec⁻¹
γ̇ = 150 sec⁻¹
γ̇ = 100 sec⁻¹
γ̇ = 75 sec⁻¹
γ̇ = 50 sec⁻¹
γ̇ = 30 sec⁻¹
γ̇ = 20 sec⁻¹
γ̇ = 10 sec⁻¹

FIGURE II-7

NARROW DISTRIBUTION POLYSTYRENE

Mw = 20,400 Mw/Mn ≤ 1.06

T = 140°C

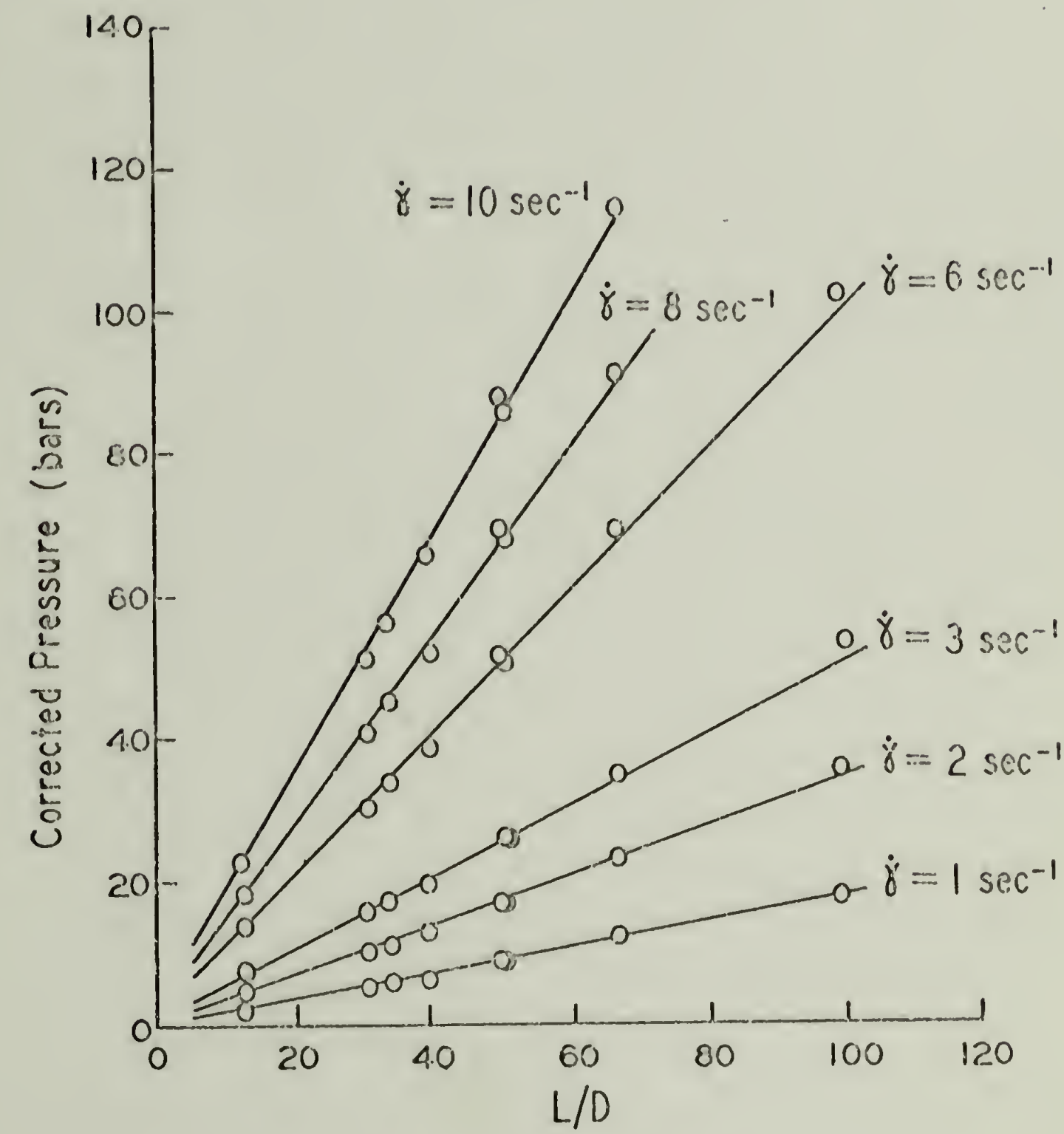

FIGURE II-8

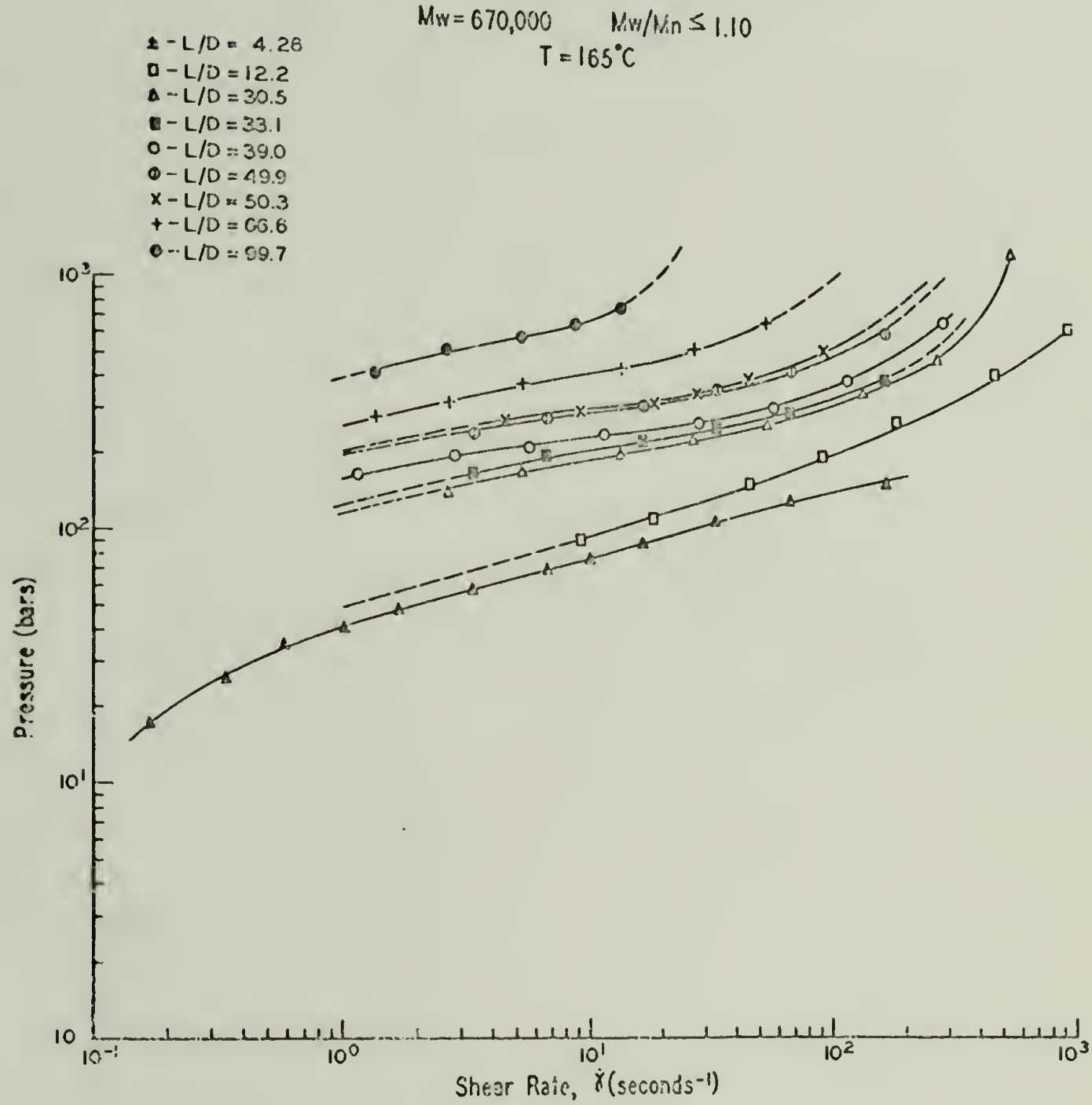
NARROW DISTRIBUTION POLYSTYRENE
Mw = 670,000 Mw/Mn ≤ 1.10
T = 165°C
± - L/D = 4.26
□ - L/D = 12.2
△ - L/D = 30.5
■ - L/D = 33.1
○ - L/D = 39.0
◐ - L/D = 49.9
X - L/D = 50.3
+ - L/D = 66.6
● - L/D = 99.7
Pressure (bars)
10³
10²
10¹
10
10⁻¹
10⁰
10¹
10²
10³
Shear Rate, γ̇(seconds⁻¹)

FIGURE II-9

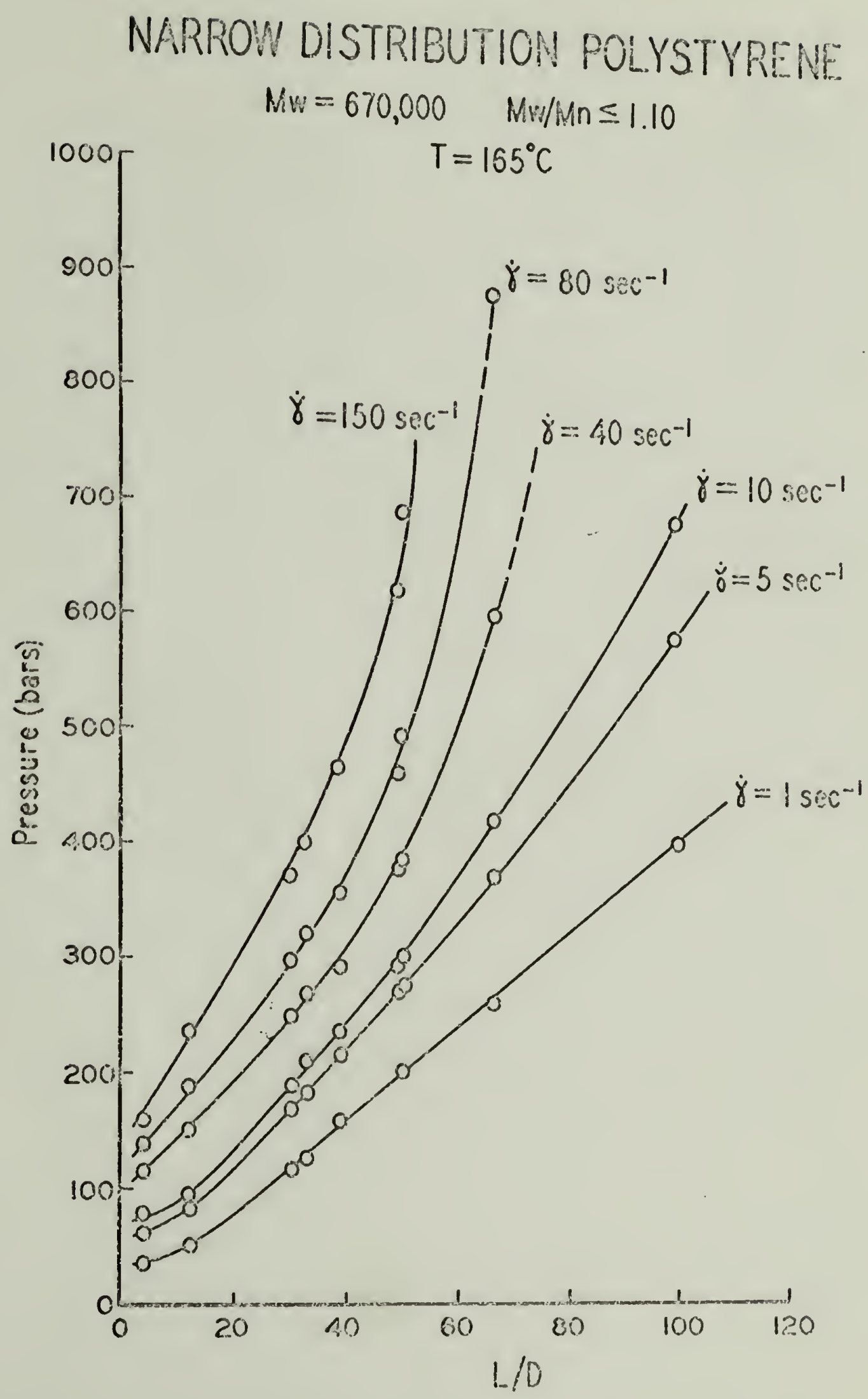
NARROW DISTRIBUTION POLYSTYRENE
Mw = 670,000 Mw/Mn ≤ 1.10
T = 165°C
Pressure (bars)
L/D
0
100
200
300
400
500
600
700
800
900
1000
0
20
40
60
80
100
120
γ̇ = 80 sec⁻¹
γ̇ = 150 sec⁻¹
γ̇ = 40 sec⁻¹
γ̇ = 10 sec⁻¹
γ̇ = 5 sec⁻¹
γ̇ = 1 sec⁻¹

FIGURE II-10

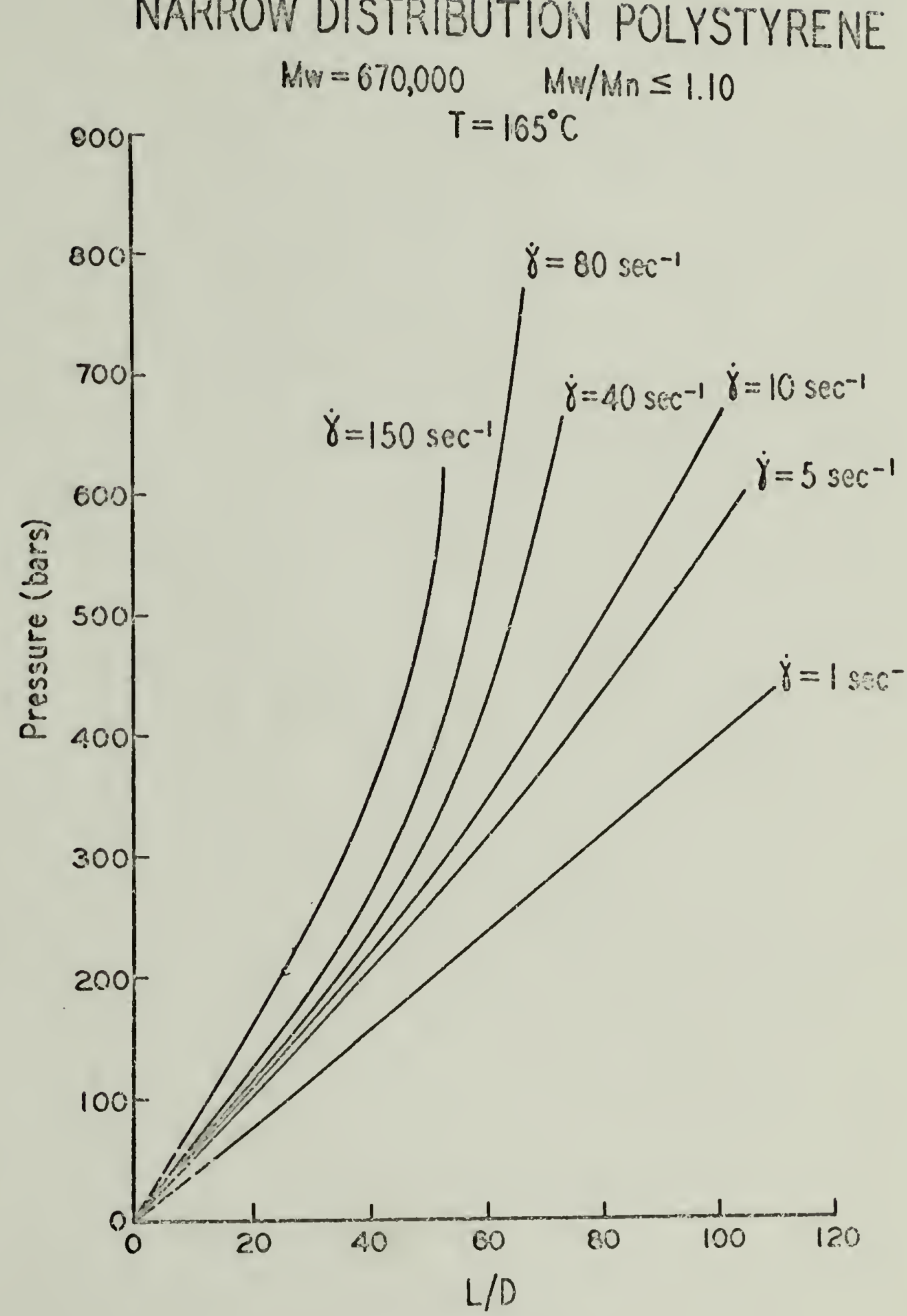
NARROW DISTRIBUTION POLYSTYRENE
Mw = 670,000 Mw/Mn ≤ 1.10
T = 165°C
Pressure (bars)
900
800
700
600
500
400
300
200
100
0
0
20
40
60
80
100
120
L/D
γ̇ = 80 sec⁻¹
γ̇ = 150 sec⁻¹
γ̇ = 40 sec⁻¹
γ̇ = 10 sec⁻¹
γ̇ = 5 sec⁻¹
γ̇ = 1 sec⁻¹

FIGURE II-11

NARROW DISTRIBUTION POLYSTYRENE

Mw = 670,000 Mw/Mn ≤ 1.10

T = 165°C

● - L/D = 12.2
σ - L/D = 30.5
o - L/D = 33.1
α - L/D = 39.0
ϙ - L/D = 49.9
ρ - L/D = 50.3
-o - L/D = 66.6
ϑ - L/D = 99.7

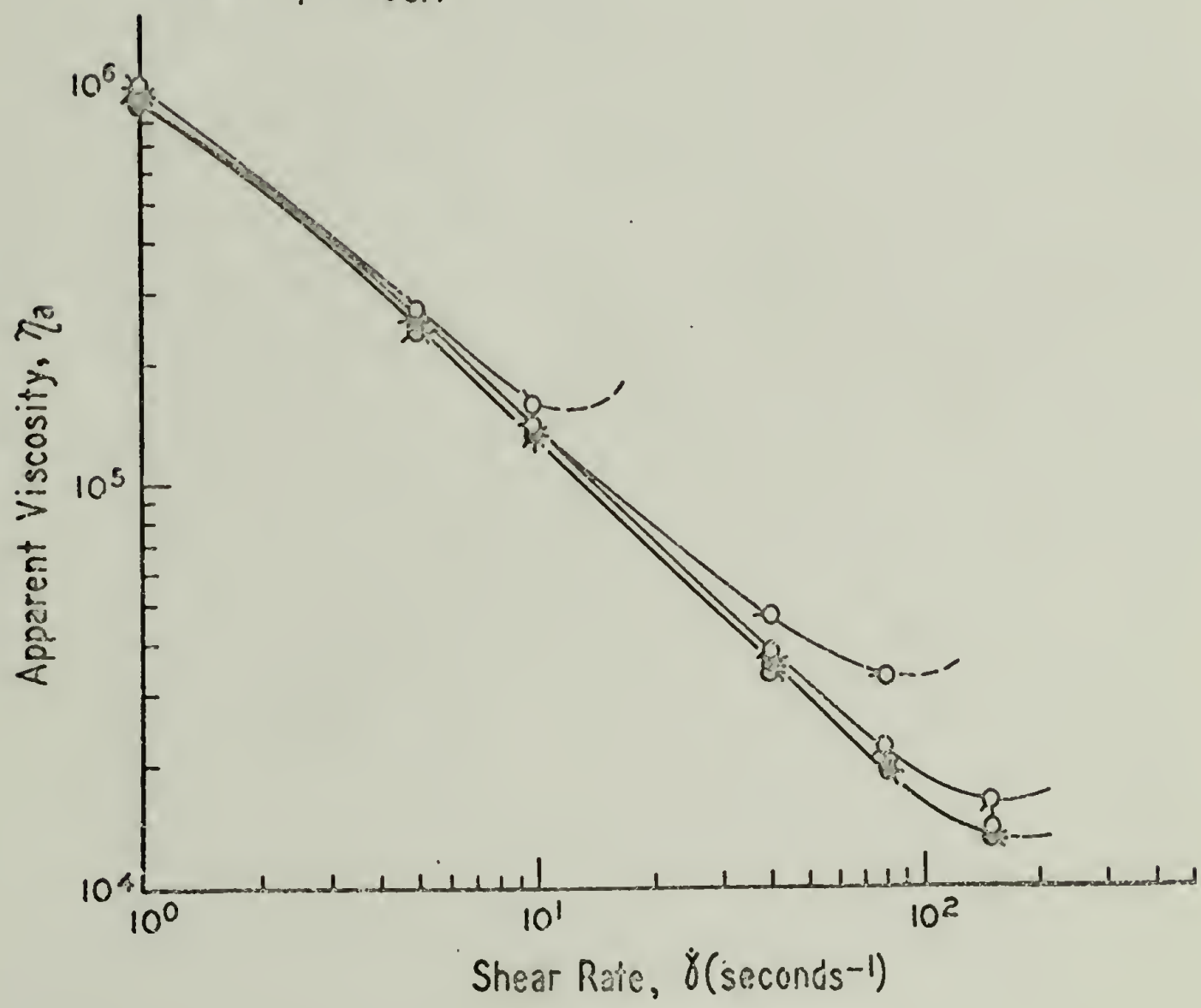

FIGURE II-12

NARROW DISTRIBUTION POLYSTYRENE

Mw = 670,000 Mw/Mn ≤ 1.10

T = 165°C

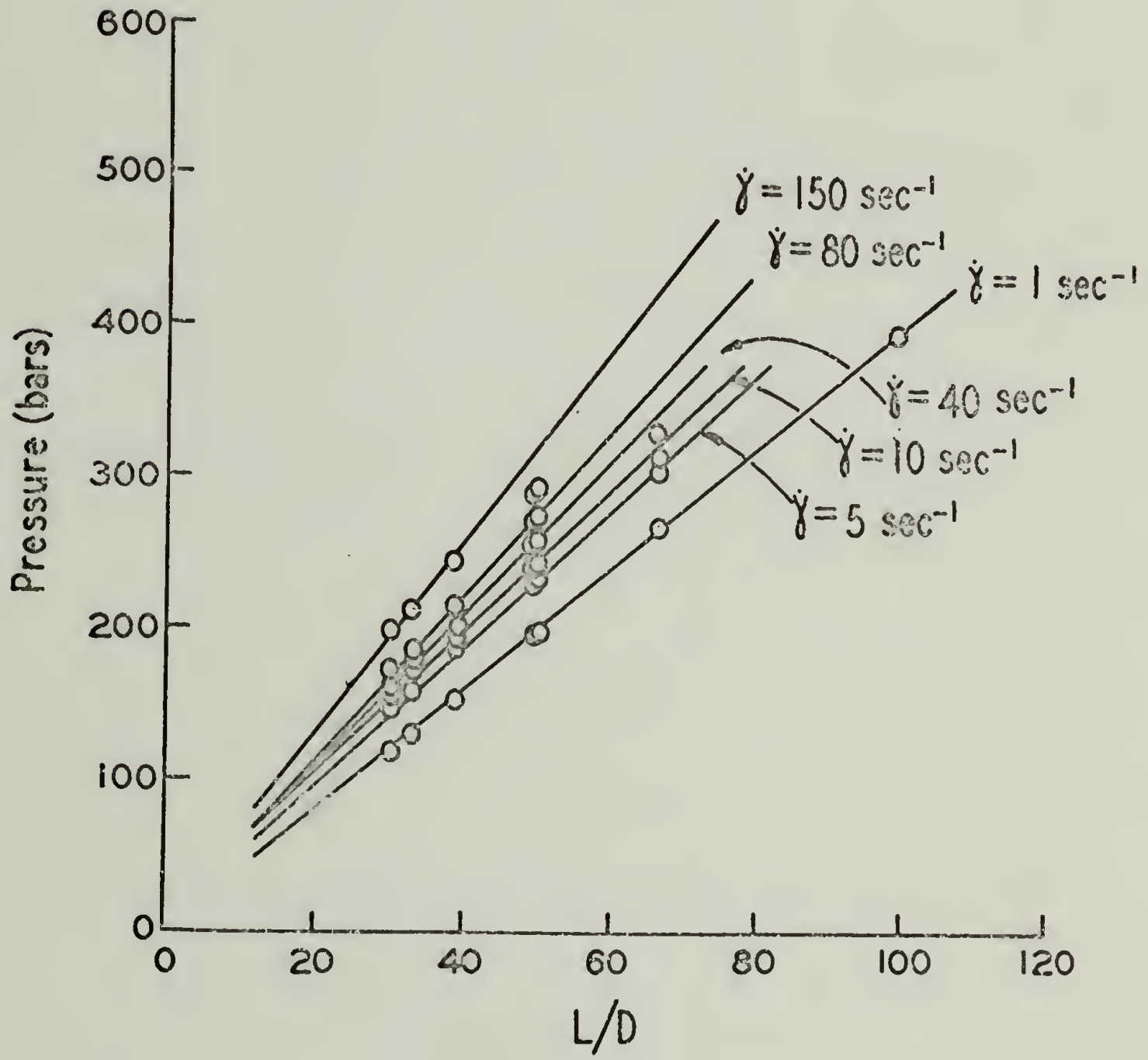

FIGURE II-13

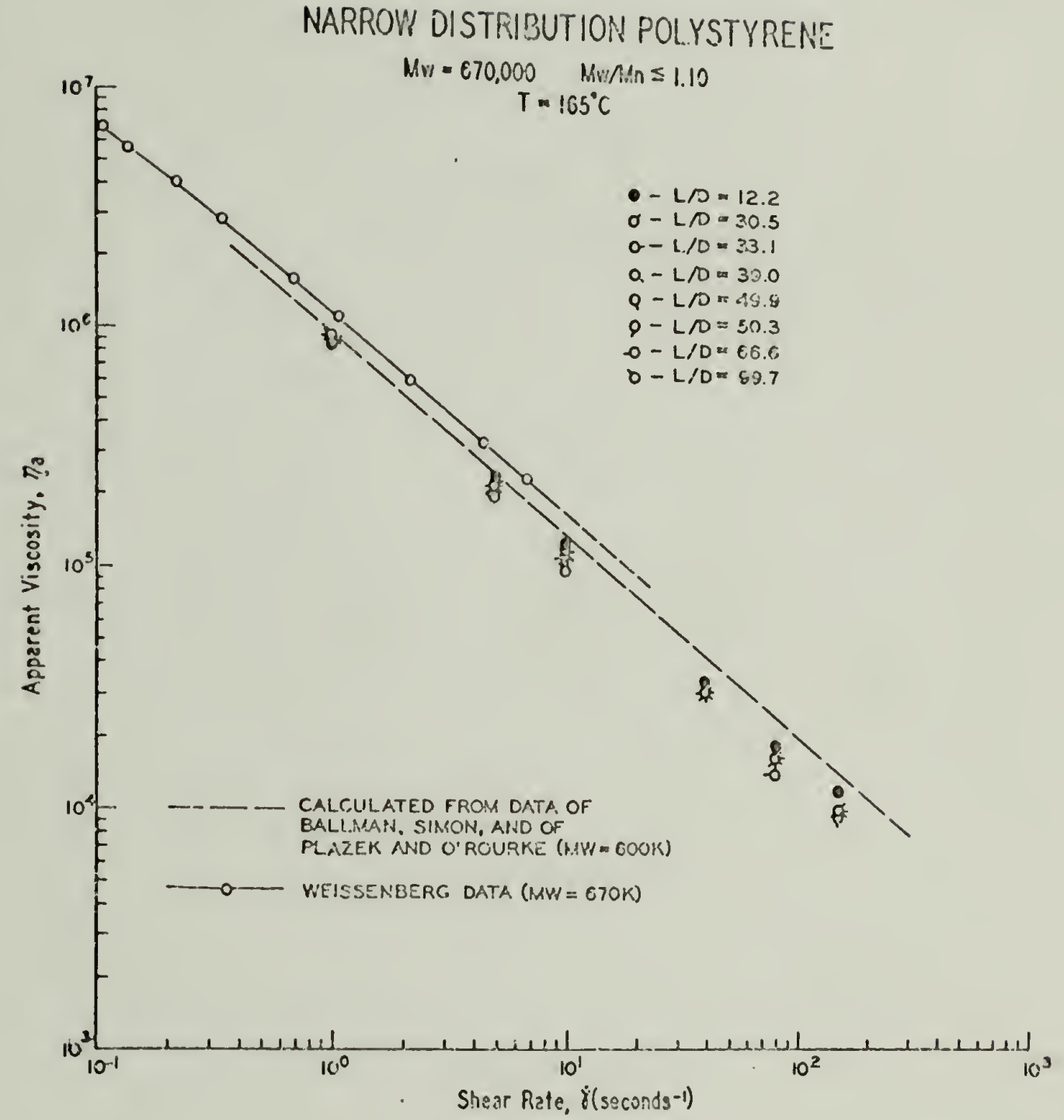
NARROW DISTRIBUTION POLYSTYRENE
Mw = 670,000 Mw/Mn ≤ 1.10
T = 165°C
● – L/D = 12.2
σ – L/D = 30.5
o – L/D = 33.1
o – L/D = 39.0
o – L/D = 49.9
o – L/D = 50.3
o – L/D = 66.6
o – L/D = 99.7
Apparent Viscosity, η_a
10^7
10^6
10^5
10^4
10^3
CALCULATED FROM DATA OF BALLMAN, SIMON, AND OF PLAZEK AND O'ROURKE (MW = 600K)
WEISSENBERG DATA (MW = 670K)
10^{-1}
10^0
10^1
10^2
10^3
Shear Rate, $\dot{\gamma}$(seconds^{-1})

FIGURE II-14

CHAPTER III

THE DETERMINATION OF THE PRESSURE COEFFICIENT AND PRESSURE EFFECTS IN CAPILLARY FLOW

Richard C. Penwell and Roger S. Porter
Polymer Science and Engineering

and

Stanley Middleman
Chemical Engineering
University of Massachusetts
Amherst, Massachusetts 01002

SYNOPSIS

General expressions for determining the pressure coefficient and axial distribution of the viscosity and pressure in capillary flow are derived for Newtonian and shear-thinning fluids. The pressure dependent viscosity model is obtained from the WLF equation as derived from Doolittle's free volume theory. The model has also been derived from Eyring's hole theory for viscosity. Poiseuille's equation is modified to correct for the pressure effect on viscosity.

A Newtonian, low molecular weight polystyrene and a shear-thinning, high molecular weight polystyrene were tested in an Instron capillary rheometer. The axial velocity distribution was found to be negligibly affected by pressure while the viscosity was shown to increase markedly with a decrease in density. The resulting pressure effects on the viscosity of both samples were analyzed using the derived expressions.

INTRODUCTION

Several investigators have recently suggested that under certain conditions, pressure can effectively influence the capillary flow of amorphous polymers.[1-8] The phenomenon generally appears as an unexpected increase in pressure or stress with increasing shear rate. The effect becomes more pronounced with the use of longer capillaries and lower melt temperatures. In particular, the increase in apparent viscosity with increasing capillary shear rate for a Newtonian fluid and for a shear-thinning polystyrene has been attributed to the effect of pressure in decreasing the free volume available for flow[1,2] (Chapters I and II).

A form of the WLF equation derivable from Doolittle's free volume expression has been used to determine the pressure dependence of viscosity.[2] At a particular shear rate and temperature, an average viscosity can be calculated based on an average pressure. To determine the average pressure, a linear pressure drop down the capillary was assumed.[1,2] However, in considering the viscosity to be pressure dependent, the axial pressure distribution is expected to be non-linear.[8-10] The calculated average pressure would then depend on the non-linearity of the pressure drop over the capillary length.

The present work is an attempt to calculate the effect of pressure in capillary flow and to apply the results to the capillary flow of a low and high molecular weight polystyrene. Initially, a pressure dependent model for the viscosity is chosen which can be obtained from the WLF equation and Eyring hole theory[11,12] and, when combined with the momentum equation, provides a reasonable solution to the problem. A general method

for determining the pressure coefficient in the model is given. It is thus possible to calculate the pressure and viscosity at any axial position in a capillary and the average pressure and viscosity at each shear rate. This has been done for both a low (Newtonian) and a high (shear-thinning) molecular weight polystyrene. A pressure corrected version of Poiseuille's equation is also presented and compared with experimental data.

EXPERIMENTAL

Samples

The narrow distribution polystyrene samples used in the tests were obtained from the Pressure Chemical Company, Pittsburgh, Pennsylvania. The 20.4K molecular weight sample has a $M_w/M_n \leq 1.06$ and the 670K sample has a $M_w/M_n \leq 1.10$.

Capillary Measurements

For the study on the low molecular weight polystyrene, a tungsten carbide capillary 0.030 inches in diameter and 0.922 inches long was used in an Instron capillary rheometer. A capillary 0.050 inches in diameter and 1.964 inches long was used for the high molecular weight sample. The test temperatures were 140°C for the 20.4K polystyrene and 165°C for the 670K polystyrene. Pressure losses in the barrel and the kinetic energy correction were negligible for these tests.[2] Based on data taken with other capillaries, an end correction was applied to the data of the high molecular weight sample.[2]

Cone and Plate Measurements

A Weissenberg rheogoniometer (Model No. 17) was used to measure the apparent viscosity as a function of shear rate for the two polystyrenes

at atmospheric pressure. Measurements were made using a 5.0 centimeter plate and a 2° cone angle. The samples were inserted into the rheogoniometer at their respective test temperatures. Therefore, the time required for thermal equilibrium had little effect on their degradation.[13]

DISCUSSION

It has been previously suggested and illustrated that pressure can influence the flow of amorphous polymers in capillary viscometry.[1-8,14,15] If the test temperature is in a region where the flow is determined by the probability of sufficient free volume being available, then the glass transition can be significantly shifted at high pressures.[16-20] The WLF equation has been used successfully to predict an average viscosity increase with pressure by insertion of the shift in the glass transition temperature, T_g.[2] The shift in T_g has been calculated using an average pressure of an assumed linear pressure drop in the capillary.[2] Since the viscosity is pressure dependent, this may have been a limiting assumption. One possible way of determining the variation in the average pressure is to select a pressure dependent viscosity model and solve the appropriate component of the momentum equation.

Model for a Pressure Dependent Viscosity

The model selected for the pressure dependent viscosity should be the simplest possible for the realistic solution of the problem. The WLF equation has been used previously to calculate the pressure dependence of apparent viscosity,[2] and is given below:

$$\log \eta/\eta_g = \frac{-C_1(T - T_g)}{C_2 + T - T_g} \qquad \text{(III-1)}$$

where T_g is the glass transition temperature, T is the test or reference temperature, η_g is the viscosity at T_g and C_1 and C_2 are usually considered constants for a given material.

By using the following equation for the pressure dependence of T_g, an increase in the apparent viscosity can be calculated with increasing pressure;

$$T_g = T_{g_o} + A_1 P \qquad \text{(III-2)}$$

where T_{g_o} is the glass transition at atmospheric pressure, $A_1 = \partial T_g / \partial P$ and P is the pressure.

Inserting equation 2 into 1 gives the following:

$$\eta = \eta_g \exp\left[2.303\left(\frac{A_2 + A_3 P}{A_4 - A_1 P}\right)\right] \qquad \text{(III-3)}$$

where $A_2 = -C_1(T - T_{g_o})$, $A_3 = C_1 A_1$ and $A_4 = C_2 + T - T_{g_o}$. At low pressures ($P < 200$ bars), $A_1 P$ will be a small percentage of A_4 and as a first approximation can be ignored. Equation 3 then simplifies to the form

$$\eta = \eta_o \, e^{bP} \qquad \text{(III-4)}$$

where $\eta_o = \eta_g \, e^{2.303 \, A_2/A_4}$ and $b = 2.303 \, A_3/A_4$. To obtain an estimate of η_o and b, consider the following values for low molecular weight polystyrene at 140°C:[2] $\eta_g \cong 10^{13}$ poise, $T_{g_o} = 90°C$, $C_1 = 14.4$, $C_2 = 36.2$ and $A_1 = 0.028$.[18] The values of η_o and b are found to be 4.36×10^4 poise and 1.07×10^{-2} $bars^{-1}$ respectively. The zero shear viscosity of this sample at 140°C is 4.0×10^4 poise which is in good agreement with the value calculated for η_o.[2] Since C_2 is pressure dependent, the expression for b indicates that it will decrease in value with increasing temperature and pressure.

A relationship equivalent to equation 4 has been previously and independently derived through considerations of the Eyring hole theory for viscosity.[11,12] The parameter b in equation 4 is equal to v_h/RT where v_h equals the volume of the holes. Using the compressibility data for polystyrene of Maxwell and Matsuoka,[22] Hirai and Eyring evaluated v_h.[12] With their value for v_h and at 140°C, b is found to be 4.43×10^{-3} $bars^{-1}$, which should be considered only an estimate.

Equation 4 should thus be a reasonable approximation describing the pressure dependence of viscosity. Indeed this empirical form has been used previously for this purpose.[3,7,8,21] At extreme pressures, it would be expected to fail based on its derivation from the WLF equation and from the assumptions made in the Eyring hole theory.[11,12] For high pressures, possibly equation 3 could be then used, noting that A_4 may also vary with increasing pressure.

The Continuity, Constitutive and Momentum Equations

Equation 4 has been established as a reasonable pressure dependent model for viscosity. It can therefore be used for problems of isothermal, compressible, Newtonian and shear-thinning capillary flows. Heat generation and its effect on the temperature and velocity profiles in both the radial and axial directions of a capillary has been well discussed for both Newtonian and non-Newtonian liquids.[23-29] Considering these previous results and the conditions of the present tests, the assumption of an isothermal problem appears acceptable.

Gerrard, Steidler and Appeldoorn have discussed the adiabatic and isothermal flow of a Newtonian fluid.[28,29] They used a fluid with a

previously determined pressure-temperature relationship. One consequence of their numerical solution was the calculated, non-linear pressure drop down the capillary. Duvdevani and Klein have studied the pressure effect in the capillary flow of polyethylene using the pressure-viscosity relationship of equation 4.[3] Expressions were derived for the shear stress at the entrance and exit which were subsequently used to determine the pressure coefficient. As the pressure coefficient of viscosity for polyethylene is much less than that for polystyrene, they were able to incorporate a limiting series expansion (assuming $b\Delta P<1$) into their solution involving regression analysis. Brenschede and Klein also used equation 4 in their determination of the pressure coefficient and of the error involved by neglecting the pressure dependence of viscosity.[7] An iteritive technique was used as one means of determining the pressure coefficient. They found that the compressibility of the melt is insignificant when considering a possible pressure effect on the flow rate.

The present discussion is an attempt to determine general expressions for the pressure dependent flow behavior of Newtonian and shear-thinning polymers whose viscosities are given by equation 4 and for which the following assumptions apply. The assumptions in this analysis, using cylindrical coordinates (r, θ, z) are: steady state flow, no gravitational effects, no slip at the boundary, $v_\theta = \tau_{r\theta} = \tau_{\theta z} = 0$ (from considerations of the symmetry) and $v_r = 0$ (fully developed flow).

The equation of continuity is represented by:

$$\frac{D\rho}{Dt} = -\rho(\nabla\cdot\bar{v}) \qquad \text{(III-5)}$$

where D/Dt is the material derivative, ρ the density and $\bar{v}$ the velocity field. With the given assumptions, equation 5 reduces to

$$\frac{\partial}{\partial z}(\rho v_z) = 0 \qquad \text{(III-6)}$$

Rearranging equation 6, the following equivalent form is obtained; $d(\ell n\ \rho) = d(\ell n\ v_z)$ (6a). This states that the relative axial change of v_z is equal to the relative change in density. For polystyrene, the expected change in density with pressure would be approximately 1%[2] (See Table II-II). Therefore, the axial velocity distribution will be negligibly dependent on pressure and the assumption of incompressible flow in the calculation of the velocity field for polystyrene is reasonable. To determine the relative effect of pressure on viscosity, a similar procedure can be applied to equation 4. Using $V = V_o + \beta P$, where β is the compressibility coefficient, the relative change in viscosity with density is;

$$d(\ell n\ \eta) = \frac{-b}{\beta\rho}\, d(\ell n\ \rho) \qquad \text{(III-7)}$$

Inserting average values for the parameters of polystyrene into equation 7 indicates that the relative change in viscosity would be approximately 80 times the relative change in density.

The momentum equation is represented by;

$$\rho \frac{D\bar{v}}{Dt} = -\nabla p - [\nabla \cdot \bar{\tau}] - \rho\bar{g} \qquad \text{(III-8)}$$

where $\bar{\tau}$ is the stress tensor, $\bar{g}$ the gravitational field and the other parameters are as defined previously. The z-component of equation 8 reduces to

$$0 = -\frac{\partial P}{\partial z} + \frac{1}{r}\frac{\partial}{\partial r}(r\tau_{rz}) \qquad \text{(III-9)}$$

The constitutive equation for a Newtonian fluid is

$$\bar{\tau} = 2\eta_o\left(\frac{1}{2}\nabla\bar{v} + \frac{1}{2}\nabla\bar{v}^T\right) - \left(-2/3\ \eta_o + \kappa\right)(\nabla\cdot\bar{v})\ \delta \qquad \text{(III-10)}$$

where η_o is the zero shear viscosity, κ is the bulk viscosity and the other parameters are as defined previously. In cylindrical coordinates, equation 10 gives $\tau_{rz} = \eta_o \left(\frac{\partial v_z}{\partial r}\right)$ (III-11) when the given assumptions are applied.

The substitution of equations 4 and 11 into equation 9 and separation of the variables gives;

$$- \frac{1}{\eta_o} e^{-bP} \frac{\partial P}{\partial z} = C = \frac{1}{r} \frac{\partial}{\partial r} \left(r \frac{\partial v_z}{\partial r}\right) \qquad \text{(III-12)}$$

With atmospheric pressure as a reference, C is given by

$$C = - \frac{1}{b\eta_o L} \left(1 - e^{-b\Delta P}\right) \qquad \text{(III-13)}$$

From equations 12 and 13, the velocity distribution is found to be

$$v = \frac{1 - e^{-b\Delta P}}{b\ \Delta P} \left[\frac{\Delta P R^2 \left(1 - \frac{r^2}{R^2}\right)}{4\eta_o L}\right] \qquad \text{(III-14)}$$

The velocity distribution is modified from the classical result by the pressure correction term $(1 - e^{-b\Delta P})/b\Delta P$, which is also applicable to Poiseuille's law as given below:

$$\eta_o = \frac{\pi \Delta P R^4}{8LQ} \left[\frac{1 - e^{-b\Delta P}}{b\Delta P}\right] \qquad \text{(III-15)}$$

Using equations 12 and 13 the following expression for the axial pressure distribution is obtained.

$$P = \frac{\ell n \left[e^{-b\Delta P} + \left(1 - e^{-b\Delta P}\right) z/L\right]}{-b} \qquad \text{(III-16)}$$

From this, the pressure gradient is given as

$$\frac{\partial p}{\partial z} = \frac{-\left(1 - e^{-b\Delta P}\right)}{bL\left\{e^{-b\Delta P} + \left(1 - e^{-b\Delta P}\right) z/L\right\}} \qquad \text{(III-17)}$$

The average pressure is given by $\bar{p} = \int_0^L P \frac{dz}{L}$. (III-18)

Substituting equation 16 for P and defining $\xi = z/L$ and $\delta = e^{b\Delta P} - 1$ gives

$$\bar{P} = \Delta P - \frac{1}{b} \int_0^1 \ell n \, [1 + \delta\xi] \, d\xi \qquad \text{(III-19)}$$

By expanding the logarithm and integrating, equation 19 becomes

$$\bar{p} = \Delta P + \frac{1}{b} \sum_{i=1}^{n} \frac{\delta^i (-1)^i}{i(i+1)} \qquad \text{(III-20)}$$

Equation 20 is valid only when $b\Delta P<1$ and the number of terms included in the series depends on how much less than 1 is $b\Delta P$. If $b\Delta P>1$, then $\bar{p}$ must be found by numerical integration of the p - z curve.

The average flow rate, given below, can be calculated and compared to either the measured flow rate or the flow rate calculated from the plunger motion.

$$Q = \frac{\pi R^4 \, (1 - e^{-b\Delta P})}{8b\eta_o L} \qquad \text{(III-21)}$$

Determination of the Pressure Coefficient b

To determine the parameter b in equation 4, the actual Newtonian viscosity η_o, given by equation 15, and the uncorrected viscosity η^o are used. The uncorrected viscosity η^o is given by Poiseuille's law as $\eta^o = \frac{\pi \Delta P R^4}{8LQ}$. The volume flow rate can be calculated from the plunger speed V_p and the cross section πR_p^2, so that $\eta^o = \Delta P R_c^4 / 8L_c R_p^2 V_p$ (III-22) where the subscript c and p refer respectively to the capillary and reservoir dimensions. Functions ϕ and θ can be defined as $\phi = \eta_o/\eta^o$ and $\theta = \phi_1/\phi_2$ (III-23) where the number subscripts refer to different size capillaries and reservoirs.

Combining equations 22 and 23 gives

$$\theta = \phi_1/\phi_2 = \eta^o{}_1/\eta^o{}_2 = \frac{\Delta P_2}{\Delta P_1}\frac{L_{c1}}{L_{c2}}\frac{V_{p1}}{V_{p2}}\frac{R_{p1}{}^2}{R_{p2}{}^2}\frac{R_{c2}{}^4}{R_{c1}{}^4} = KC_1V_R \qquad \text{(III-24)}$$

where $K = \Delta P_2/\Delta P_1$, $V_R = V_{P1}/V_{P2}$ (ratio of plunger speeds) and

$$C_1 = \frac{L_{c1}}{L_{c2}}\frac{R_{p1}{}^2}{R_{p2}{}^2}\frac{R_{c2}{}^4}{R_{c1}{}^4} \quad \text{(geometrical factor).}$$

Combining equations 15 and 23,

$$\theta = K\left[\frac{1 - e^{-b\Delta P_1}}{1 - e^{-bK\Delta P_1}}\right] \qquad \text{(III-25)}$$

Equating equations 24 and 25 gives,

$$C_1V_R = \frac{1 - e^{-b\Delta P_1}}{1 - e^{-bK\Delta P_1}} \qquad \text{(III-26)}$$

Equation 26 is a general expression for determining the pressure coefficient of a Newtonian fluid. Using one capillary in the same rheometer $C_1 = 1$ and b can be determined in the following manner. For convenience, the pressure required for flow at the lowest shear rate can be used as the reference pressure, ΔP_1. From earlier calculations, an estimate of b is available. Therefore, a suitable range of values for $b\Delta P_1$ can be selected. The range of K values can also be determined from the experimental data, using ΔP_1 as the reference pressure. For different values of K, V_R can be calculated as a function of $b\Delta P_1$. Since the velocity ratios are pre-determined, it is convenient to plot this information with K and $b\Delta P$ as variables as shown in Figure 1. From experimental values of K and $V_R(n=1)$, $b\Delta P_1$ and therefore b can be determined. Although one curve is sufficient to determine b, several can be used to calculate any possible change in b with increasing pressure. For low

molecular weight polystyrene at 140°C, b was found to be 5.51×10^{-3} $bars^{-1}$. The variation in b over the pressure range studied was approximately 10%. A second means of determining b is to calculate η^o using equation 22 and then using equation 4,

$$b = \ell n \frac{(\eta^o/\eta_o)}{P} \qquad \text{(III-27)}$$

Modifications for a Shear-Thinning Polymer

By a separation of the pressure and shear rate dependence of the apparent viscosity, the problem is similar to the Newtonian case. The power law expression $\tau = K'\dot{\gamma}^n$ (III-28) is assumed applicable at atmospheric pressure. The corrected shear rate, $\dot{\gamma}$, is obtained from the measured shear rate times a factor of $\frac{3n+1}{4n}$ (III-29).[30] Equation 4 now becomes

$$\eta = \eta_{atm.}\, e^{bP} = K'\dot{\gamma}^{n-1} e^{bP} \qquad \text{(III-30)}$$

Following the same procedure as before, equation 9 can be solved and equation 13 now becomes

$$C = \frac{e^{-b\Delta P} - 1}{bK'L} \qquad \text{(III-31)}$$

Using a single capillary, the expression for determining b is

$$V_R^{\,n} = \frac{1 - e^{-b\Delta P_1}}{1 - e^{-bK\Delta P_1}} \qquad \text{(III-32)}$$

where V_R is the ratio of the plunger speeds and $K = \Delta P_2/\Delta P_1$. The expressions for p, $\partial P/\partial z$ and $\bar{p}$ remain the same.

The procedure for determining the pressure coefficient b, is identical to that for the Newtonian case. The Weissenberg rheogoniometer was used to obtain the data at atmospheric pressure required to calculate the power law exponent, n. Figure 1 was used to calculate a value of 2.90×10^{-3} for the pressure coefficient of the high molecular weight polystyrene.

RESULTS

A study of the low molecular weight polystyrene at 140°C was performed in an Instron rheometer using a capillary 0.030 inches in diameter and 0.922 inches long. At this temperature and in the shear rate range studied, a negligible capillary end correction and extrudate expansion have been reported.[2]

For the low molecular weight polystyrene, the pressure coefficient had values of 5.51×10^{-3} bars^{-1} and 5.54×10^{-3} bars^{-1} as calculated by equations 26 and 27 respectively. Figure 2 represents the axial pressure distribution, given by equation 16, at various shear rates. The deviation from a linear pressure drop increases with increasing shear rate. The greater the non-linearity in the pressure drop, the greater the deviation of the average pressure from $\Delta P/2$. The magnitude will affect the value of the average viscosity calculated using equation 3. The variation in the average pressure with the total pressure is illustrated in Figure 3. At low pressure, the average is adequately represented by $\Delta P/2$, but decreases significantly from this value at higher pressures.

With a pressure dependent viscosity, an appreciable change in viscosity with total pressure and axial position can be anticipated. The magnitude of this variation is illustrated in Figure 4, in which the apparent viscosity is plotted as a function of the axial distance at various shear rates. These curves may be integrated to obtain an average viscosity which can be compared to the viscosity calculated by equation 4 using an average pressure. This comparison is made in Table I which also includes the viscosity calculated as the stress/shear rate.

The corrected version of Poiseuille's equation presented in equation 15 predicts the Newtonian behavior of a polymer with a pressure dependent viscosity. Figure 5 is a comparison of the viscosity calculated using equation 15 and the viscosity obtained from measurements in the Instron and Weissenberg rheometers. The Weissenberg data, taken at atmospheric pressure, is Newtonian within the range studied. The capillary data deviates from Newtonian behavior with increasing shear rate, reflecting the pressure dependence of the viscosity. The calculated curve is Newtonian with a slight increase in viscosity at the highest shear rates. The deviation of equation 15 at higher shear rates is possibly a consequence of the limitations stated in deriving the pressure dependent viscosity model from equation 3.

Figure 6 is a comparison of the pressure corrected flow rate, equation 21, and the flow rate calculated from the plunger motion of the Instron rheometer. It has been previously observed that no appreciable difference exists between measured flow rates and those calculated from the plunger motion.[2] The flow rate calculated with equation 21 begins to deviate at higher shear rates, again indicating the limits of the model have been exceeded.

It may be reasonably assumed that the pressure effect is independent of shear-thinning. Thus flow data on the high molecular weight polystyrene may be treated similar to the approach used for the Newtonian case. Data from the Weissenberg rheogoniometer were used to evaluate the power law exponent, n having a value of 0.19. Figure 1, a graphical representation of equation 32, was used to evaluate the pressure coefficient, b having a

value of 2.90×10^{-3} bars^{-1}. An appropriate end correction had been previously applied to the capillary data.[2]

The axial pressure distribution is given in Figure 7 for several shear rates at 165°C. The deviation from a linear pressure drop is not as great as for the low molecular weight polystyrene, which is a consequence of the lower value of the pressure coefficient obtained for the high molecular weight polystyrene. The value of $\Delta P/2$, used previously in calculations involving an average pressure, does not appear to cause serious error.

Figure 8 represents the axial variation of viscosity at shear rates of 1, 40 and 150 seconds^{-1}. As with the low molecular weight polystyrene, the viscosity varies considerably with the axial position and total pressure. Average values of the viscosity obtained from Figure 8 are within 1% of the values calculated with equation 4 using the calculated average pressure.

SUMMARY

The influence of pressure on the viscosity in capillary flow has been discussed for Newtonian and shear-thinning fluids. A pressure dependent viscosity model, derivable from Doolittle's free volume equation and the Eyring hole theory for viscosity, was combined with the momentum equation to derive general expressions for determining the pressure coefficient and the axial pressure and viscosity distributions. From these, an average pressure and viscosity can be determined.

The resulting expressions were applied to a Newtonian, low molecular weight polystyrene and a shear-thinning high molecular weight polystyrene.

From a consideration of the continuity equation, the axial velocity was found to be negligibly affected by pressure for the test conditions used. The axial pressure distributions for both the low and high molecular weight samples were non-linear at moderate shear rates, resulting in average capillary pressures less than $\Delta P/2$. The viscosities averaged over several intervals of the capillary agreed well with the viscosities calculated using an average pressure representing the entire capillary. Values calculated using the pressure corrected flow rate and Poiseuille equations agreed well with the experimental data.

REFERENCES

III-1. R.C. Penwell and R.S. Porter, J. Appl. Polym. Sci., 13, 2427 (1969).

III-2. R.C. Penwell and R.S. Porter, submitted to J. Polym. Sci.

III-3. I. Duvdevani and I. Klein, SPE J., 23, 41 (1967).

III-4. K. Ito, Rept. Prog. Polym. Phys. (JAPAN), 12, 131 (1969).

III-5. G.A. Toelke, C.G. Gogas and J.A. Biesenberger, SPE 13th Antec, 98 (1967).

III-6. D. P. Thomas and R.S. Hagan, Polym. Engr. Sci., 9, 164 (1969).

III-7. Von E. Brenschede and J. Klein, Rheol. Acta, 8, 71 (1969).

III-8. V. Semjonow, Rheol. Acta, 4, 133 (1965).

III-9. B.C. Sakiadis, A.I.Ch.E. J., 8, 317 (1962).

III-10. T. Arai, I. Suzuki and N. Akino, Proc. Fujihara Memorial Faculty of Engr., Keio University, Tokyo, Japan, 20, 39 (1967).

III-11. S. Glasston, K. Laidler and H. Eyring, The Theory of Rate Processes, p. 512, McGraw-Hill, 1941.

III-12. N. Hirai and H. Eyring, J. Polym. Sci., 37, 51 (1959).

III-13. K. Arisawa and R.S. Porter, J. Appl. Polym. Sci., 14, 879 (1970).

III-14. R.L. Ballman, Nature, 202, 288 (1964).

III-15. A.K. Van der Vegt and P.P.A. Smit, S.C.I. Monograph No. 26, 313, (1967).

III-16. A. Miyake and M. Sakakibara, Rpts. Prog. in Polym. Phys. in Japan, 6, 93 (1963).

III-17. R.W. Warfield, J. Appl. Chem., 17, 263 (1967).

III-18. G. Gee, Polymer 7, 177 (1966).

III-19. A.J. Matheson, J. Chem. Phys., 44, 695 (1966).

III-20. A. Eisenberg. J. Phys. Chem., 67, 1333 (1963).

III-21. E. Kuss, Chem. Ingr. Techn., 37, 465 (1965).

III-22. B. Maxwell and S. Matsuoka, SPE J., 27, 13 (1957).

III-23. H.L. Toor, A.I.Ch.E. J., 4, 319 (1958).

III-24. H.C. Brinkman, Appl. Sci. Res., A2, 120 (1950).

III-25. R.B. Bird, SPE J., 11, 35 (1955).

III-26. H.L. Toor, Ind. and Engr. Chem., 48, 922 (1956).

III-27. R.E. Gee and J.B. Lyon, Ind. and Engr. Chem., 49, 956 (1957).

III-28. J.E. Gerrard, F.E. Steidler and J.K. Appeldoorn, I. and E.C. Fund., 4, 332 (1965).

III-29. J.E. Gerrard, F.E. Steidler and J.K. Appeldoorn, I. and E.C. Fund., 5, 260 (1966).

III-30. S. Middleman, The Flow of High Polymers, Interscience, New York, 1968, p. 15.

TABLE III-I

PRESSURE DEPENDENT VISCOSITY FOR LOW MOLECULAR WEIGHT POLYSTYRENE AT T=140°C(1)

$\dot{\gamma}$ sec^{-1}	ΔP_{Total} bars	$\Delta P_{average}$ bars	$\eta_a \times 10^{-4}$ (2) poises	$\eta_a \times 10^{-4}$ (3) poises	$\eta_a \times 10^{-4}$ (4) poises
1.34	6.71	3.34	3.95	4.02	4.02
2.68	13.86	6.84	4.08	4.10	4.10
5.36	28.57	13.91	4.20	4.27	4.27
13.4	82.57	38.18	4.86	4.90	4.88
26.8	205.7	83.95	6.05	6.47	6.29

(1) Capillary diameter = 0.030 inches, length = 0.922 inches

(2) Calculated from $\tau/\dot{\gamma}$

(3) Numerically integrated from Figure 3

(4) Calculated from Equation 4

CAPTIONS FOR FIGURES

III-1. General curve for the determination of the pressure coefficient of Newtonian and shear-thinning fluids.

III-2. The axial pressure distribution of the 20.4K polystyrene for several shear rates at 140°C.

III-3. The average pressure as a function of the total pressure drop for the 20.4K polystyrene at 140°C.

III-4. The axial variation in viscosity at several shear rates for the 20.4K polystyrene at 140°C.

III-5. Comparison of Instron and Weissenberg data with the pressure corrected Poiseuille equation for the 20.4K polystyrene at 140°C.

III-6. Comparison of the flow rate calculated from the plunger motion and the pressure corrected flow rate equation.

III-7. The axial pressure distribution of the 670K polystyrene at 165°C and for various shear rates.

III-8. The axial variation in viscosity at several shear rates for the 670K polystyrene at 165°C.

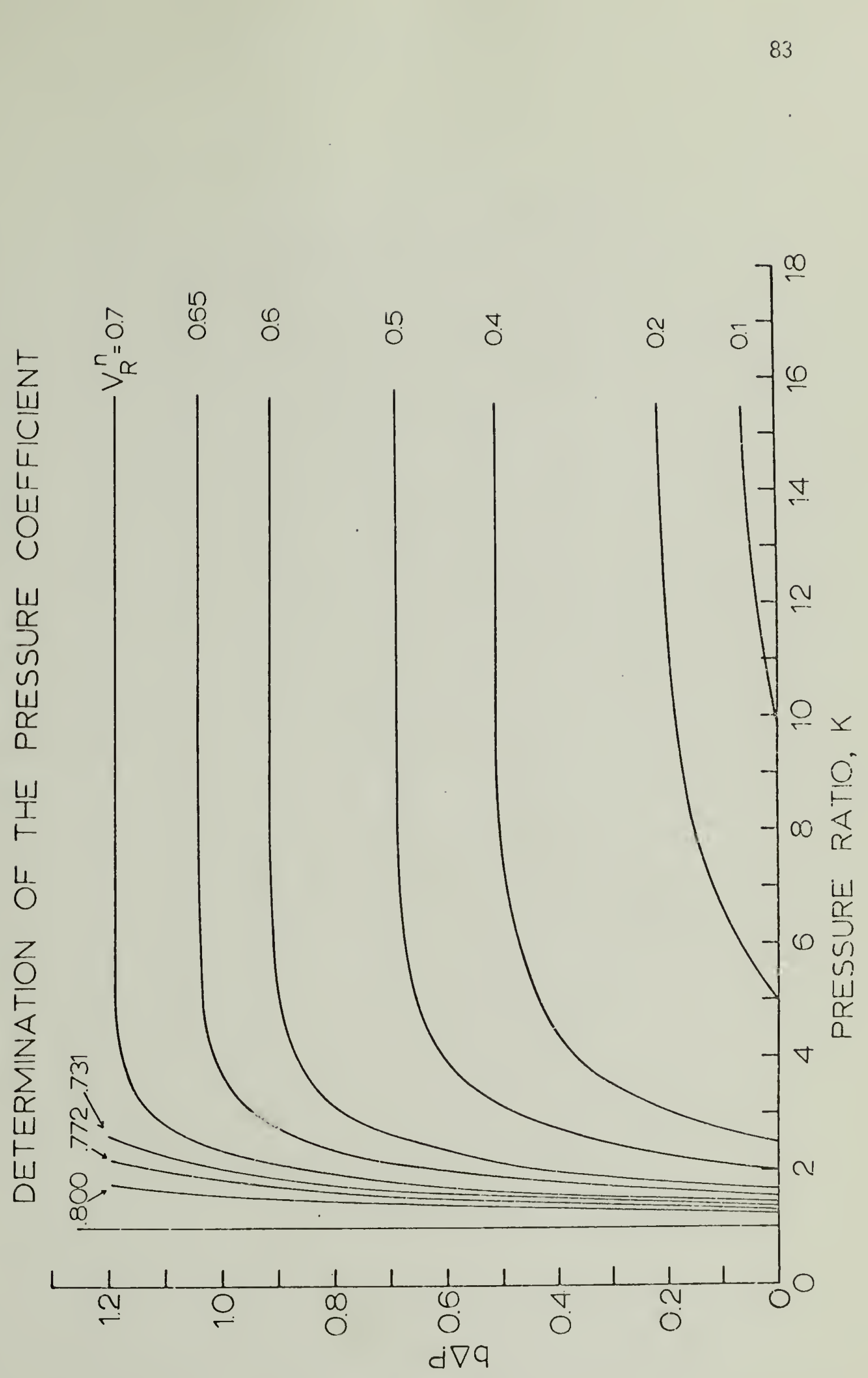
DETERMINATION OF THE PRESSURE COEFFICIENT
V_R^n=0.7
0.65
0.6
0.5
0.4
0.2
0.1
.800
.772
.731
$b\Delta p$
1.2
1.0
0.8
0.6
0.4
0.2
0
2
4
6
8
10
12
14
16
18
PRESSURE RATIO, K

FIGURE III-1

AXIAL PRESSURE DISTRIBUTION FOR THE CAPILLARY FLOW OF A POLYSTYRENE

MW = 20.4 K T = 140°C

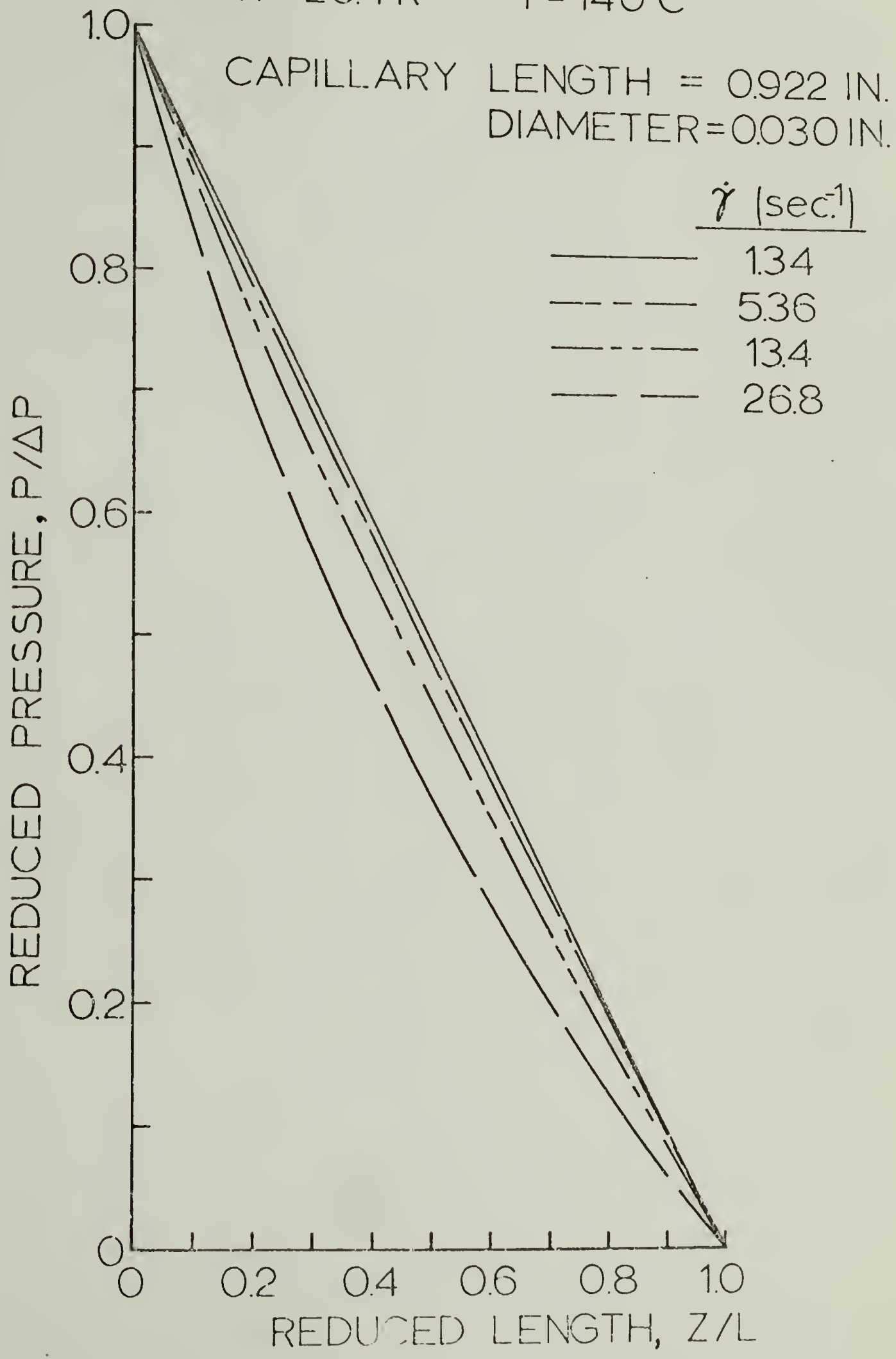

FIGURE III-2

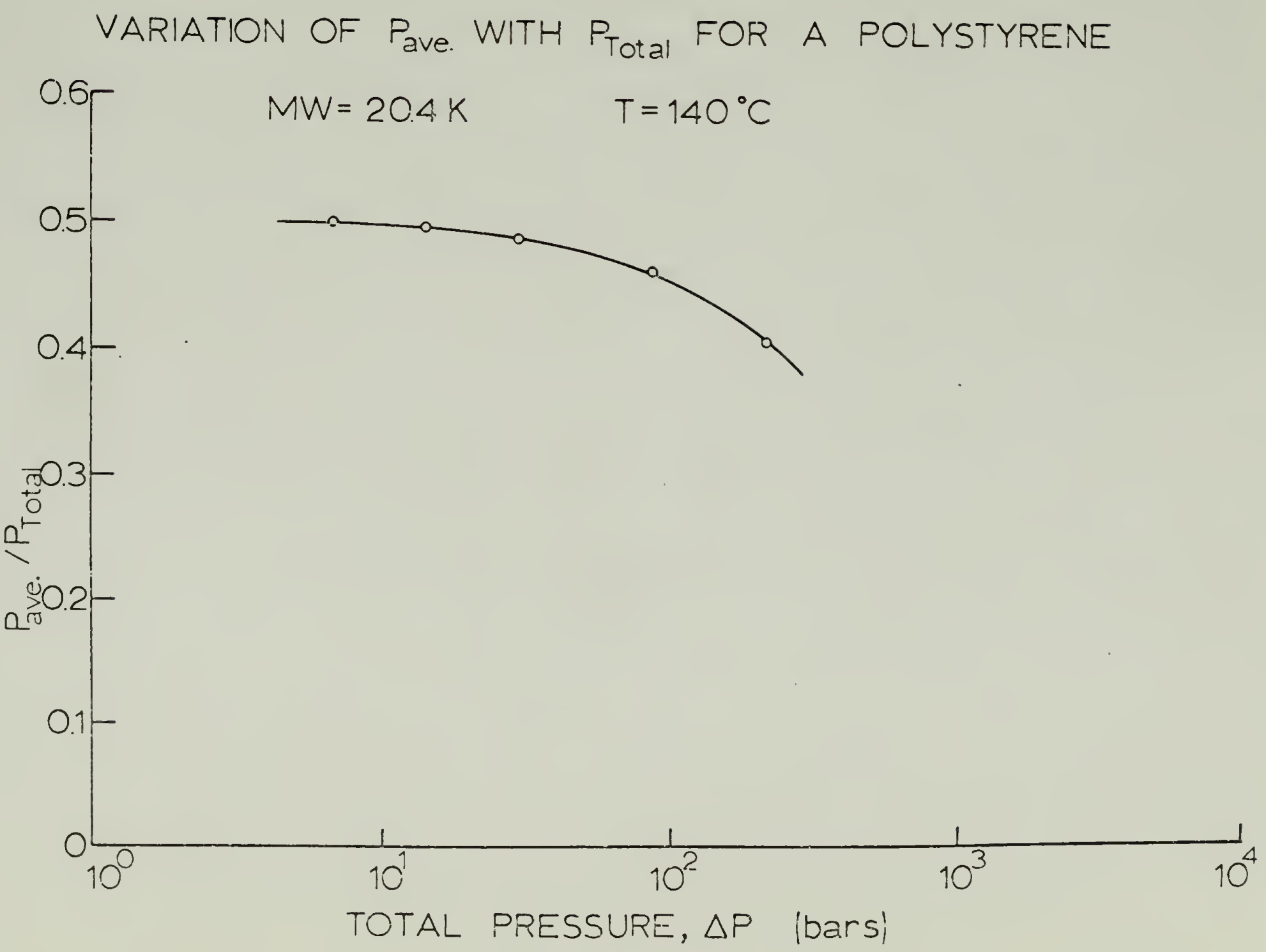
VARIATION OF $P_{ave.}$ WITH P_{Total} FOR A POLYSTYRENE
MW = 20.4 K
T = 140 °C
0.6
0.5
0.4
0.3
0.2
0.1
0
$P_{ave.}/P_{Total}$
10^0
10^1
10^2
10^3
10^4
TOTAL PRESSURE, ΔP (bars)

FIGURE III-3

AXIAL CHANGE IN VISCOSITY FOR THE CAPILLARY FLOW OF A POLYSTYRENE

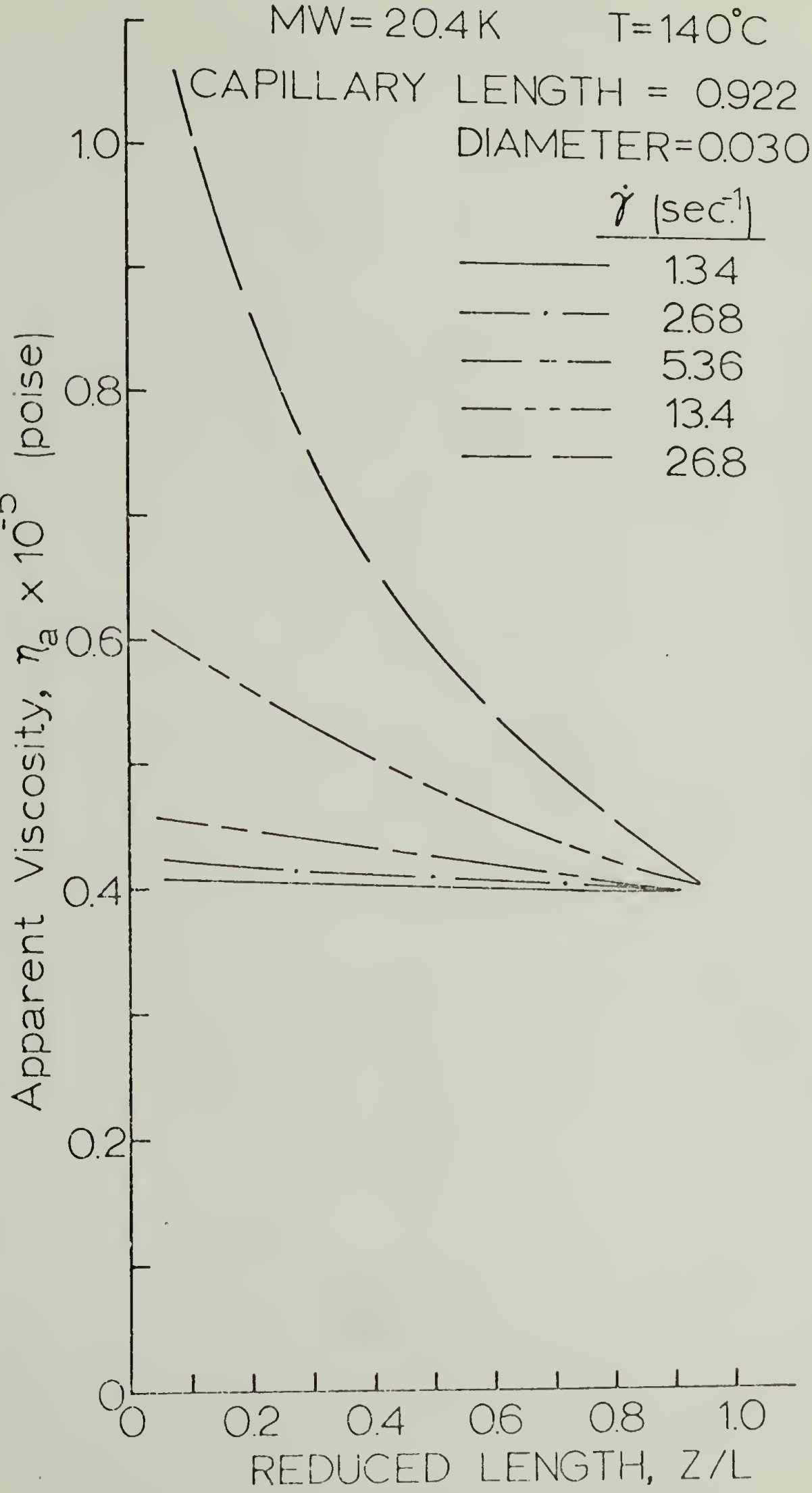

FIGURE III-4

FIGURE II-5

FLOW PROPERTIES OF A POLYSTYRENE

MW = 20.4 K T = 140°C

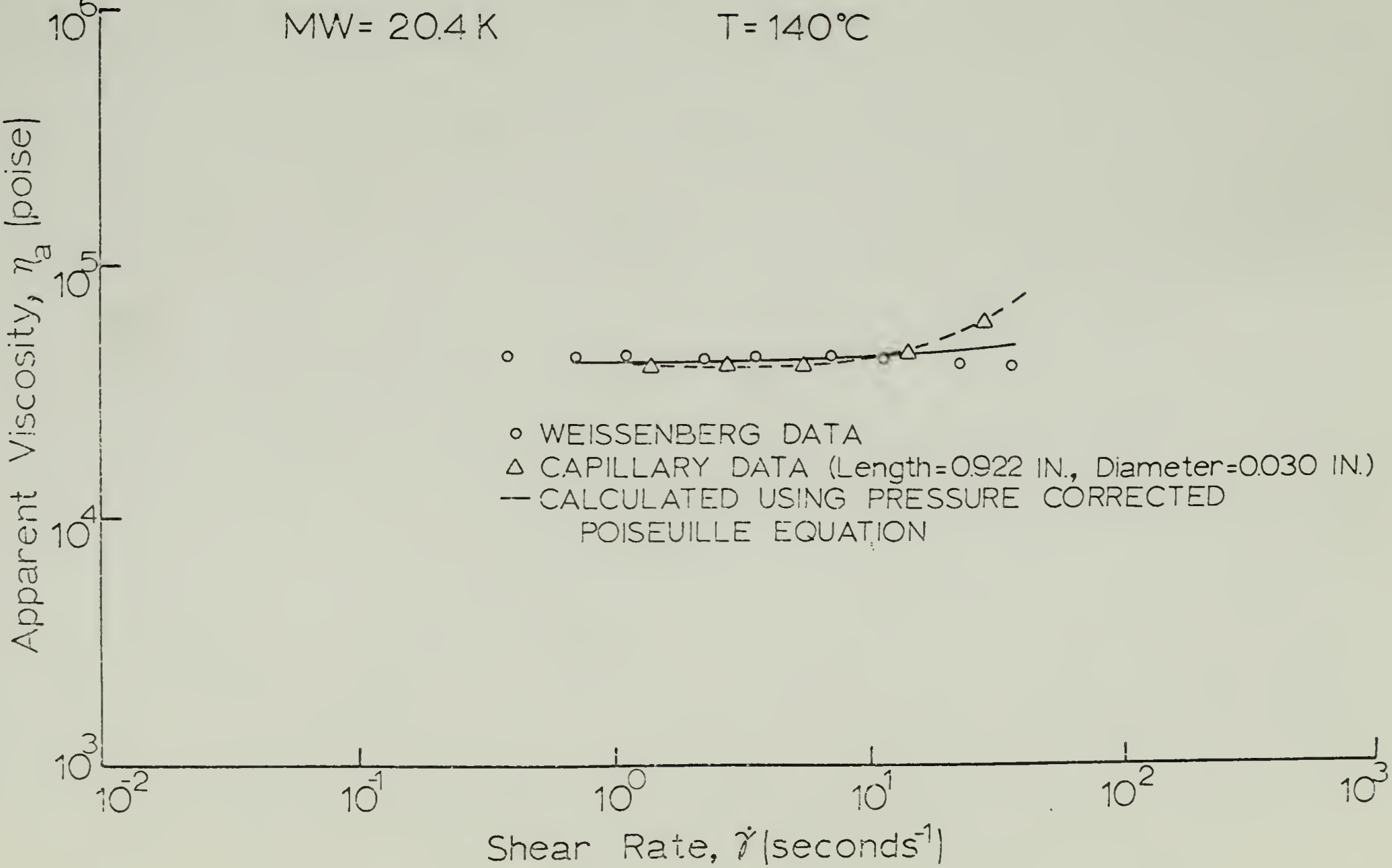

A COMPARISON OF CALCULATED CAPILLARY FLOW RATES FOR A POLYSTYRENE

MW = 20.4 K T = 140°C

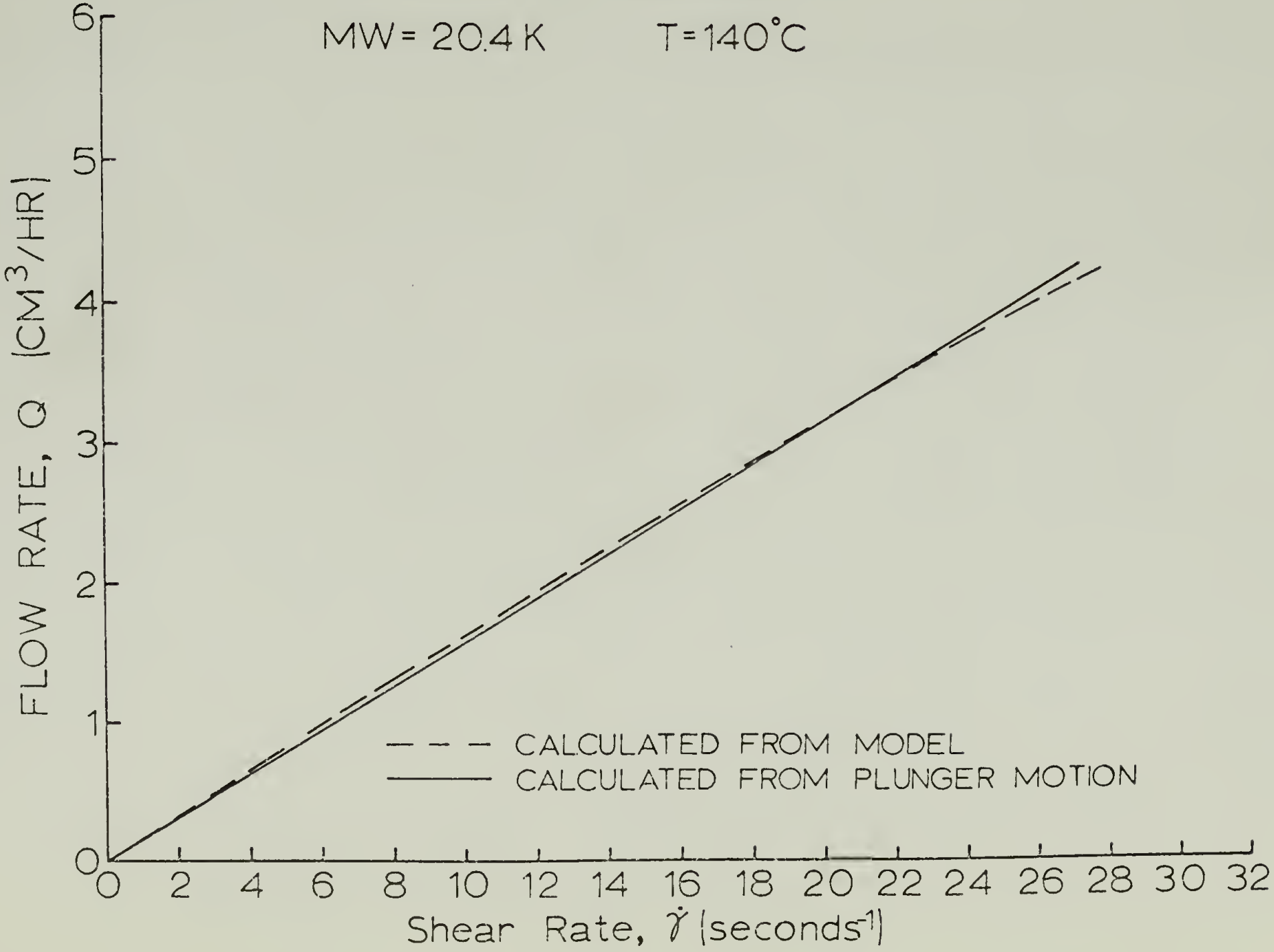

FIGURE III-6

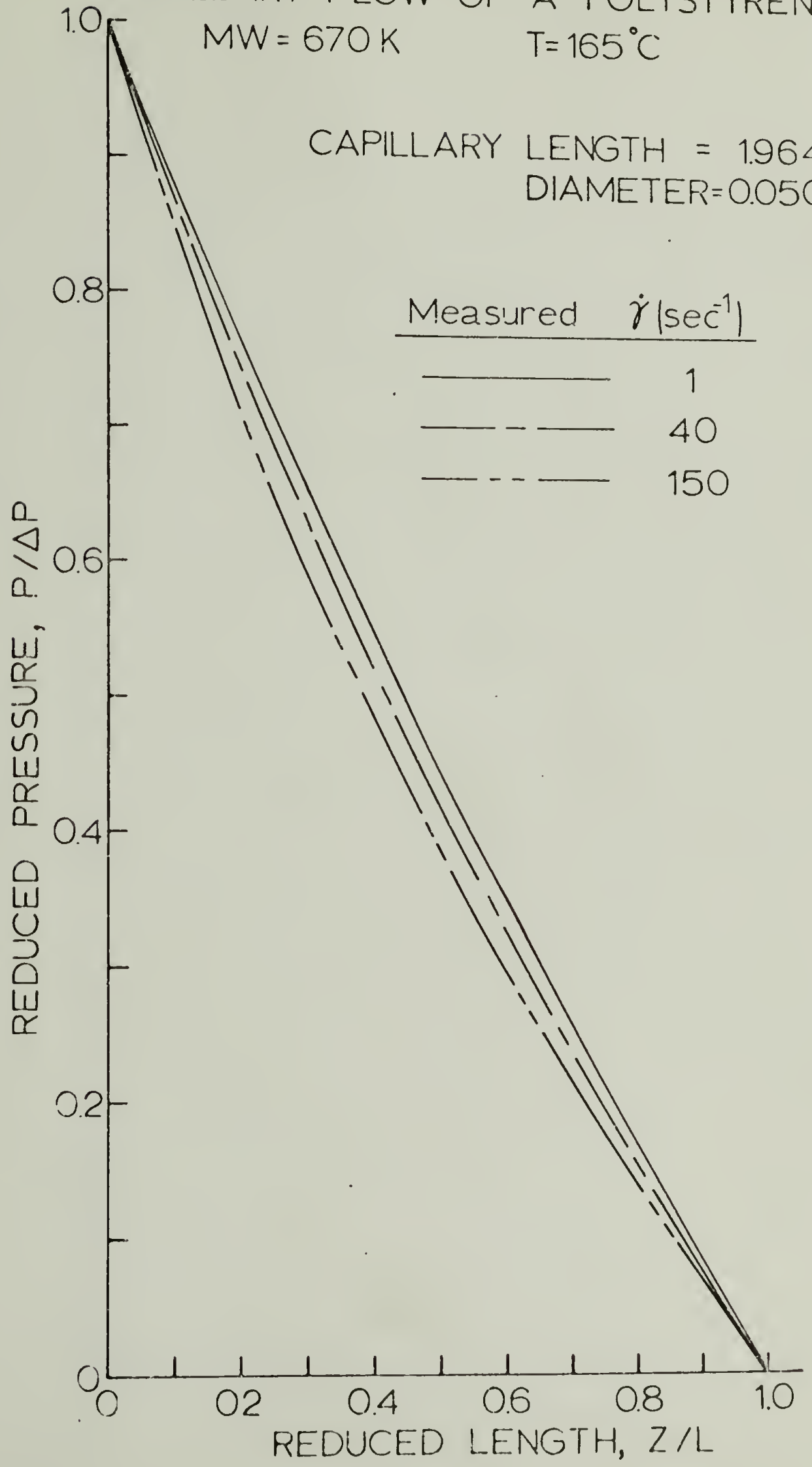
AXIAL PRESSURE DISTRIBUTION FOR THE CAPILLARY FLOW OF A POLYSTYRENE
MW = 670 K
T = 165 °C
CAPILLARY LENGTH = 1.964 IN.
DIAMETER = 0.050 IN.
Measured $\dot{\gamma}$ (sec^{-1})
1
40
150
REDUCED PRESSURE, P/ΔP
1.0
0.8
0.6
0.4
0.2
0
0
02
0.4
0.6
0.8
1.0
REDUCED LENGTH, Z/L

FIGURE III-7

AXIAL CHANGE IN VISCOSITY FOR THE CAPILLARY FLOW OF A POLYSTYRENE
MW=670 K T=165°C

CAPILLARY LENGTH = 1.964 IN.
DIAMETER=0.050 IN.

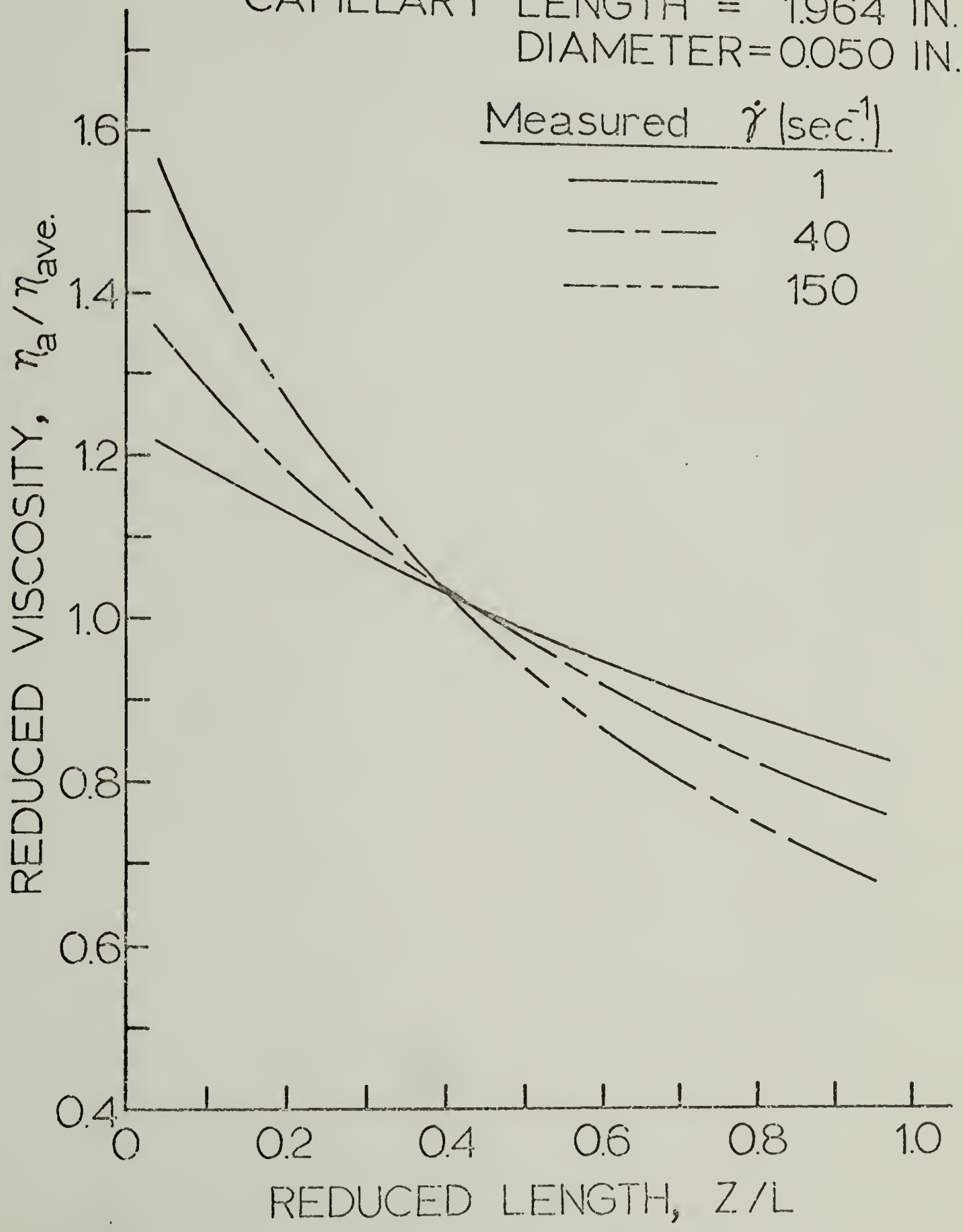

FIGURE III-8

CHAPTER IV

THE INFLUENCE OF PRESSURE IN THE CAPILLARY FLOW OF POLY(METHYL METHACRYLATE)

By

Antonio Casale*, Richard C. Penwell and Roger S. Porter
Polymer Science and Engineering
University of Massachusetts
Amherst, Massachusetts 01002

SYNOPSIS

Pressure effects in the capillary flow of a single sample of poly-(methyl methacrylate), M_v = 1.33 x 10^5, were evaluated. The length/diameter ratios of the different capillaries used varied from 4 to 100. The tests were made with an Instron rheometer in the range 160-250°C. The pressure-viscosity model, derived from the free volume-WLF equation, was used to pressure correct the capillary data. The corrected data agreed well with data obtained at atmospheric pressure using a Weissenberg rheogoniometer. A derived expression to calculate an increase in the flow activation energy with increasing stress predicts the observed increase in activation energy.

INTRODUCTION

Recently, several attempts have been made to account for the effect of pressure on the apparent viscosity in the capillary flow of amorphous polymers.[1-7] The phenomenon is generally observed as an increase in viscosity with increasing shear rate for Newtonian polymers and as a deviation from "power law" behavior for shear-thinning polymers.[1,8,9]

---

* On leave from Montecatini Edison, Milan, Italy.

A more prominent manifestation of the pressure effect on viscosity is the nonlinearity reported in plots of pressure versus capillary length/diameter ratio.[2,10,11] Such behavior has been previously analyzed for polystyrene based on the reduction of free volume available for flow and by the shifting of the glass transition temperature, T_g, with increasing pressure. The WLF equation, derived from the Doolittle free volume theory, was used to relate shifts in T_g to possible viscosity increases due to pressure.[1,2] (Chapters I and II).

The free volume-WLF equation has also been used to derive a viscosity-pressure model of general and simplified form.[3] The model has been combined with the momentum equation to derive general expressions for determining the pressure coefficient and the axial pressure and viscosity distributions for Newtonian and shear-thinning fluids.

Capillary data of poly(methyl methacrylate) (PMMA) indicates an additional and important case where pressure is significantly affecting the flow at relatively low melt temperatures.[11a] The pressure effect is analyzed using previously derived expressions for determining the pressure coefficient and axial pressure distribution (Chapter III). Capillaries of different dimensions were used at 180° and 190°C for the purpose of estimating the entrance losses before pressure correcting the data. Below 180°C the larger L/D capillaries cannot be used and above 190°C the magnitude of the pressure effect decreases rapidly, particularly for the smaller L/D capillaries.

The flow activation energy of PMMA was observed to increase with increasing stress in the uncorrected data. Using the viscosity-pressure

model and the Eyring activation energy equation, an expression was derived which predicts the increase in activation energy with increasing stress. Comparisons of the pressure corrected viscosity and the viscosity measured in a Weissenberg rheogoniometer are presented in the shear-thinning region.

EXPERIMENTAL

Studies were conducted on a single poly(methyl methacrylate) with an $M_v = 1.33 \times 10^5$. Tungsten carbide capillaries were used in an Instron rheometer, Instron Corporation, to investigate the effect of pressure on the apparent viscosity. The length to diameter (L/D) ratios of the capillaries varied from approximately 4 to 100. The temperature uncertainty along their lengths was estimated to be within 1°C.

The pressure effect on viscosity was analyzed at 180 and 190°C with data from several capillaries. Additional tests were made at temperatures ranging from 160 to 250°C, to illustrate the variation in onset and magnitude of the viscosity increase with pressure. Pressure losses in the sample reservoir above the capillary were negligible for all but the lowest L/D capillary. The kinetic energy correction was assumed to be negligible for the conditions of these tests.

Viscosity data at atmospheric pressure were also obtained in a Weissenberg rheogoniometer (Model No. 17) using a 5.0 centimeter diameter plate and a 2° angle cone. To minimize degradation, the samples were preformed and tested in a nitrogen atmosphere. The sample, nonetheless, degraded after prolonged periods of time as indicated by discoloration and nonreproducibility of the data. Several samples were used for short periods to minimize this problem.

RESULTS AND DISCUSSION

An increase in the glass transition temperature, T_g, with increasing pressure can be quantitatively related to viscosity through the WLF equation which has foundation in free-volume theory. Also, nonlinear plots of the pressure drop versus capillary length/diameter ratio can be linearized with this approach.[1-3] Capillary flow studies indicate that these same phenomenon occur for PMMA, particularly at the lower test temperatures. The effect of pressure on viscosity is illustrated by the uncorrected viscosity-shear stress curves in Figure 1. The curve shapes in the shear-thinning region change continuously with temperature. At the lowest temperatures, a definite upturn in the viscosity is indicated. In this region, the stress limits of the Instron rheometer are readily exceeded.

The pressure effect on the viscosity suggested in Figure 1 is better illustrated in Figure 2 where the pressure is plotted as a function of the length/diameter ratio for the several capillaries which were used. The curves become increasingly nonlinear as the temperature is decreased and the shear rate increased. Similar data at 190°C suggested a decrease in the pressure effect with increasing temperature (See Appendix D, Figure 1). An appreciable entrance loss is also indicated for all the shear rates in Figure 2.

Before considering the pressure effect on viscosity, the entrance losses must be estimated and applied to the capillary data. Figure 3 represents the corrected pressure data at 180°C. The entrance losses were determined by the best approximated linear portions of the curves shown in Figure 2. A similar procedure was used for the data at 190°C (See

Appendix D, Figure 2). The effect of pressure on the entrance losses is neglected. From the minimum scatter observed in the data of Figure 2, this assumption appears reasonable.

The behavior of the PMMA in Figures 1 and 2 indicates that pressure is influencing the flow in a manner similar to that discussed previously for polystyrene.[1-3] At equal shear rates, the increase in viscosity becomes quite noticeable as the temperature is decreased. Since the glass transition temperature of PMMA can be increased with the application of pressure,[12] the free volume approach for the calculation of viscosity changes appears valid. As with the polystyrene, this approach assumes the decrease in free volume at high pressures greatly reduces the mobility of the molecules, resulting in an appreciable deviation from power law behavior.

The variation in the WLF parameters, the thermal expansion and compressibility coefficients and the absence of other pertinent data for PMMA in the literature prohibits the application of the free volume-WLF equation used previously for polystyrene.[13-19] Also, the high pressures obtained in the tests of PMMA would be expected to result in nonlinear axial pressure distributions in the capillary[3,5,6]. The average pressure for the nonlinear distributions would deviate significantly from $\Delta P/2$. If unaccounted for, the variation in the average pressure with total pressure could cause significant error in the analysis.

The form of the WLF equation used to analyze the pressure dependence of viscosity has subsequently been reduced to a simple and widely used empirical pressure-viscosity model.[3] This model;

$$\eta = \eta_{atm.}\, e^{bP} \qquad \text{(IV-1)}$$

has also been shown to be derivable from the Eyring hole theory for viscosity[20] and has been applied in previous attempts to account for the pressure dependence of viscosity.[3-6] Recently, equation 1 was used to derive general expressions for determining the pressure coefficient, b, for the capillary flow of Newtonian and shear-thinning fluids.[3] Expressions for calculating the average pressure and axial pressure and viscosity distributions were also derived. Since the WLF equation does not consider shear-thinning characteristics, and the available data for PMMA is not adequate, the expressions derived elsewhere with equation 1 are applied in this analysis of the pressure effect on PMMA.

Expressing the pressure dependence of the glass transition by $T_g = T_{go} + A_1 P$ (IV-2) where T_{go} is the glass transition at atmospheric pressure, $A_1 = \partial T_g / \partial P$ and P is the pressure, the WLF equation has been reduced to equation 1.[3] Using the approximation necessary for this reduction of the WLF equation, an initial maximum error of 5% is introduced for PMMA.

The pressure coefficient is given in terms of the WLF parameters as $b = 2.303\ A_3/A_4$ where $A_3 = C_1 A_1$, $A_4 = C_2 + T - T_{go}$ and C_1, C_2 may be considered constants. The value of b is 4.24×10^{-3} using the following values for PMMA at 190°C: $T_{go} = 105°C$[13,15-17], $C_1 = 11.1$, $C_2 = 90.7$ and $A_1 = 0.023$.[12] The WLF parameters C_1 and C_2 were evaluated using the Weissenberg data by a procedure given elsewhere.[21] The value of b determined in this manner is considered only as an estimate.

The general procedure and curve for determining the pressure coefficient for shear-thinning fluids has been described elsewhere and is only briefly reconsidered here.[3] Using one capillary, the pressure

coefficient can be determined from the following relationship:

$$V_R^n = \frac{1 - e^{-b\Delta P_1}}{1 - e^{-Kb\Delta P_1}} \qquad \text{(IV-3)}$$

where V_R is the plunger velocity ratio V_{P1}/V_{P2}, n is the power law exponent, ΔP_1 is a reference pressure and K is equal to $\Delta P_2/\Delta P_1$. The pressure, ΔP_2, is that required for flow at a plunger speed V_{P2}. The power law exponent is obtained from atmospheric viscosity-shear rate data, conveniently obtained with a Weissenberg rheogoniometer or other suitable viscometer that operates without pressure. Equation 3 is presented graphically for PMMA in Figure 4. The values of K are the actual pressure ratios obtained at 180° and 190°C for a capillary 0.050 inches in diameter and 1.964 inches long. The reference pressure, ΔP_1, at each temperature is the pressure required for flow at the lowest shear rate. The velocity ratio, V_R, is known at any shear rate and the pressure coefficient b can be found. The variation of b with pressure can be determined by calculation at successively higher K values.

The axial pressure distribution can be calculated using the expression[3]

$$p = \ln \frac{[e^{-b\Delta P} + (1 - e^{-b\Delta P})\ z/L]}{-b} \qquad \text{(IV-4)}$$

By numerical integration of the p - z curve, the average pressure as a function of the total pressure can be determined. The data in Figure 5 illustrate the decrease in the average pressure with the total pressure drop at 180° and 190°C. For the high pressures obtained in these tests, serious error would result if this decrease in the average pressure were

not considered. At low pressures, the average pressure approaches the incompressible limit, $\Delta P/2$.

The magnitude of the pressure effect at 180°C for various capillaries is shown in Figure 6. The Weissenberg data, taken at atmospheric pressure, is used as a reference for comparison of the corrected viscosity data. As the length/diameter (L/D) ratio of the capillary is increased, the stress to maintain the same shear rate in the power law region deviates significantly from the viscosity-shear rate behavior at atmospheric pressure. The power law exponent is also observed to decrease with increasing L/D ratio. Similar results were obtained at 190°C (See Appendix D, Figure 3).

With equations 1, 3 and 4, the data in Figure 6 can be pressure corrected. The graphical representation of equation 3, given in Figure 4, is used to determine b. Average values of 2.07×10^{-3} and 4.26×10^{-3} $bars^{-1}$ were calculated at 180° and 190°C respectively. These values represent the average of the higher pressure ranges and since b is slightly pressure dependent are inaccurate for the two lowest L/D capillaries used. With the known pressure coefficients, the average pressures at each shear rate are found from equation 4. The pressure corrected viscosity, $\eta_{atm.}$ is calculated from equation 1.

This pressure correcting procedure applied to the data of Figure 6 and also to the data at 190°C gives the results shown in Figure 7. Since the procedure is applicable to the power law region, the greatest deviation of calculated and experimental data occurs at 1 $second^{-1}$, where the experimental data approaches the Newtonian region and are outside the power law correlation. The assumption of a constant pressure coefficient

over the entire pressure range results in a consistent error in the data. A comparison of Figures 6 and 7, however, indicates that the method for pressure correcting the capillary data is appropriate and reliable.

The successively higher levels of stress required at equal shear rates for capillaries of increasing L/D ratio are explained by the observed pressure dependence of viscosity. Therefore, if an Arrhenius plot is made at the various stress levels, the slope of the linear plots might be expected to vary. Considering the Eyring activation energy equation $\eta = Ae^{E^*/RT}$ (IV-5), this implies the flow activation energy, E^*, is some function of pressure.

Importantly, Arrhenius plots of data similar to Figure 1 for a capillary 0.030 inches in diameter and 3.00 inches long indicate that the activation energy increases with increasing pressure. Combining equations 1 and 5 gives,

$$\eta_{atm.} e^{bP} = Ae^{E^*/RT}. \qquad \text{(IV-6)}$$

Rearranging equation 6 to solve for the activation energy and using $\tau = \frac{\Delta PD}{4L}$ results in

$$E^* = 2.303\ RT\ \log\ (\eta_{atm}/A) + \frac{RTb4\tau L}{D} \qquad \text{(IV-7)}$$

where R is the gas constant, T is the temperature, η_{atm} is the apparent viscosity at atmospheric pressure, b is the pressure coefficient, τ is the stress and L and D are the length and diameter of the capillary.

The parameters T, τ, L and D are known. The apparent viscosity, η_{atm}, is obtained from the Weissenberg data. The pre-exponential factor A is known as a $f(\tau)$ from Arrhenius plots of the experimental capillary data. The pressure coefficient can also be determined at any stress from the curves of Figure 4.

The variation in the activation energy with increasing stress or pressure can now be calculated using equation 7. The resulting curve is compared with the activation energies determined from Arrhenius plots in Figure 8. With the excellent agreement of the calculated and experimental activation energies, the pressure dependence of the viscosity and the activation energy are well described by equations 1 and 7.

REFERENCES

IV-1. R.C. Penwell and R.S. Porter, J. Appl. Poly. Sci., 13, 2427 (1969).

IV-2. R.C. Penwell and R.S. Porter, accepted J. Poly. Sci.

IV-3. R.C. Penwell, R.S. Porter and S. Middleman, submitted for publication.

IV-4. I. Duvdevani and I. Klein, SPE-J., 23, 41 (1967).

IV-5. Von E. Brenschede and J. Klein, Rheol. Acta, 8, 71 (1969).

IV-6. U. Semjanow, Rheol. Acta., 4, 133 (1965).

IV-7. J.D. Ferry and R.A. Stratton, Kolloid-Z., 171, 107 (1960).

IV-8. R.L. Ballman, Nature, 202, 288 (1964).

IV-9. A.K. Van der Vegt and P.P.A. Smit, S.C.I. Monograph No. 26, 313 (1967).

IV-10. G.A. Toelke, C.G. Gogos and J.A. Biesenberger, SPE 13th Antec, 98 (1967).

IV-11. D.P. Thomas and R.S. Hagan, Poly. Engr. Sci., 9, 164 (1969).

IV-11a. G. Pezzin, SPE Trans. 3, 260 (1963).

IV-12. A. Miyake and M. Takakibara, Repts. Prog. in Poly. Phys. (Japan), 6, 93 (1963).

IV-13. S. Loshaek, J. Poly. Sci., 15, 391 (1955).

IV-14. T.G. Fox and S. Loshaek, J. Poly. Sci., 15, 371 (1955).

IV-15. L.A. Wood, J. Poly. Sci., 28, 319 (1958).

IV-16. R. Simha and R. Boyer, J. Chem. Phys., 37, 1003 (1962).

IV-17. S.S. Roger and L. Mandelkern, J. Phys. Chem., 61, 985 (1957).

IV-18. G. Gee, Polymer 7, 177 (1966).

IV-19. S. Onogi, T. Masuda and T. Ibaragi, Kolloid-Z., 2, 110 (1968).

IV-20. N. Hirai and H. Eyring, J. Poly. Sci., 37, 51 (1959).

IV-21. J.D. Ferry, Viscoelastic Properties of Polymers, pg. 212, Wiley and Sons, Inc., 1961.

CAPTIONS FOR FIGURES

IV-1. Pressure effect on the viscosity in the capillary flow of poly(methyl methacrylate) (PMMA) in the range 160 - 250°C.

IV-2. Pressure versus the L/D ratio of several capillaries at several shear rates at 180°C.

IV-3. End correction applied to the data of Figure 2.

IV-4. Determination of the pressure coefficient for PMMA.

IV-5. Variation of the average capillary pressure with total pressure for PMMA at 180 and 190°C.

IV-6. Pressure effect on the apparent viscosity of PMMA at 180°C for several capillaries.

IV-7. Pressure corrected viscosity data at 180 and 190°C for several capillaries.

IV-8. Pressure effect on the activation energy of PMMA.

PRESSURE EFFECT ON THE CAPILLARY FLOW OF POLY (METHYLMETHACRYLATE)

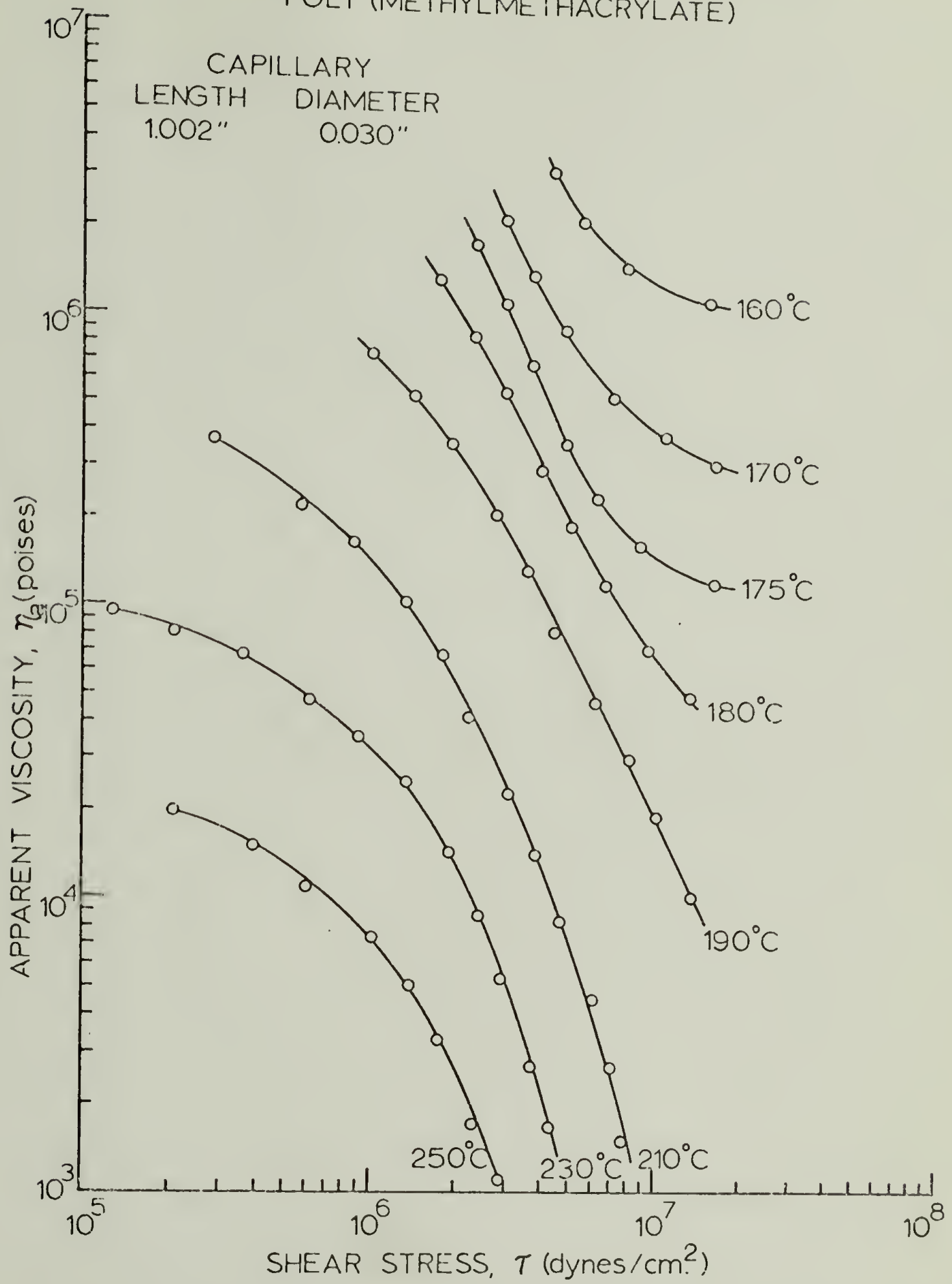

FIGURE IV--1

CAPILLARY FLOW OF POLY(METHYL-METHACRYLATE). PRESSURES REQUIRED AT DIFFERENT SHEAR RATES

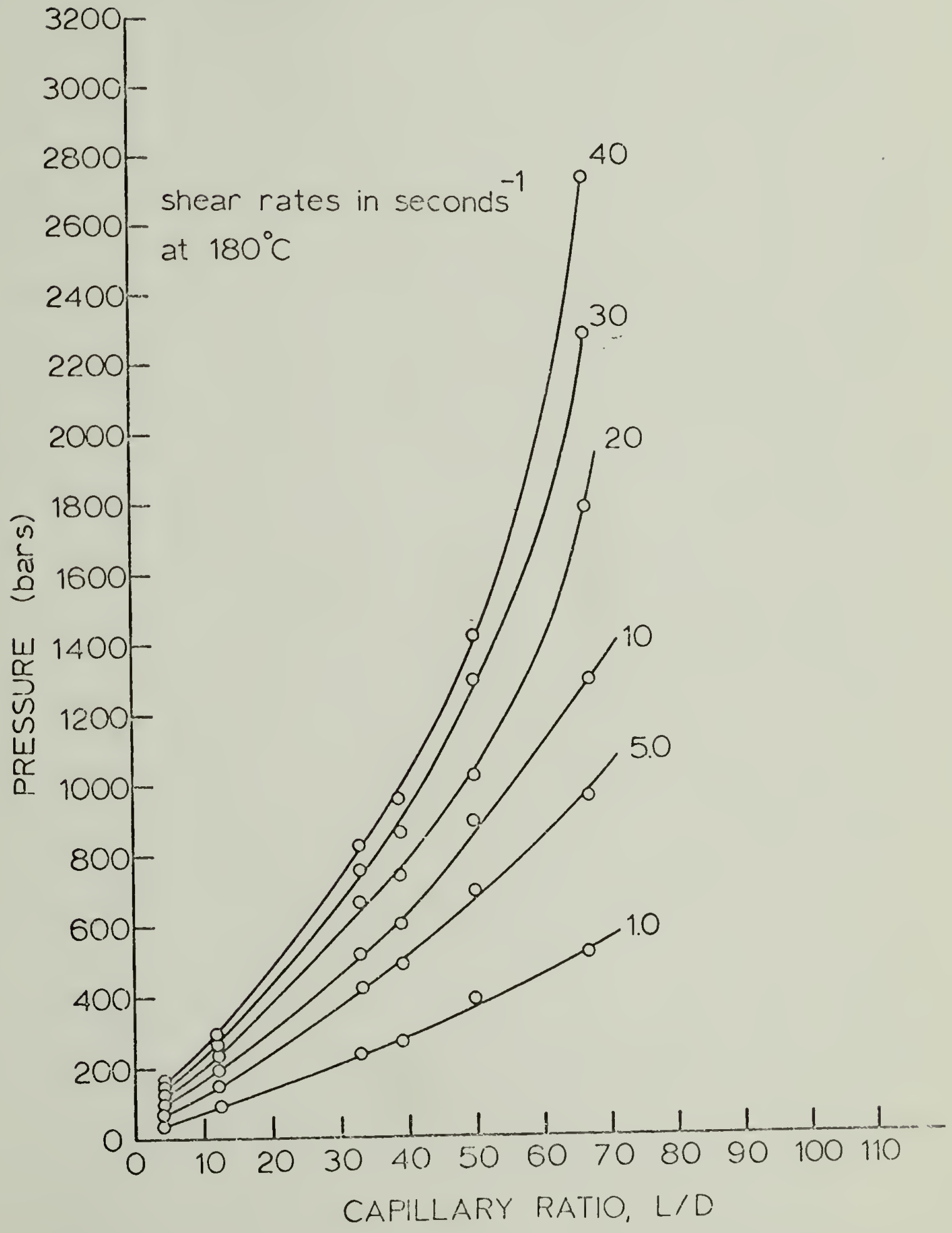

FIGURE IV-2

END-CORRECTED PRESSURE VERSUS CAPILLARY RATIO FOR POLY(METHYLMETHACRYLATE)

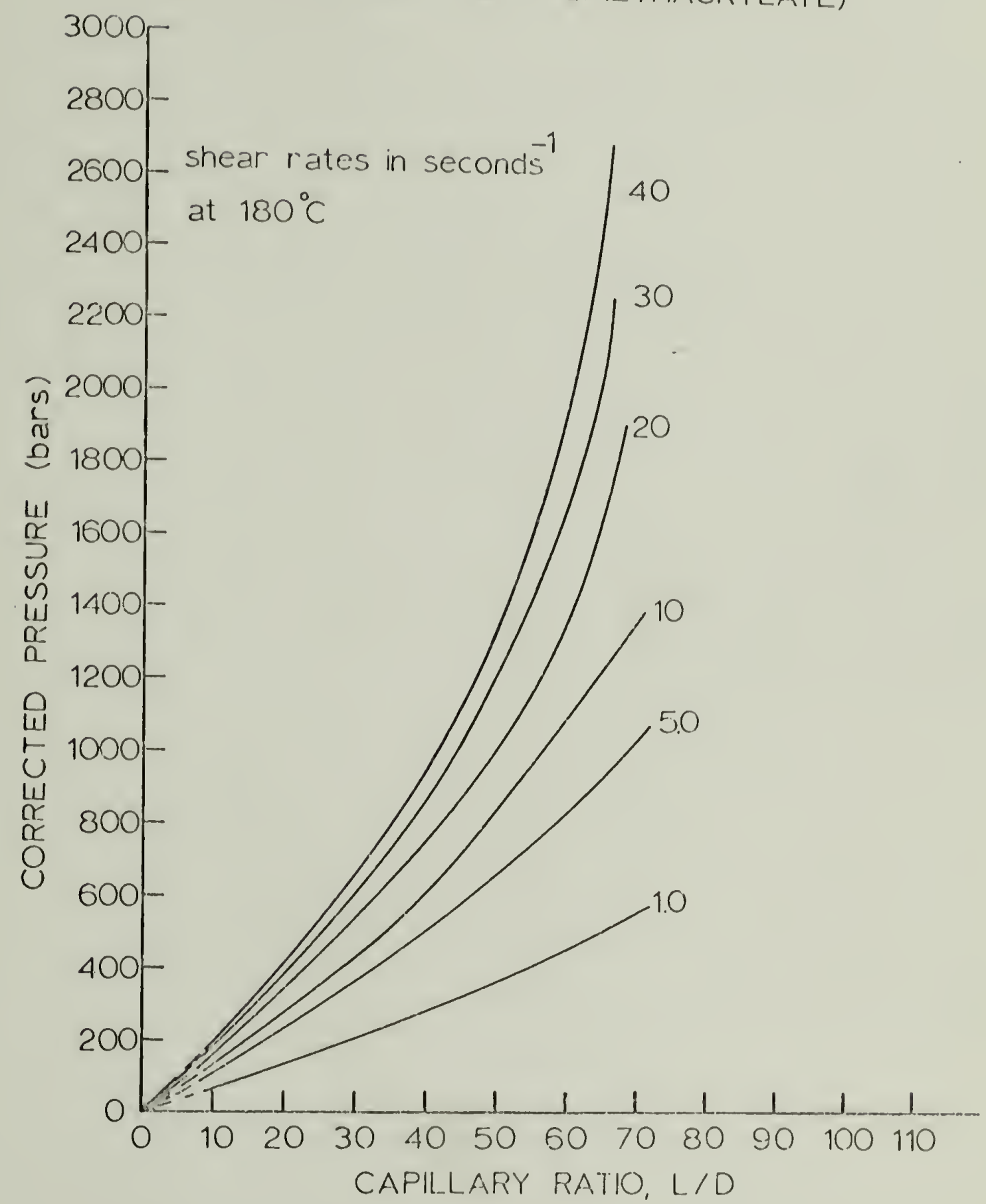

FIGURE IV-3

DETERMINATION OF THE PRESSURE COEFFICIENT FOR POLY(METHYLMETHACRYLATE)

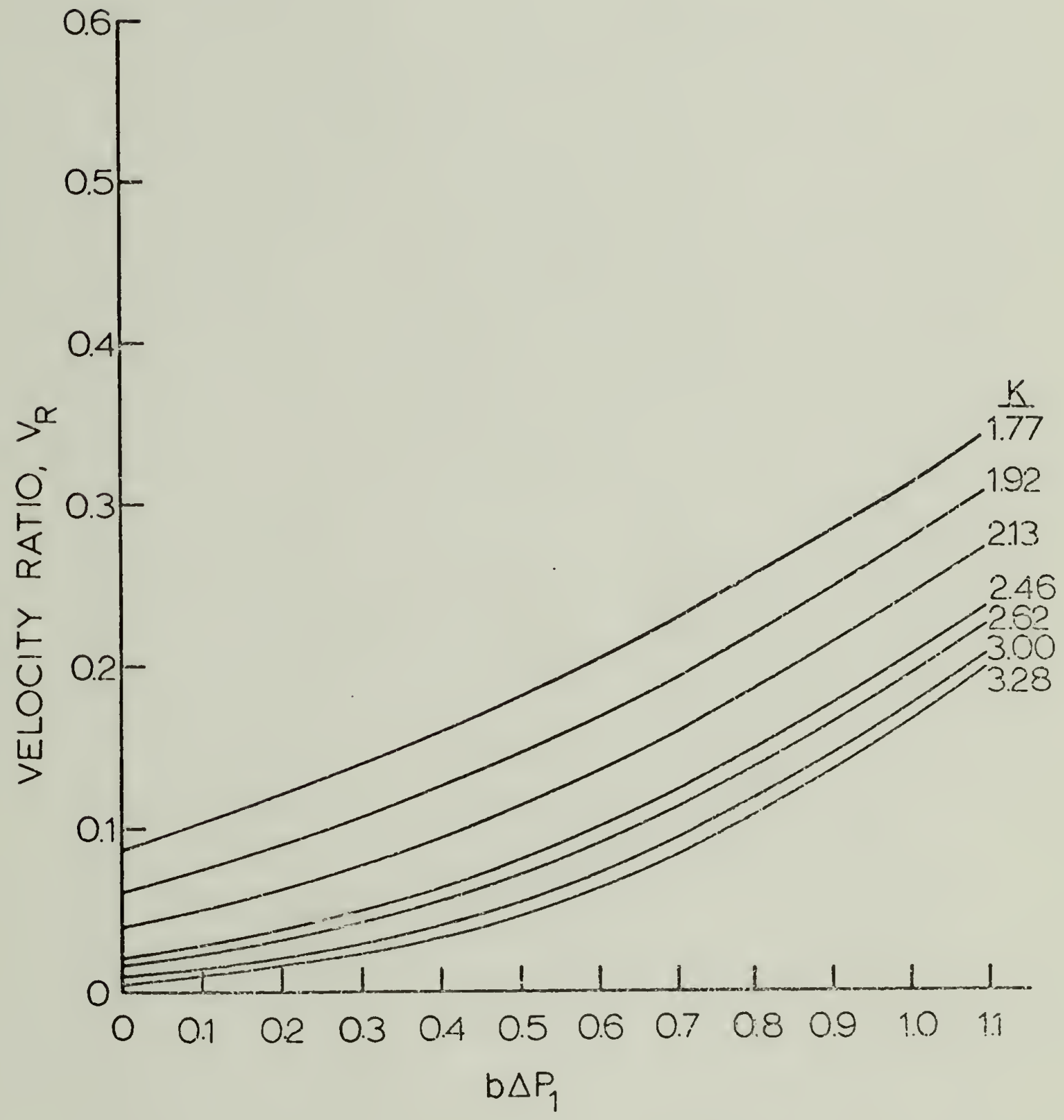

FIGURE IV-4

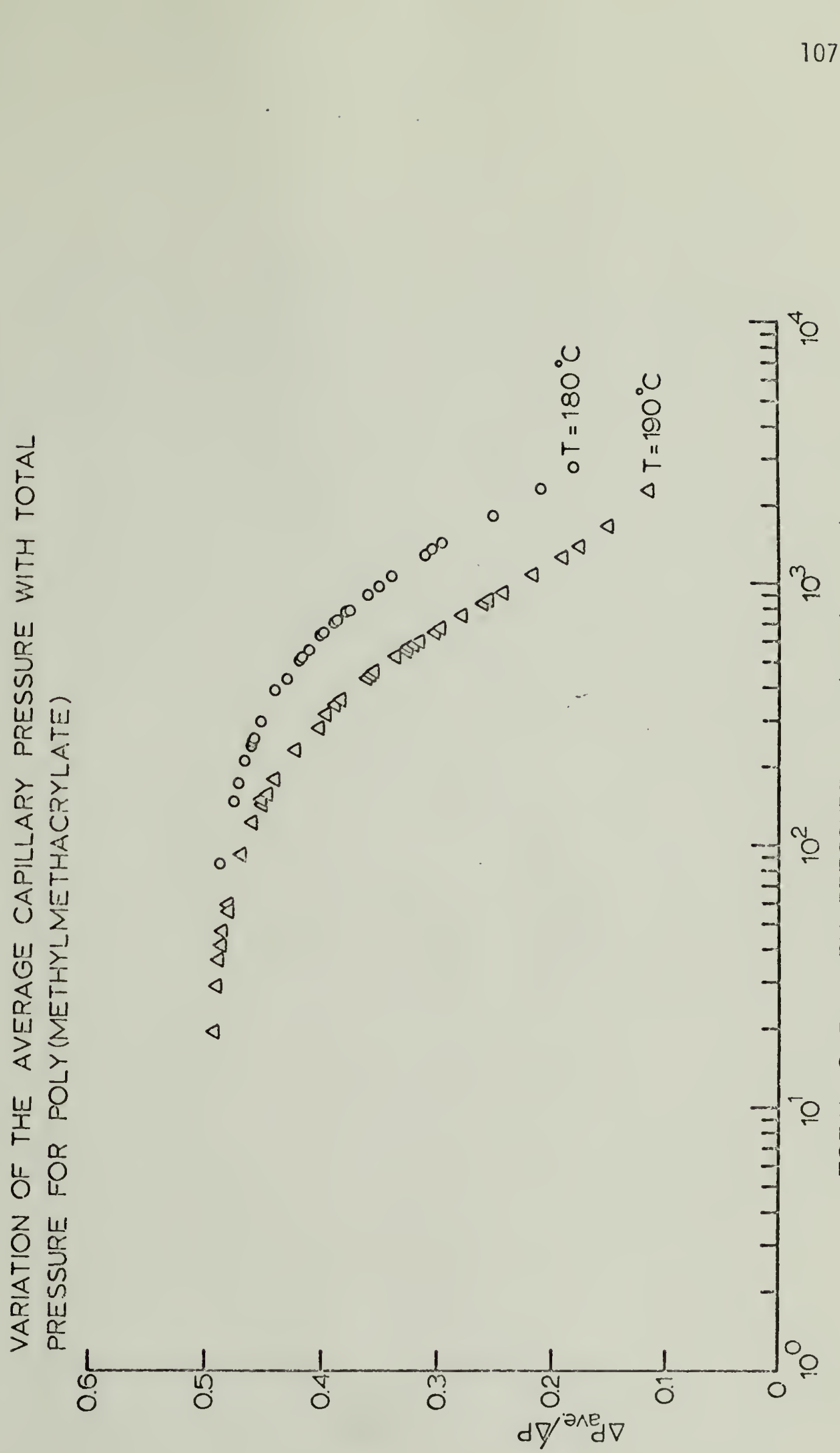
VARIATION OF THE AVERAGE CAPILLARY PRESSURE WITH TOTAL PRESSURE FOR POLY(METHYLMETHACRYLATE)
o T = 180°C
Δ T = 190°C
$\Delta P_{ave.}/\Delta P$
0.6
0.5
0.4
0.3
0.2
0.1
0
10^0
10^1
10^2
10^3
10^4
TOTAL CAPILLARY PRESSURE, ΔP (bars)

FIGURE IV-5

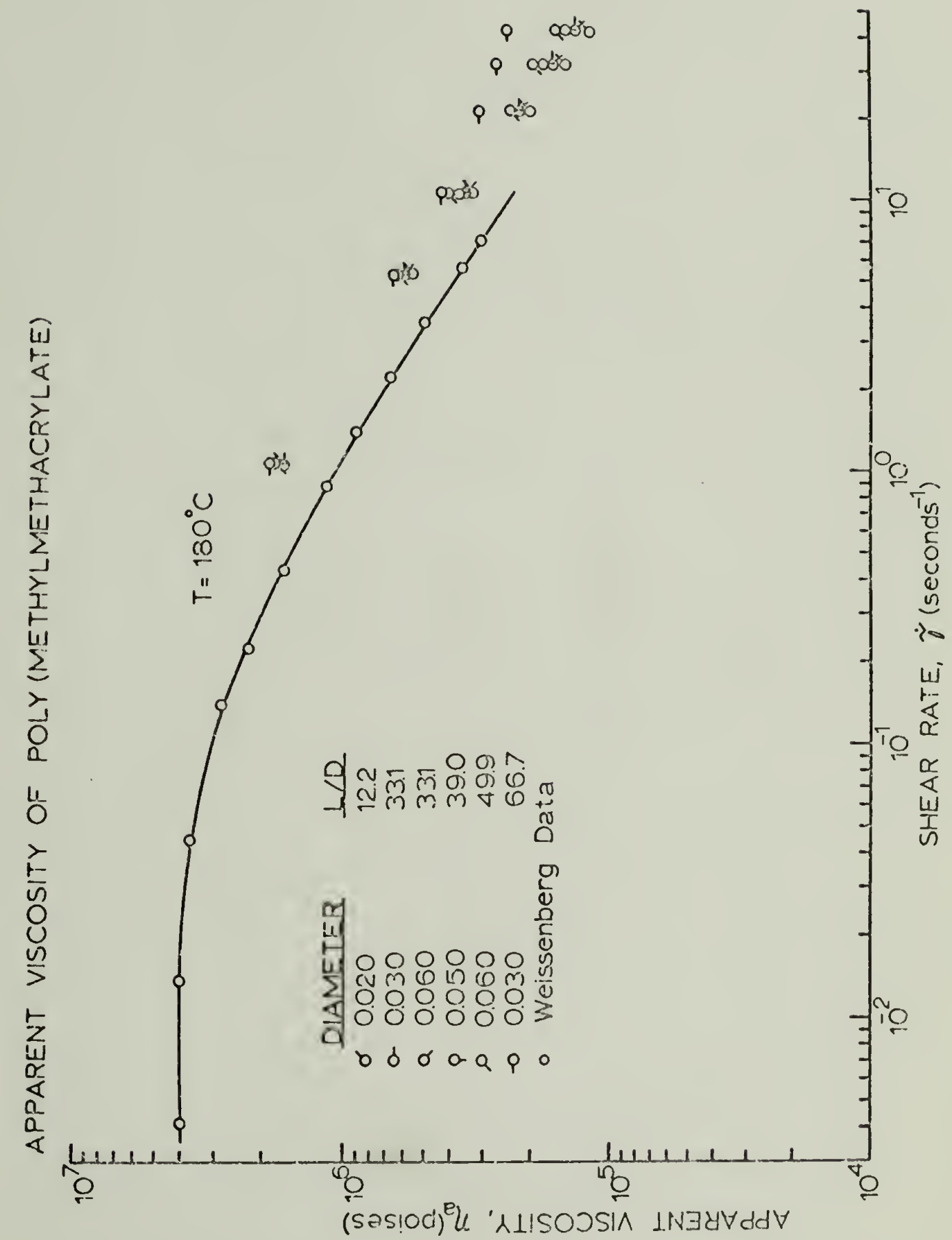
APPARENT VISCOSITY OF POLY (METHYLMETHACRYLATE)
T = 180°C
DIAMETER L/D
0.020 12.2
0.030 33.1
0.060 33.1
0.050 39.0
0.060 49.9
0.030 66.7
Weissenberg Data
APPARENT VISCOSITY, η_a (poises)
SHEAR RATE, $\dot{\gamma}$ (seconds^{-1})
10^7
10^6
10^5
10^4
10^{-2}
10^{-1}
10^0
10^1

FIGURE IV-6

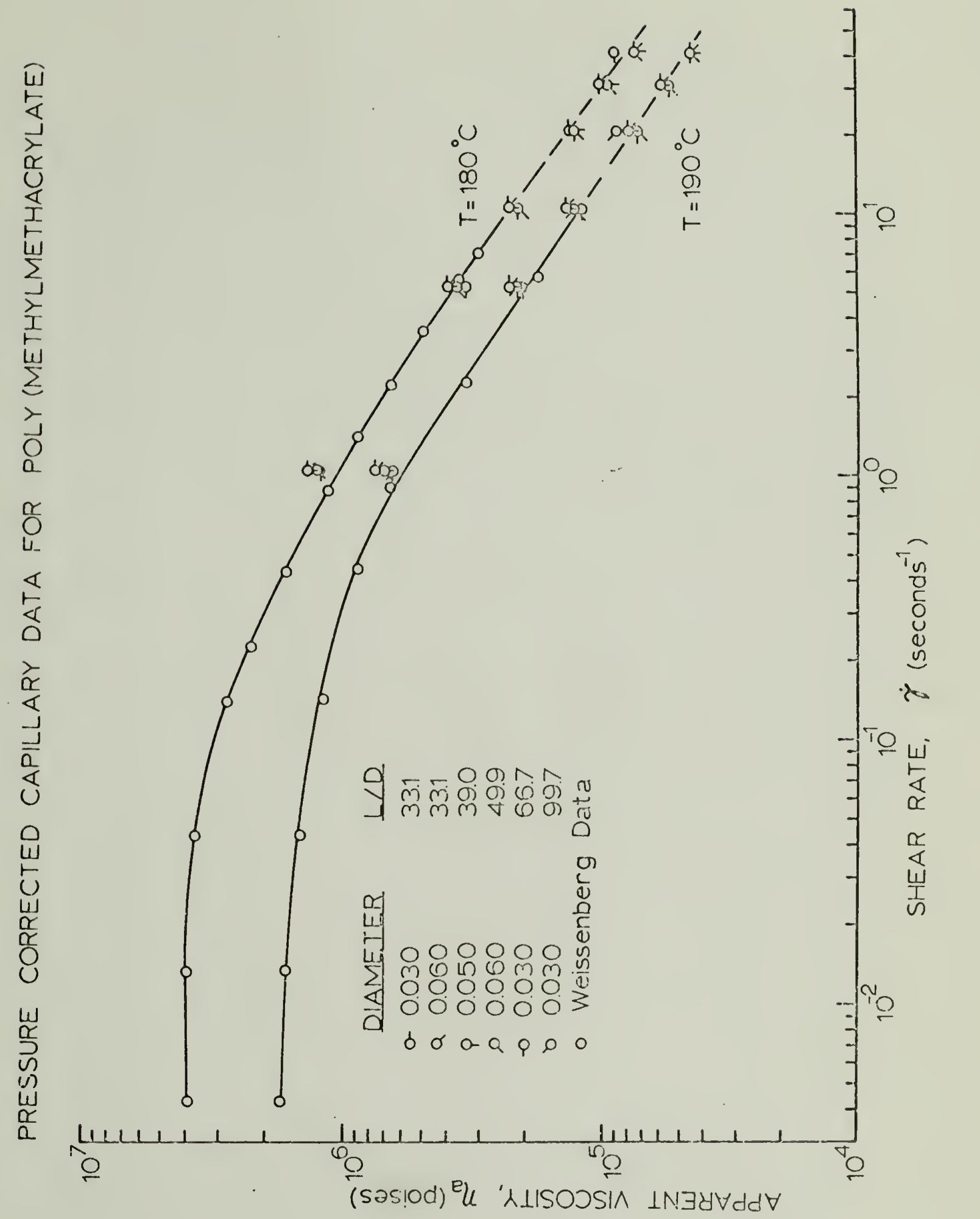
PRESSURE CORRECTED CAPILLARY DATA FOR POLY (METHYLMETHACRYLATE)
T=180°C
T=190°C
DIAMETER L/D
0.030 33.1
0.060 33.1
0.050 39.0
0.060 49.9
0.030 66.7
0.030 99.7
Weissenberg Data
APPARENT VISCOSITY, η_a (poises)
SHEAR RATE, $\dot{\gamma}$ (seconds^{-1})
10^7
10^6
10^5
10^4
10^{-2}
10^{-1}
10^0
10^1

FIGURE IV-7

PRESSURE EFFECT ON THE ACTIVATION ENERGY OF POLY(METHYLMETHACRYLATE)

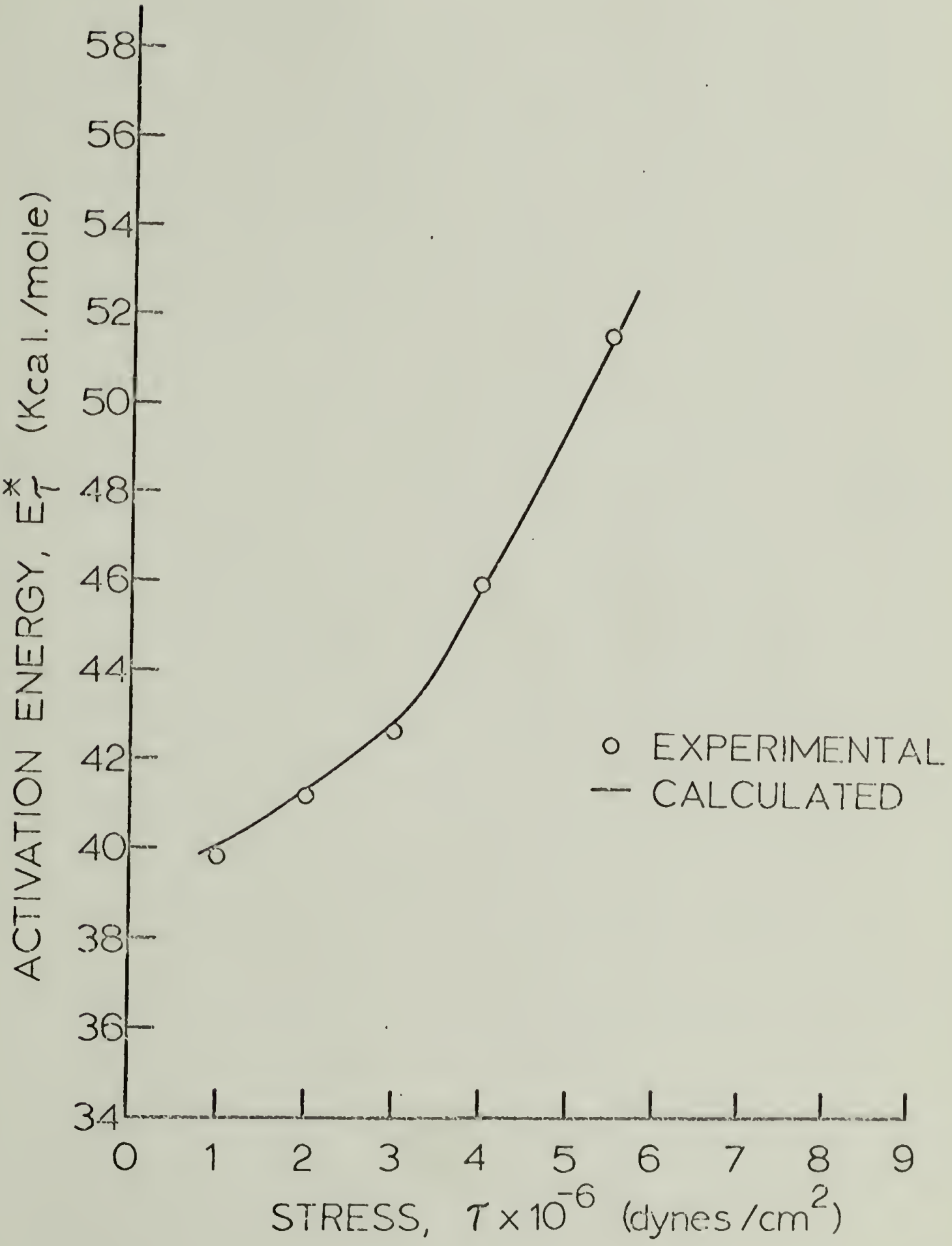

FIGURE IV-8

CHAPTER V

CONSIDERATIONS FOR FUTURE STUDY

INTRODUCTION

This chapter contains possible future studies arising from the work done and discussions involved with this thesis. In some cases, a brief review of the previous work and initial references precede the suggestions for future work.

DISCUSSION

Polycarbonate

In Chapter 4, the knowledge of the pressure effects in capillary flow gained in Chapters I-III was applied to the capillary data of another widely used amorphous polymer, poly(methyl methacrylate). One important consequence of that work was the explanation of the apparent viscosity increase in activation energy with increasing stress. Polycarbonate (PC) is another commercial amorphous material whose capillary flow might be affected by pressure over an experimentally measureable region. It would then be of interest to analyze any pressure dependence by either of the procedures described in Chapters II and III.

Preliminary apparent viscosity measurements were made on a PC of bisphenol-A, lot number J-168 (grade 141), obtained from General Electric, Pittsfield, Massachusetts. An Instron capillary rheometer was used with a tungsten carbide capillary 0.030 inches in diameter and 0.922 inches long to obtain data in the range 245-270°C. To obtain reproducible data and to

avoid bubble formation during extrusion, especially at temperatures greater than 270°C, the samples should be dried very well.

From Figure 1, there is a definite indication that pressure is affecting the flow of PC. At the two lowest test temperatures, a definite upturn in the apparent viscosity with increasing shear rate is indicated. The dashed points and curves represent estimates since the capacity of the Instron rheometer was rapidly exceeded. It would be particularly interesting to investigate the flow in the range of 245°C as the PC appears to be in the Newtonian region. As described in Chapter II, the WLF pressure-viscosity model can be applied in the Newtonian region.

O'Reilly, Karasz and Bair have made dielectric, mechanical and volumetric measurements to detect the transitions in PC.[1] A glass transition, T_g, of 142°C and an initial crystalline melting point of 227°C were determined. They further state PC is very difficult to crystallize and that it can be accomplished only by solvent treatment. No trace of crystallization was found on slow cooling from the melt.[1] Warfield found a T_g of 140°C and a P_g of 1200 atmospheres at 193°C in his compressibility studies of PC[2]. P_g is the pressure required to induce the glass transition at any given temperature. Ishida and Matsuoka used dielectric measurements to detect a T_g of 150°C[3]. They also present data on the thermal expansion coefficient and compressibility of PC. O'Reilly has reported a T_g of 143°C for PC in addition to thermal expansion data and a $\partial T_g/\partial P$ value of 0.044[4]. Baumann and Steingiser, in their rheological measurements on PC, indicate a critical entanglement molecular weight less than 13,000 and a flow activation energy of 26-30 k cal/mole at low shear rates in the range of 260-316°C. The activation energy calculated from an Arrhenius plot of the

Newtonian viscosities of Figure 1 was 26 k cal/mole.

Davis has made a thermal and oxidative degradation study of PC.[6] Using TGA, he reported an appreciable weight loss for PC at approximately 350°C. Davis and Golden, in their review paper on PC, found that M_v decreases very little below 300°C.[7] No appreciable degradation should therefore occur near 240°C.

From the preliminary results of Figure 1 and other relevant data available in the literature, it appears feasible to further investigate the pressure effects on the capillary flow of PC.

Measurement of P_g

P_g is defined as the pressure necessary to induce the glass transition at any test temperature. If the P_g - T relations were known for the amorphous polymers studied in Chapters I-IV, the WLF and mathematical models used to describe the pressure-viscosity relations could be tested for use near the glass transition temperature. Also, by experimentally knowing the volume and pressure needed to induce the glass transition, calculations such as presented in Table II-II could be verified. This is essentially a check on the use of the Tait equation to calculate the volume as a function of the pressure at a given temperature. It might be possible to evaluate the Tait equation constants by an iterative technique for amorphous systems heretofore uninvestigated. Knowing the pressure necessary to induce the glass transition at any test temperature would also aid in selecting proper operating temperatures to observe the desired behavior within the limits of the test equipment.

The Instron capillary rheometer can be used for qualitative and possibly quantitative determinations of P_g. By inserting a plug in the

rheometer and using the load cycling system, a P-V curve can be obtained at any temperature. Within the proper temperature range, P_g should be observed as a sudden change in the slope of the P-V curve. The accuracy of the experiment will depend, in part, on the absence or presence of air in the sample in addition to any leakage which might occur.

Measurement of the Pressure Effect in the Low Shear Rate, Newtonian Region of Shear-Thinning Fluids

For the high molecular weight polystyrene and poly(methyl methacrylate) samples studied in Chapters I-IV, it was not possible to obtain data in the low shear rate, Newtonian region. Data in this region would complete the study of the pressure effect on the flow of shear-thinning polymers. More importantly, any effect of pressure on viscosity in the onset region of shear-thinning should be obvious by comparison of the capillary data with Weissenberg rheogoniometer data.

The Instron rheometer could be used to conduct such a study by the use of two capillaries in series. The first capillary would be large enough in diameter to give relatively small shear rates. The second capillary would be of smaller diameter and would create sufficient back pressure on the exit side of the first capillary to see an appreciable effect of pressure on viscosity. For steady state condition, this is equivalent to applying a hydrostatic pressure to the first capillary, comparable to the operation of a Westover rheometer. The advantages in using two capillaries of different diameters to increase the pressure in the first capillary are that it can be done on existing equipment and that it is a continuous extrusion experiment.

Effect of Pressure on the Viscosity of Polymer Solutions

The use of polymer solutions to study the effect of pressure on viscosity would be an interesting area for further investigation as it might provide additional insight concerning the interdependence of concentration, free volume and their effect on the onset of shear-thinning in high molecular weight systems. Any observation of the pressure dependence of the onset of shear-thinning detected in bulk flow by the method given prior to this section could be further analyzed by solution studies.

Miller's work on the compressibility of alkanes and other liquids indicates they are more compressible than polymers by approximately a factor of ten.[8] If this is generally the case, then any pressure dependence of the polymer might be insignificant when compared to its solvent. However, the compressibilities might easily be separable, particularly if the polymer or solvent undergoes or approaches a first or second order transition. Matheson has studied the role of free volume in the pressure dependence of the viscosity of liquids.[9] Kuss determined the pressure coefficients of viscosity for several hydrocarbons using a high pressure falling ball viscometer.[10] Hogenboom, Webb and Dixon have also measured the viscosity as a function of temperature, pressure and free volume for several liquid hydrocarbons and have calculated the respective Tait equation constants.[11] The works of Cutler and Rossini, et al may be referred to for other possible pertinent solvent properties.[12]

Initial systems which might be considered are ethyl acetate and polystyrene and ethyl acetate and poly(methyl methacrylate). Miller presents compressibility and free volume data for the solvent, ethyl acetate.[8]

Possible Solution for Isothermal, Compressible, Newtonian Flow at High Pressures

The pressure-viscosity model, $\eta = \eta_o e^{bP}$, would be expected to fail at high pressures based on the assumptions made in its derivation from the WLF-free volume model (Chapter III). The WLF expression could be used at higher pressures and therefore its solution with the momentum equation is of interest.

Using equations III-3 and III-9,

$$\frac{1}{\eta_g}\partial P e^{-2.3\left[\frac{A_2 + A_3P}{A_4 - A_1P}\right]} = c\partial z \qquad \text{(V-1)}$$

Letting $x = \frac{A_2 + A_3P}{A_4 - A_1P}$ or $P = A_4 - \frac{A_1A_2 + A_3A_4}{A_1(A_3 + xA_1)}$ and $a = 2.303$, $\alpha = A_1A_2 + A_3A_4$, $\beta = A_1A_3$, $\gamma = A_1^2$, and $b' = \frac{\alpha\gamma}{\eta_g}$, equation 1 thus simplifies to:

$$b'\int_{x_o}^{x} \frac{e^{-ax}dx}{(\beta+\gamma x)^2} = c\int \partial z \qquad \text{(V-2)}$$

where $x_o = A_2/A_4$.

Integration of equation 33 by parts yields

$$-\left\{\frac{b'e^{-ax}}{\gamma(\beta+\gamma x)} + \frac{ab'e^{a\beta/\gamma}}{\gamma^2}\left[\ell n(\beta+\gamma x) - \frac{a}{\gamma}(\beta+\gamma x) + \left(-\frac{a}{\gamma}\right)^2\frac{(\beta+\gamma x)^2}{2!} + \left(-\frac{a}{\gamma}\right)^3\frac{(\beta+\gamma x)^3}{3\cdot 3!} + \ldots\right]\right\}\Bigg]_{x_o}^{x} = cz\Big]_L^z \qquad \text{(V-3)}$$

Equation 3 could be used to evaluate x and then P as a function of z. Additional work could be done to simplify equation 3 and in applying it to the experimental data.

Energy Considerations for a Viscoelastic Fluid

Bagley first suggested the possibility of applying an end correction to capillary flow data, based on the extrapolation of linear plots of pressure drop versus L/D ratios for several capillaries.[13] He defined the corrected shear stress as $\tau = \frac{\Delta P}{2(L/R+n)}$ (V-4), where n equals the extrapolated abscissa intercept in a ΔP versus L/D plot. Philippoff and Gaskins next suggested that perhaps the end correction could be subdivided into a Couette or entrance loss, and for viscoelastic fluids, also an elastic energy loss.[14] Neglecting kinetic energy effects, they defined the total pressure drop, P_T as;

$$P_T = P_C + (P_{11})_R \qquad \text{(V-5)}$$

where P_C is the pressure drop over the length of the capillary and $P_{11} = \tau S_R$. τ is the shear stress and S_R is the recoverable shear. The corrected shear stress now becomes

$$\tau = \frac{\Delta P R}{2(L+eR)} \qquad \text{(V-6)}$$

where $e = n + S_{R/2}$. Bagley, using Hooke's law in shear ($\tau = GS_R$), redefined the end correction as

$$e = \left(\frac{1}{2G}\right) \tau + n \qquad \text{(V-7)}$$

where G is the shear modulus and n is associated with the Couette losses in the entrance.[15] By plotting the total end correction versus the shear stress, it is possible to obtain n, G and S_R. Based on equation 5, the above procedure provides a means of determining the recoverable shear, S_R. The first normal stress difference can now be determined using

$$S_R = \tau_{11} - \tau_{22}/\tau_{12} \qquad \text{(V-8)}$$

Other attempts to account for the storage of elastic energy in capillary flow of viscoelastic fluids include measurements of the residual pressure and the swelling of the extrudate. Sakiadis has derived an expression relating the residual pressure at the exit of a capillary to the first and second normal stress differences when the tensile force is much smaller than the excess pressure drop associated with inlet effects.[16] Arai has also discussed the relationship of a residual pressure and extrudate swelling.[17] A problem in these considerations has been an accurate determination of the residual pressure.

Theories concerning the swelling of viscoelastic fluids emerging from a capillary have mainly been based on conservation of momentum or molecular rheology. Chapoy states, in fact, that the swelling of viscoelastic fluids can arise from a relaxation of the parabolic velocity distribution and/or a randomization of polymer molecules.[18]

Calculation of the axial stress by a momentum balance is initiated by calculating the thrust of the emerging jet as the difference between the flux of axial momentum leaving the tube and the axial stresses which exist in the fluid as it emerges.[19] Middleman has detailed the derivation to evaluate the first normal stress difference as a function of shear rate.[19] The results adequately describe the behavior of polymer solutions and first normal stress calculations have been in good agreement with those calculated from cone-plate measurements.

An equation equivalent to equation 8 given by Graessley to determine the first normal stress difference is

$$\tau_{11} - \tau_{22} = 2 J_0 \tau_{12}^2 \qquad (V\text{-}9)$$

where J_o is the steady state shear compliance.[20] Graessley has compared calculations of the first normal stress difference for polystyrene using expressions derived from a momentum balance and equation 9. The normal stresses calculated using the momentum balance were several decades lower than those predicted by equation 9. From a momentum balance, the calculation of the first normal stress difference depends on the decrease in velocity which arises from extrudate swelling. According to equation 9, $\tau_{11} - \tau_{22}$ is determined by τ_{12} at any radial position. As the viscosity is increased, comparable $\tau_{11} - \tau_{22}$ values are developed at lower velocities and the momentum becomes too small to predict the first normal stress difference.[20]

Because of the apparent failure of the momentum expressions to adequately describe extrudate swelling at higher viscosities, several attempts have been published in which the idea of randomization of the molecules has been used to explain extrudate swelling. Several conclusions and observations have been made by simply measuring the swell ratio of the extrudate.[20-23] The swelling of the extrudate has been found to increase with shear rate and decrease with longer residence times in the capillary.[21] Graessley, with measurements of a commercial polystyrene, found the swell ratio-shear stress relationship could be described by a single curve.[20] In a plot of swell ratio vs. stress, the swell ratio was independent of the shear rate and temperature.

Graessley,[20] in his analysis of die swell, considers the tensile stress, T, as given by

$$T = G_s[\alpha - \frac{1}{\alpha^2}] \qquad (V\text{-}10)$$

where G_s is the elastic shear modulus and α is $(D/D_o)^2$. He states that the

mean normal stress difference required to support this tension is

$$\langle \tau_{11} - \tau_{22} \rangle = \alpha T \qquad \text{(V-11)}$$

Combining equations 9, 10, and 11 gives

$$\alpha^2 - \frac{1}{\alpha} = 2J_o G_s \langle \tau_{12}^2 \rangle \qquad \text{(V-12)}$$

and

$$\langle \tau_{11} - \tau_{22} \rangle = G_s(\alpha^2 - \frac{1}{\alpha}) \qquad \text{(V-13)}$$

Equation 13 represents, then, a means of calculating the first normal stress difference based on the swelling of the extrudate.

The discussion to this point has briefly included several different methods of possibly calculating the first normal stress difference in capillary flow. A general verification of each of the methods and an intercomparison is lacking. In addition to this work, it would be interesting to compare calculations of the first normal stress difference to those calculated from an instrument such as the Weissenberg rheogoniometer. The equation commonly used is

$$\tau_{11} - \tau_{22} = 2F/\pi R^2 \qquad \text{(V-14)}$$

where F is the total measured force on a plate of radius R.[24]

Continued studies concerning the nature of and parameters affecting the elastic energy stored in a flowing viscoelastic fluid are necessary if it is to be taken into account in the equation of energy. In previous studies of classical fluids, all the energy is converted to heat. Graessley has suggested that the elastic energy per unit volume of a fluid element is[20]

$$e' = \frac{1}{2} J_o P_{12}^2 \qquad \text{(V-15)}$$

It would be an interesting study to evaluate the use of equation 15 and the energy equation to compare the results with a classical study of viscous

dissipation on the same system.

The Use of Liquid Crystals for Thermal Studies

A complex liquid crystal solution, obtained from the Vari-Light Corporation, undergoes visual color changes in the temperature range 27-31°C. Specifically, blue is said to appear at 31°C, green at 29.2°C, yellow at 27.6°C and red at 27°C. The solution, probably because it is a mixture, does not appear homogeneous when observed in an optical microscope with a reflecting light source.

The idea is to detect viscous heating in a mixture of the crystals and a fluid by the observation of variation in color of the liquid crystals. Because of the lack of homogeniety of the crystals and intensity of the colors, special equipment would probably be required to detect any color spectrum. It would be worthwhile to shear only the solution of crystals using a glass plate to visually observe the possibility of generating a color spectrum by viscous heating. The effects of shear on the crystals could be determined. The next step would be to blend it with a low molecular weight material to ascertain the effect of the matrix material on the liquid crystals and concentrations necessary to visually observe homogeneous color changes. This could be done in small quantities and if successful could also be studied with a glass plate-plate viscometer.

REFERENCES

V-1. J. O'Reilly, F. Karasz and H. Bair, J. Poly. Sci. 6C, 109 (1964).

V-2. R.W. Warfield, J. Appl. Chem., 17, 263 (1967).

V-3. Y. Ishida and S. Matsuoka, Poly. Prepr., 6(2), 795 (1965).

V-4. J. O'Reilly, J. Poly. Sci., 57, 429 (1962).

V-5. G. Baumann and S. Steingiser, J. Poly. Sci., Pt. A, 1, 3395 (1963).

V-6. A. Davis, Makro. Chemie, 132, 23 (1970).

V-7. A. Davis and J.H. Golden, J. Macromol. Sci., C3, 49 (1969).

V-8. A.A. Miller, J. Poly. Sci., A-2, 4, 415 (1966).

V-9. A.J. Matheson, J. Chem. Physics, 44, 695 (1966).

V-10. E. Kuss, Chem. Ingr. Tech., 37, (5), 465 (1965).

V-11. D. Hogenboom, W. Webb and J. Dixon, J. Chem. Phys., 46, 2586 (1967).

V-12. W. Cutler, R. McMickle, W. Webb and R. Schiessler, J. Chem. Phys., 29, 727 (1958).

V-13. E.B. Bagley, J. Appl. Physics, 28, 624 (1957).

V-14. W. Philippoff and F. Gaskins, Trans. Soc. Rheol., 2, 263 (1958).

V-15. E.B. Bagley, Trans. Soc. Rheol, 5, 355 (1961).

V-16. B.C. Sakiadis, A.I.Ch.E. J., 8, 317 (1962).

V-17. T. Arai, I. Suzuki and N. Akino, Proc. Fujihara Memorial Fac. of Engr., Keio Univ., Tokyo, Japan, 20, 39 (1967).

V-18. L. Chapoy, Rheol. Acta 8, 497 (1969).

V-19. S. Middleman, The Flow of High Polymers, Interscience (1968), pg. 42.

V-20. W. Graessley, S. Glasscock and R. Crawley, unpublished.

V-21. A.P. Metzger and J.D. Matlack, 13th SPE Antec, 389 (1967).

V-22. E.B. Bagley, J. Appl. Poly. Sci., 7, 1661 (1963).

V-23. C. McLuckie and M. Rogers, J. Appl. Poly. Sci., 13, 1049 (1969).

V-24. J. O'Reilly and W. Prest, Poly. Conf. on Rheol., Wayne State Univ., May (1966).

PRESSURE EFFECT ON THE CAPILLARY FLOW OF POLYCARBONATE

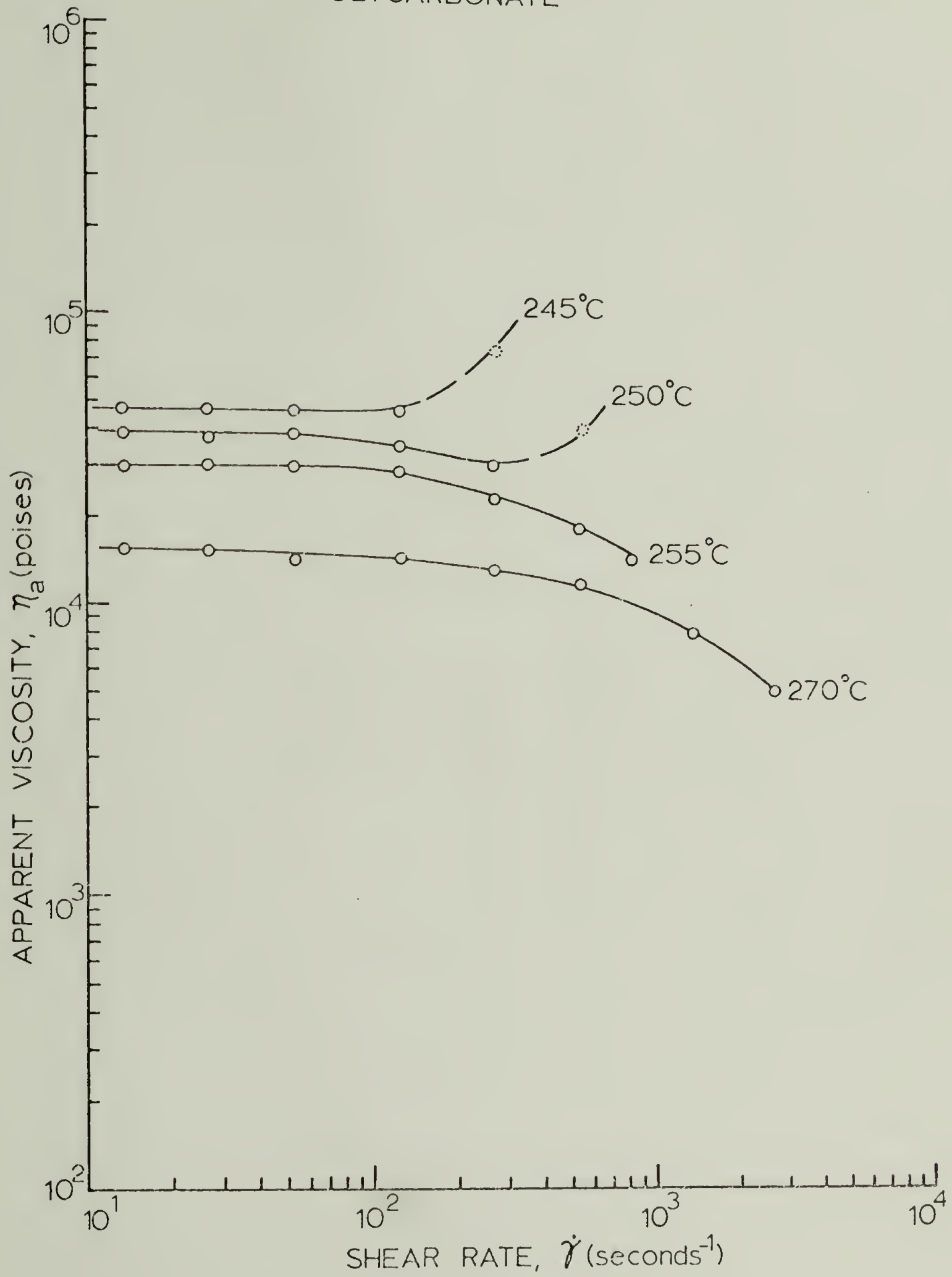

FIGURE V-1

APPENDIX A

The Figures in this appendix were not included in the original manuscript of Chapter I and are considered here only as a supplement. Figures 1-4 are referenced in Chapter I while Figures 5 and 6 are presented as complimentary information. The discussion of the Figures is limited to their brief description.

Figure 1 is a graphical representation of the shift in the dynamic glass transition with frequency for polystyrene. The data is from the work of Lewis[I-7]. Figures 2 and 3 are additional illustrations of the deviations in the calculated and experimental data of the dynamic viscosity versus frequency for a low and high molecular weight polystyrene. The curves represent the experimental data of J. O'Reilly and W. Prest. Figure 4 is the graphical relationship of the glass transition temperature, T_g, and the pressure as determined by Gee[I-12].

Figure 5 is an Arrhenius plot of a low molecular weight polystyrene. It is included to show the consistency of the experimental data and to illustrate the type of plot from which the activation energy for viscous flow is determined. The activation energy, E*, is equal to the slope of the log η_0 versus $\frac{1}{T}$ plot times 2.303 R, where R is the gas constant. Figure 6 illustrates the change in activation energy with reciprocal temperature for a polystyrene having a molecular weight of 20.4K. At higher temperatures, the activation energy approaches the limit of 23 k cal/mole. It steadily increases to greater than 70 k cal/mole as the temperature decreases to 120°C.

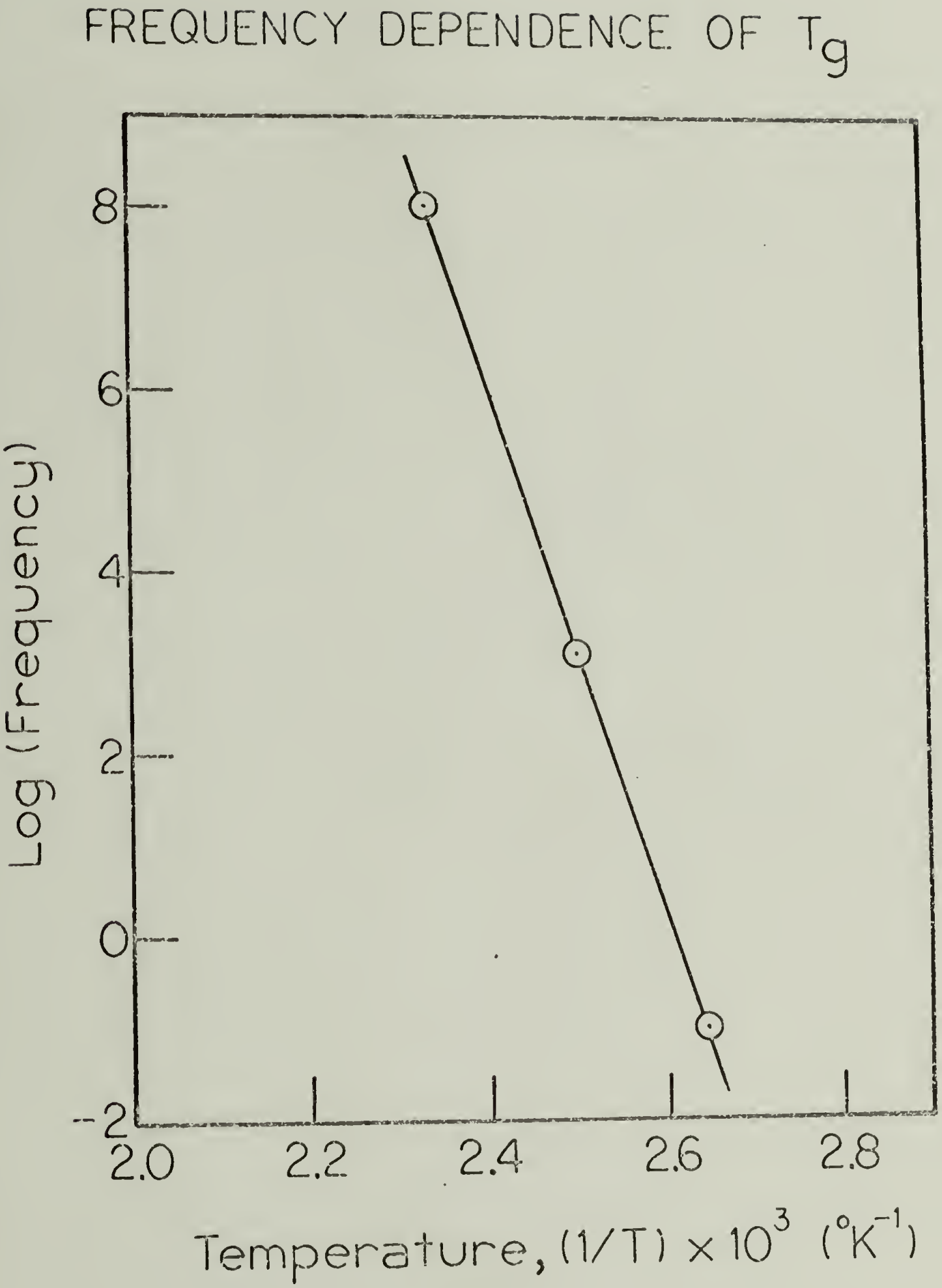
FREQUENCY DEPENDENCE OF T_g
Log (Frequency)
8
6
4
2
0
-2
2.0
2.2
2.4
2.6
2.8
Temperature, $(1/T) \times 10^3$ ($^\circ K^{-1}$)

FIGURE A-1

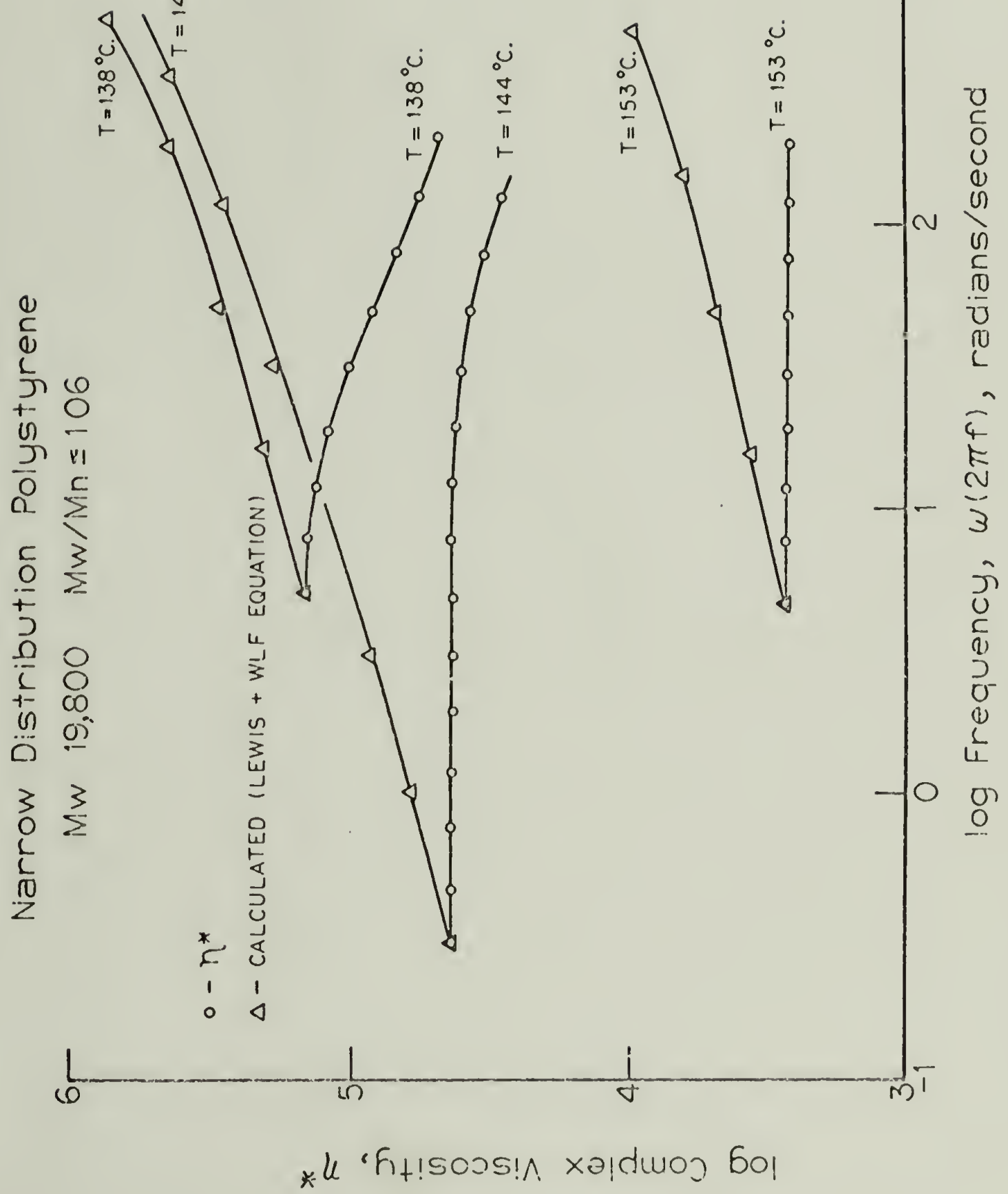
Narrow Distribution Polystyrene
Mw 19,800 Mw/Mn ≤ 106
o - η*
Δ - CALCULATED (LEWIS + WLF EQUATION)
T = 138°C.
T = 144°C.
T = 138°C.
T = 144°C.
T = 153°C.
T = 153°C.
log Complex Viscosity, η*
log Frequency, ω(2πf), radians/second
6
5
4
3
-1
0
1
2
3

FIGURE A-2

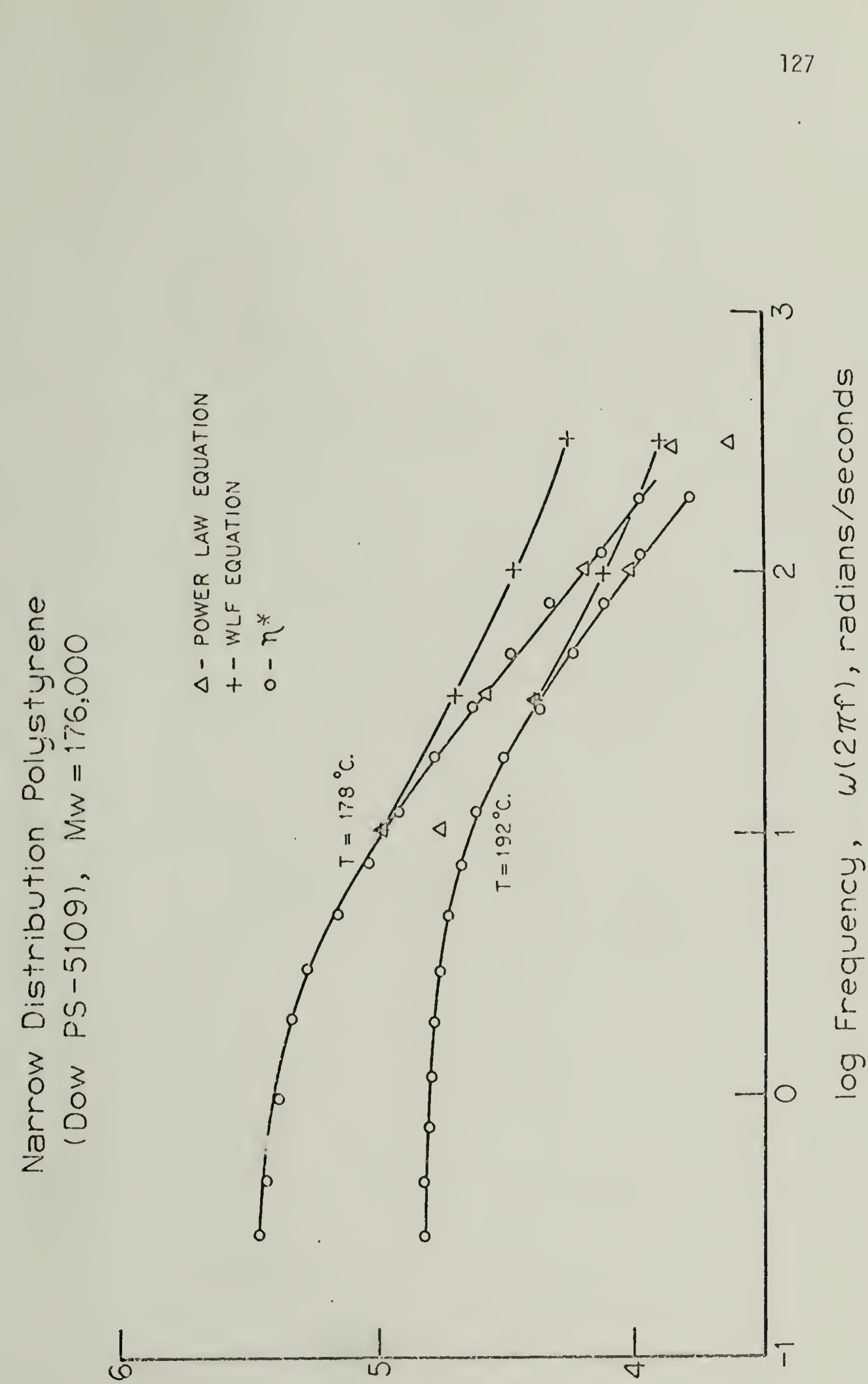
Narrow Distribution Polystyrene
(Dow PS-5109), Mw = 176,000
Δ - POWER LAW EQUATION
+ - WLF EQUATION
o - η*
T = 178 °C.
T = 192°C.
log Frequency, ω(2πf), radians/seconds
log complex viscosity, η*
6
5
4
-1
0
1
2
3

FIGURE A-3

T_g Change with Pressure for Polystyrene
after G. Gee, Polymer 1, 177 (1966)

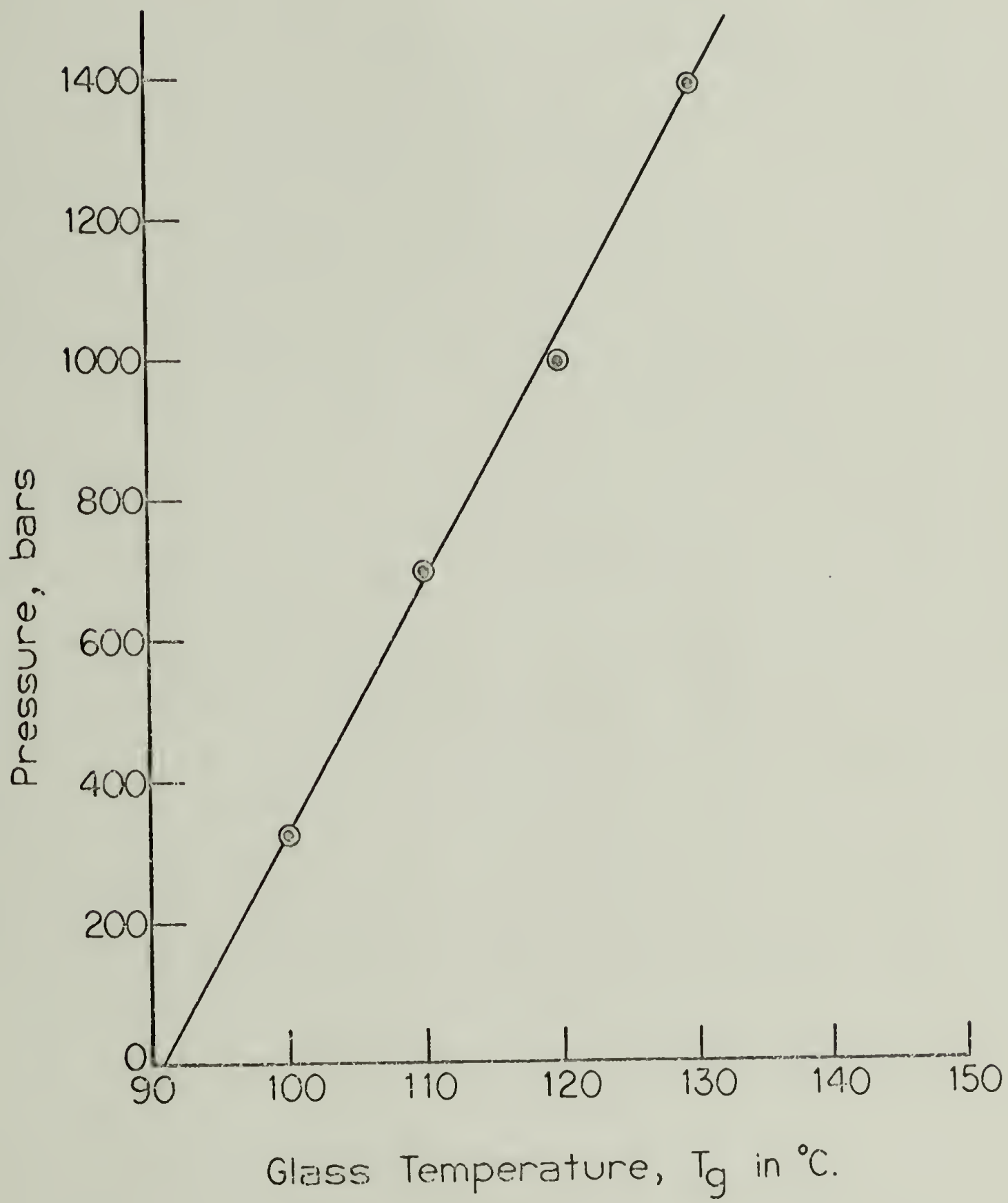

FIGURE A-4

Narrow Distribution Polystyrene
Mw 19,800 Mw/Mn ≤ 1.06

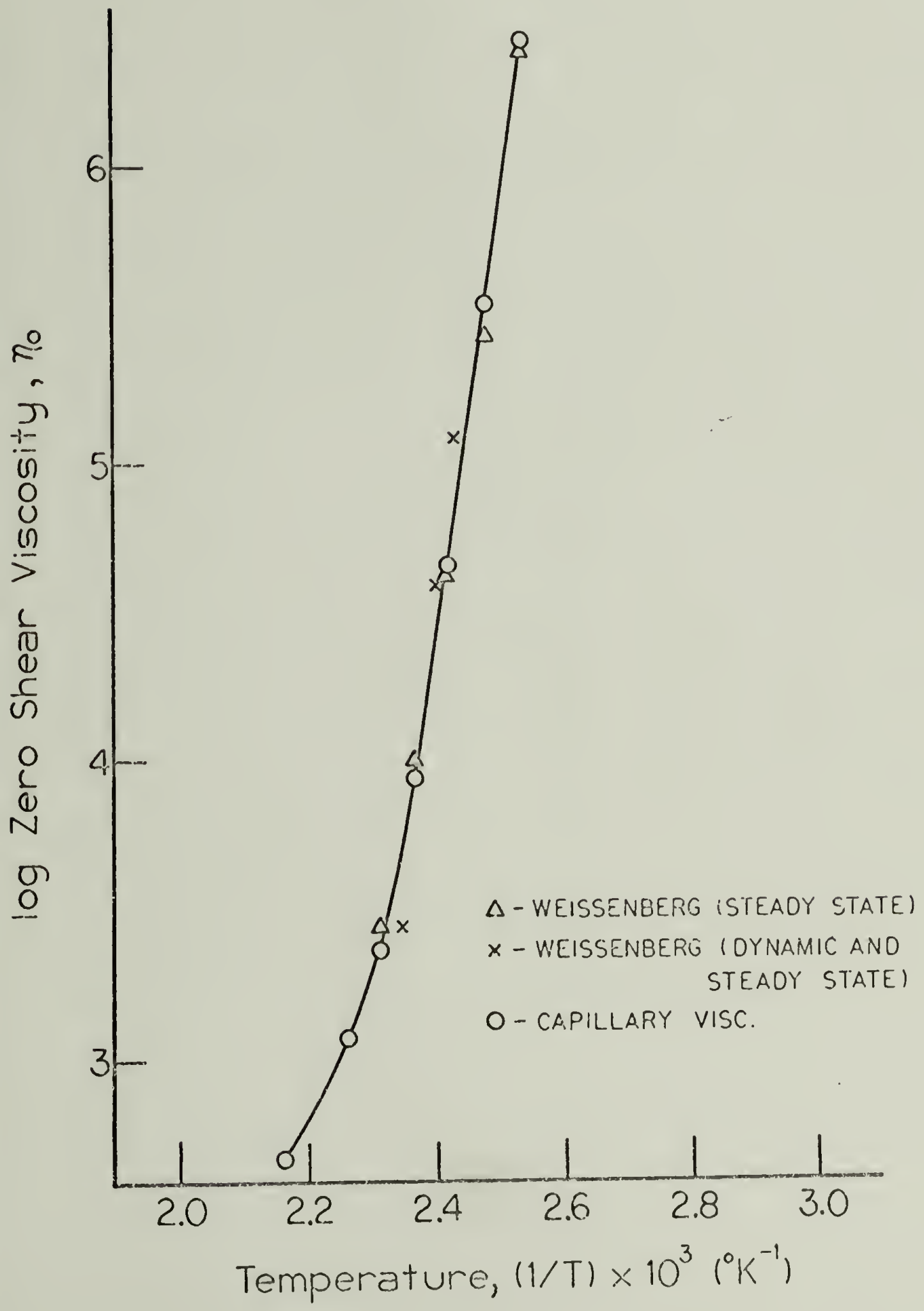

FIGURE A-5

NARROW DISTRIBUTION POLYSTYRENE
MW = 20.4K

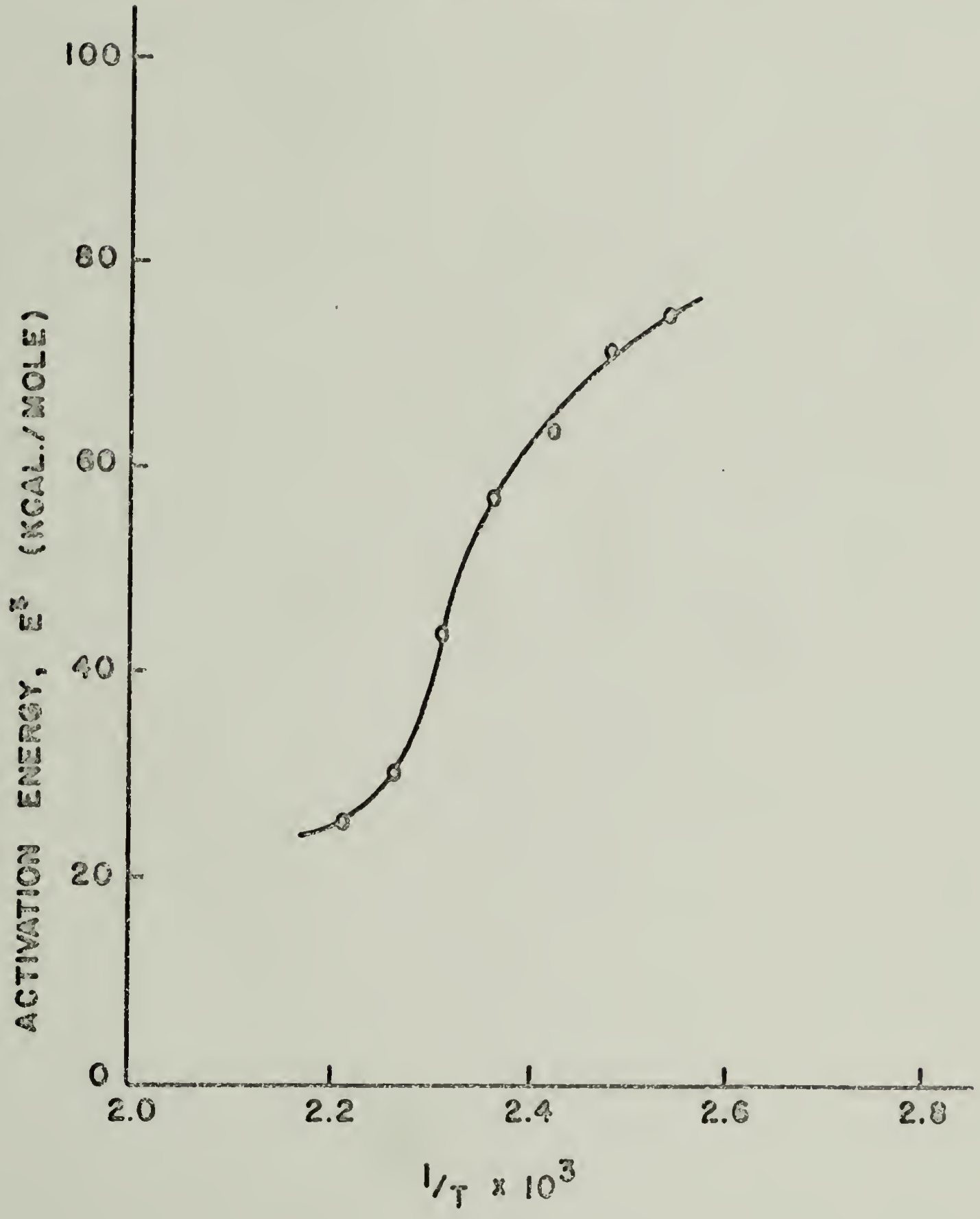

FIGURE A-6

APPENDIX B

Figures 1 and 2 in this appendix were not included in the original manuscript of Chapter II. However, they are referenced in that chapter and are included as supplementary information. As in Appendix A, the discussion of the Figures is limited to their brief description.

Figure 1 illustrates the effect of pressure on the flow of the low molecular weight polystyrene at 140°C. This is evidenced by the large increase in pressure with increasing shear rate, particularly as the length/diameter ratio of the capillary increases. Figure 2 represents the pressure corrected data of Figure 1 obtained by the method presented in Chapter II. At the highest shear rates measured, a slight over-correction of the data is indicated as a slight deviation from a linear relationship.

NARROW DISTRIBUTION POLYSTYRENE

Mw = 20,400 Mw/Mn ≤ 1.06

T = 140°C

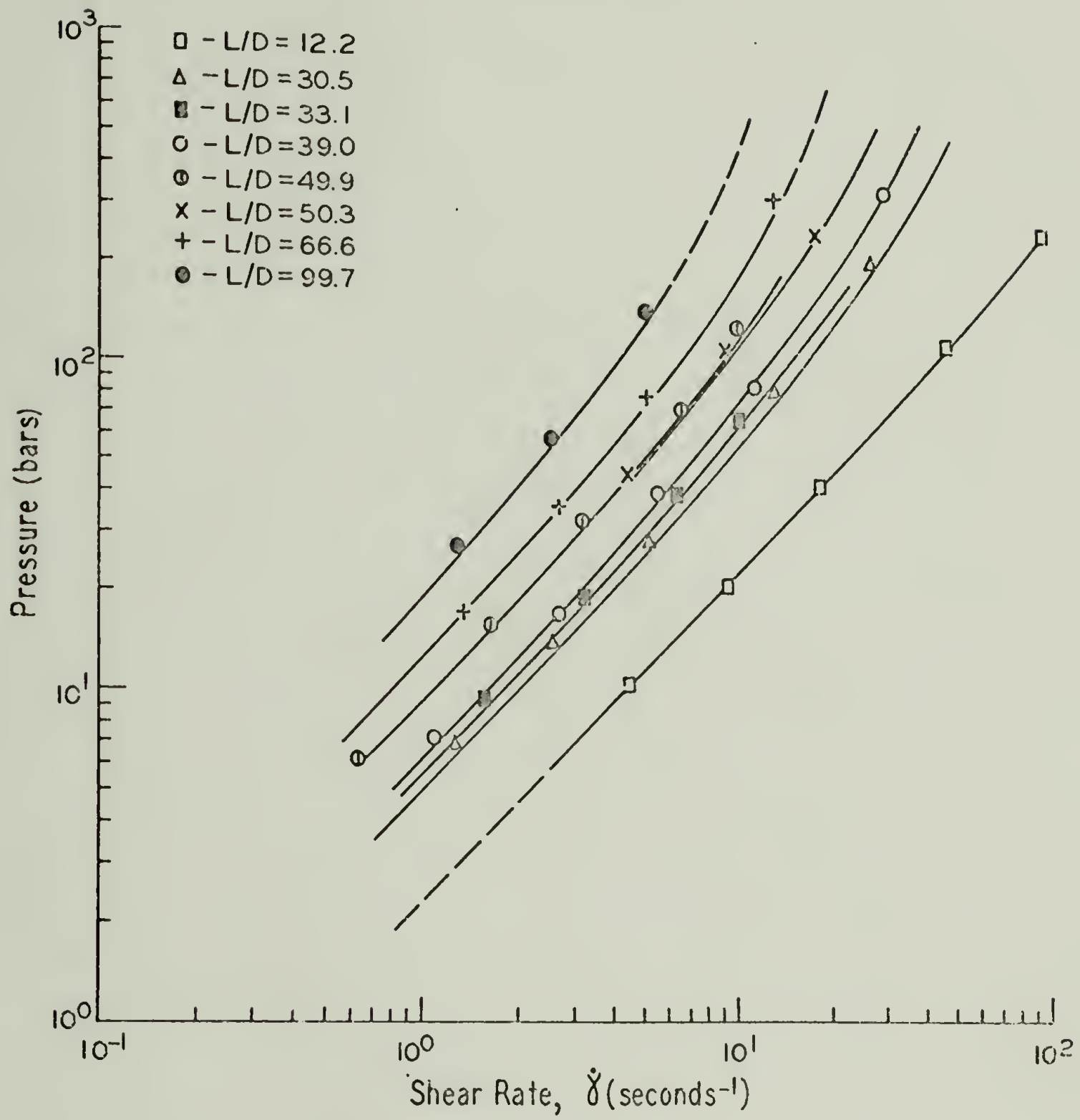

FIGURE B-1

NARROW DISTRIBUTION POLYSTYRENE

Mw = 20,400 Mw/Mn ≤ 1.06
T = 140°C

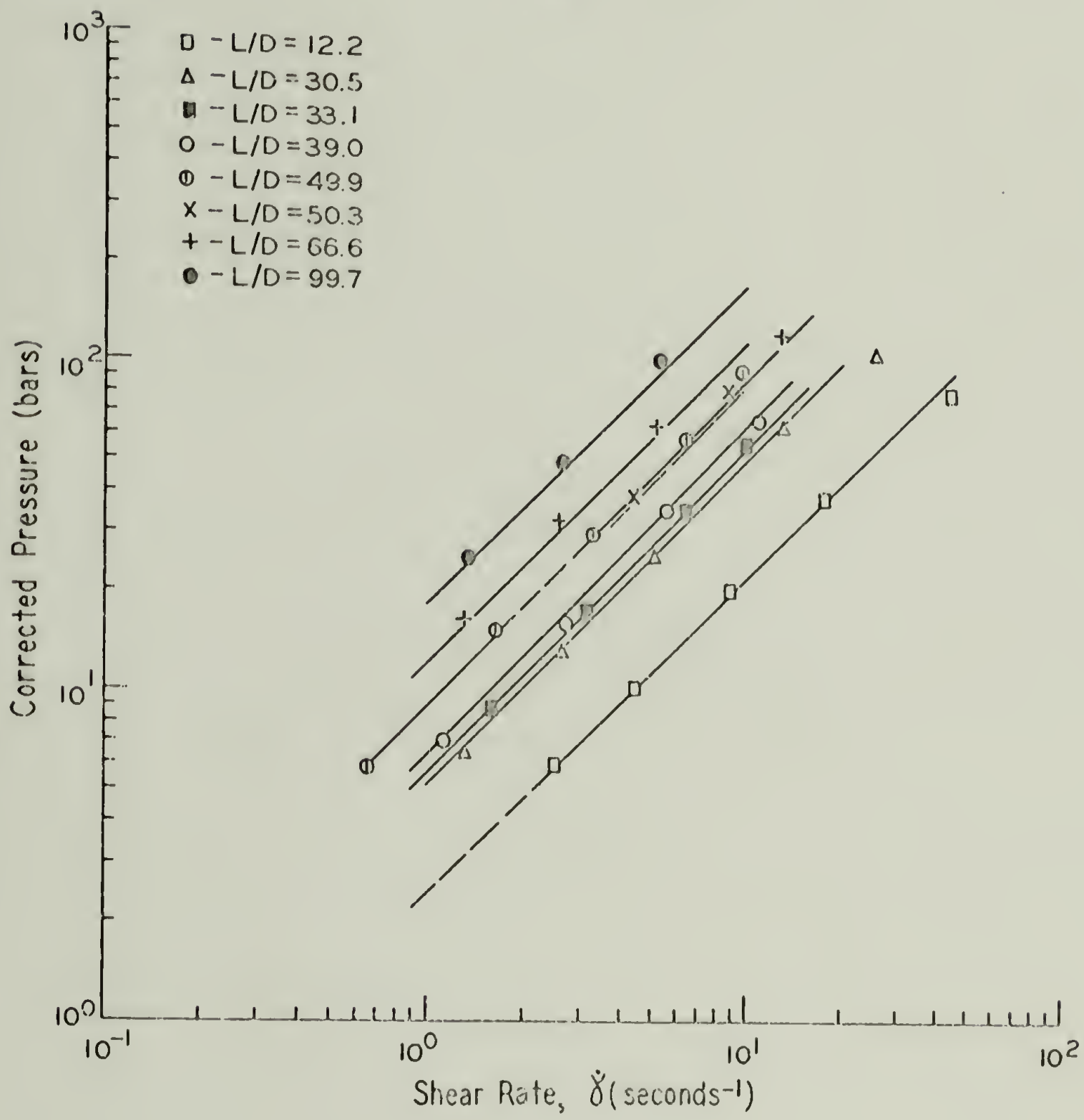

FIGURE B-2

APPENDIX C

The details in the derivation of the general expressions presented in Chapter III are given in this appendix. These include the general expressions for determining the pressure coefficient and axial distribution of the viscosity and pressure in the capillary flow of Newtonian and shear-thinning fluids. The assumptions in this analysis, using cylindrical coordinates (r,θ,z) are: steady state flow, no gravitational effects, no slip at the boundary, $v_\theta = \tau_{r\theta} = \tau_{\theta z} = 0$ (from considerations of the symmetry) and $v_r = 0$ (fully developed flow).

Calculation of the Relative Change in Viscosity with Density

Considering equation III-4, $\eta = \eta_o e^{bP}$, and $V = V_o + \beta P$:

$$\frac{d\eta}{dv} = \frac{d\eta}{dP}\,\frac{dP}{dv} = \frac{\eta_o b e^{bP}}{\beta} = \frac{\eta b}{\beta} \qquad \text{(C-1)}$$

Now
$$d\ell n\eta = \frac{b}{\beta}\,dv = -\frac{b}{\beta\rho}\,d\ell n\rho \qquad \text{(C-2)}$$

Determination of the Axial Pressure Distribution

Equation III-12 is

$$-\frac{1}{\eta_o} e^{-bP}\frac{\partial P}{\partial z} = C = \frac{1}{r}\frac{\partial}{\partial r}\left(r\frac{\partial v_z}{\partial r}\right) \qquad \text{(C-3)}$$

The left hand side of equation 3 gives,

$$-\frac{1}{b} e^{-bP}\Big]_{P_o}^{P} = \eta_o\, Cz\Big]_L^z \qquad \text{(C-4)}$$

Considering atmospheric pressure to be the reference and the pressure drop to be ΔP measured from z=0, C is found to be

$$C = - \frac{1}{bn_0 L} (1 - e^{-b\Delta P}) \qquad (C\text{-}5)$$

The axial distribution is derived from equation 4:

$$- \frac{1}{b} e^{-bP}\Big|_0^P = - \frac{1}{bL} (1 - e^{-b\Delta P}) z\Big|_L^z \qquad (C\text{-}6)$$

or $$e^{-bP} = z/L(1 - e^{-b\Delta P}) + e^{-b\Delta P} \qquad (C\text{-}7)$$

giving $$P = \frac{\ln [e^{-b\Delta P} + (1 - e^{-b\Delta P}) z/L]}{-b} \qquad (C\text{-}8)$$

The average pressure is derived using the relationship

$$\overline{P} = \frac{\int p dz}{L} = \int_0^1 p \, dz/L \qquad (C\text{-}9)$$

Using equations 8 and 9,

$$\overline{P} = \Delta P - \frac{1}{b} \int_0^1 \ln[1 + (e^{b\Delta P} - 1)\xi] \, d\xi \qquad (C\text{-}10)$$

where $\xi = z/L$

With $\delta = e^{b\Delta P} - 1$ and expanding the logarithm,

$$\overline{P} = \Delta P - \frac{1}{b}\left\{\frac{\delta\xi^2}{2} - \frac{1}{6}\delta^2\xi^3 + \frac{1}{12}\delta^3\xi^4 - \frac{1}{20}\delta^4\xi^5 + \ldots\right]_0^1\} \qquad (C\text{-}11)$$

or $$\overline{P} = \Delta P - \frac{1}{b}\{\delta/2 - \frac{1}{6}\delta^2 + \frac{1}{12}\delta^3 - \frac{1}{20}\delta^4 + \frac{1}{30}\delta^5 - \ldots\} \qquad (C\text{-}12)$$

At small pressures,

$$\overline{P} = \Delta P - \frac{1}{2b}(e^{b\Delta P} - 1) \approx \Delta P - \frac{1}{2b}(1 + b\Delta P - 1) \approx \frac{\Delta P}{2} \qquad (C\text{-}13)$$

Equation 12 can be written in the form,

$$\overline{P} = \Delta P + \frac{1}{b} \sum_{i=1}^{n} \frac{\delta^i (-1)^i}{i(i+1)} \qquad \text{(C-14)}$$

Determination of the Pressure Coefficient for a Shear-Thinning Fluid

Substituting $\tau = \eta\dot{\gamma} = K'\dot{\gamma}^n e^{bP}$ into equation III-9 gives,

$$\frac{e^{-bP}}{K'} \frac{\partial P}{\partial z} = C = \frac{1}{r} \frac{\partial}{\partial r} \left(r\left(\frac{\partial v}{\partial r}\right)^n\right) \qquad \text{(C-15)}$$

By considering the left hand side of equation 15,

$$C = -\left(\frac{1 - e^{-b\Delta P}}{bK'L}\right) \qquad \text{(C-16)}$$

Combining equations 15 and 16 with $\tau_w = \frac{\partial P}{\partial z} \frac{R}{2}$,

$$\tau_w = \frac{(1 - e^{-b\Delta P})D_c}{4bL} = K'' \left(\frac{8V_c}{D_c}\right)^n \qquad \text{(C-17)}$$

For two capillaries, equation 17 is used to obtain,

$$\frac{1 - e^{-b\Delta P_1}}{1 - e^{-bK\Delta P_2}} = \frac{K''_1}{K''_2} \frac{L_{c_1}}{L_{c_2}} \frac{D_{c_2}}{D_{c_1}} \left[\frac{V_{c1}}{D_{c_1}} \frac{D_{c_2}}{V_{c_2}}\right]^n \qquad \text{(C-18)}$$

For the same capillary, equation 18 reduces to,

$$\frac{1 - e^{-b\Delta P_1}}{1 - e^{-bK P_1}} = V_R^n \qquad \text{(C-19)}$$

Figures 1 and 2 are alternate ways of plotting the data presented in Figure III-1. The limitation imposed by Figures 1 and 2 is the loss of generality. Figures 1 and 2 are specifically for the 20.4K and 670K

polystyrenes with the experimentally determined pressure ratios K. The advantage in plotting the curves as in Figures 1 and 2 is the greater accuracy obtained in determining the pressure coefficient. This is particularly true in the range $0 < K < 2$ where $b\Delta P$ is most sensitive to changes in K as seen in Figure III-1.

DETERMINATION OF THE PRESSURE COEFFICIENT FOR POLYSTYRENE

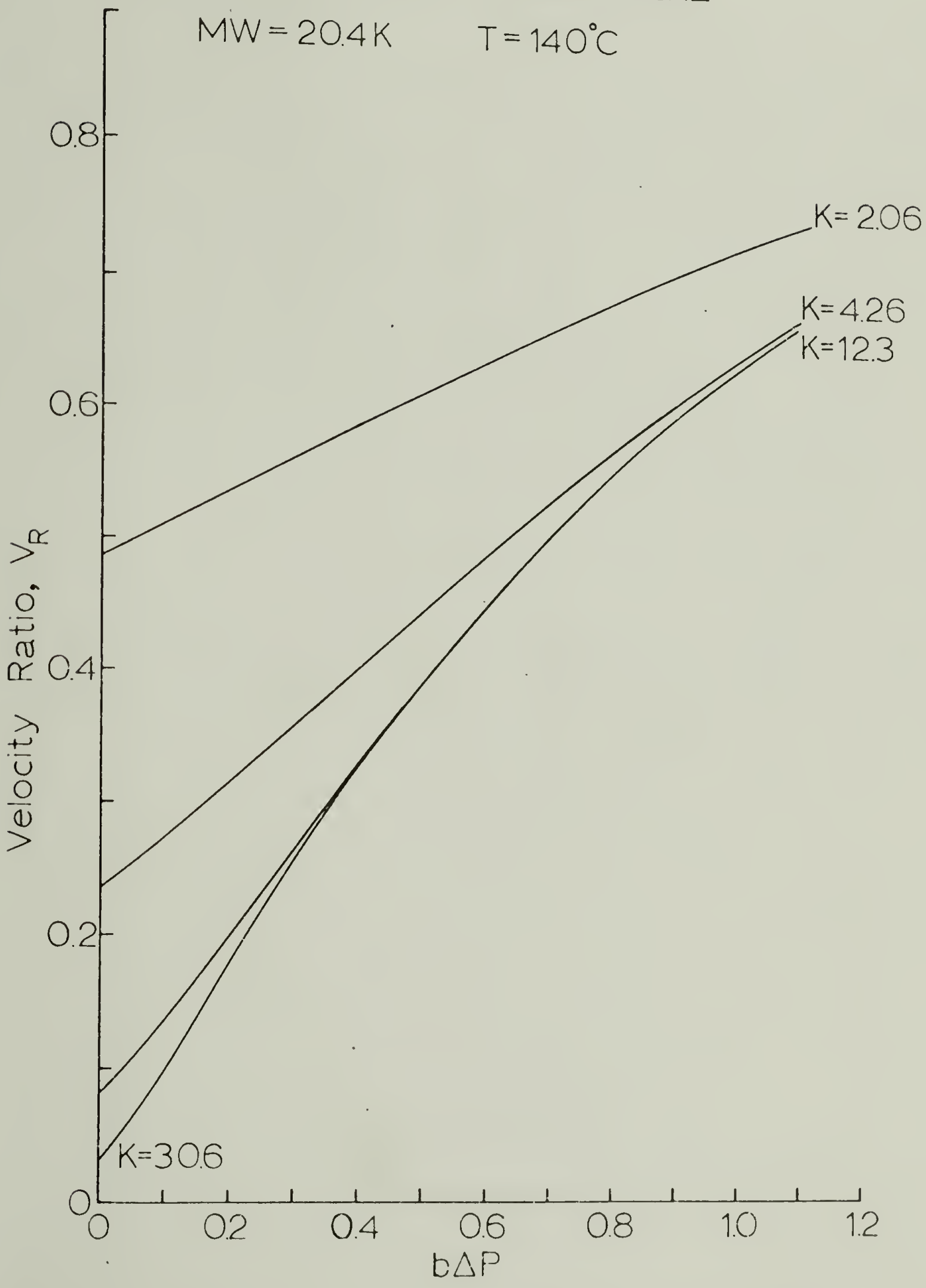

FIGURE C-1

DETERMINATION OF THE PRESSURE COEFFICIENT FOR POLYSTYRENE

MW=670K T=165°C

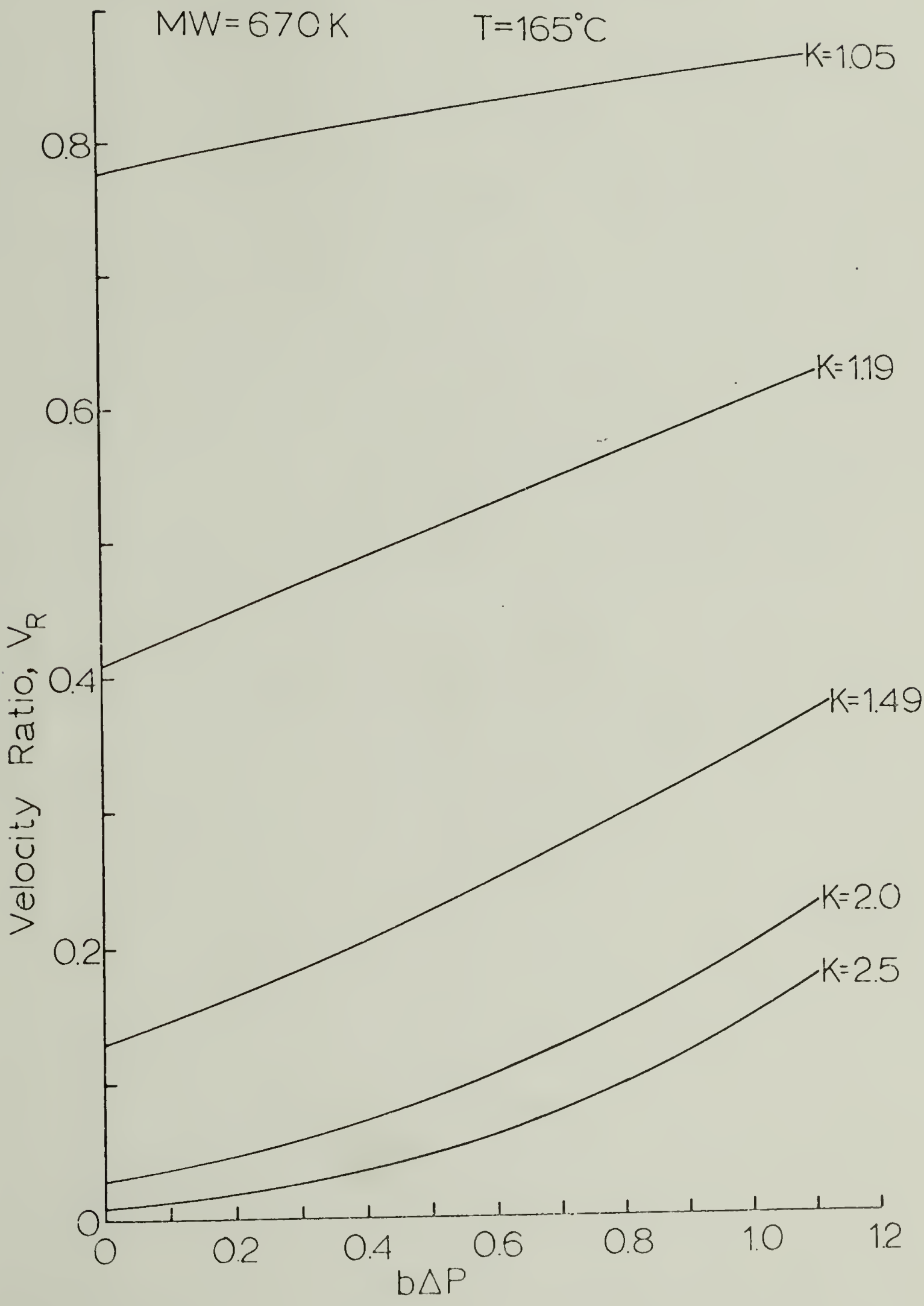

FIGURE C-2

APPENDIX D

Figures 1-3 are additional information not included in the original manuscript of Chapter IV. They are referenced in Chapter IV and their discussion here is limited to a brief description.

Figure 1 is a plot of pressure versus the length/diameter ratio of several capillaries for poly(methyl methacrylate) at 190°C. The effect of pressure on the capillary flow is evidenced by the increased nonlinearity in the curves as the shear rate is increased. Figure 2 represents the data of Figure 1 minus an estimated end correction. The effect of pressure on the apparent viscosity at 190°C is illustrated in Figure 3. The solid line is data obtained at atmospheric pressure.

CAPILLARY FLOW OF POLY (METHYL METHACRYLATE). PRESSURES REQUIRED AT DIFFERENT SHEAR RATES

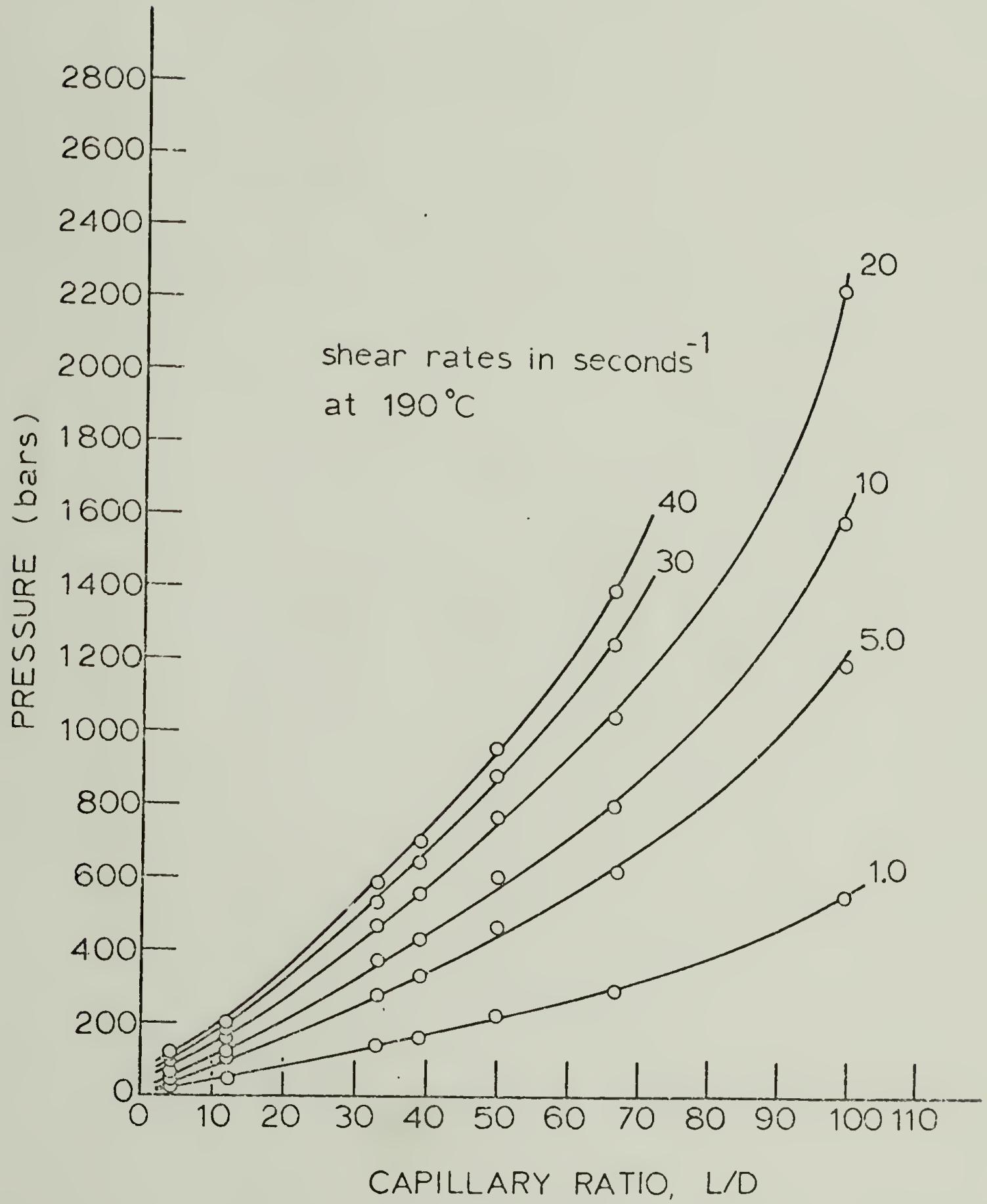

FIGURE D-1

END-CORRECTED PRESSURE VERSUS CAPILLARY RATIO FOR POLY (METHYLMETHACRYLATE)

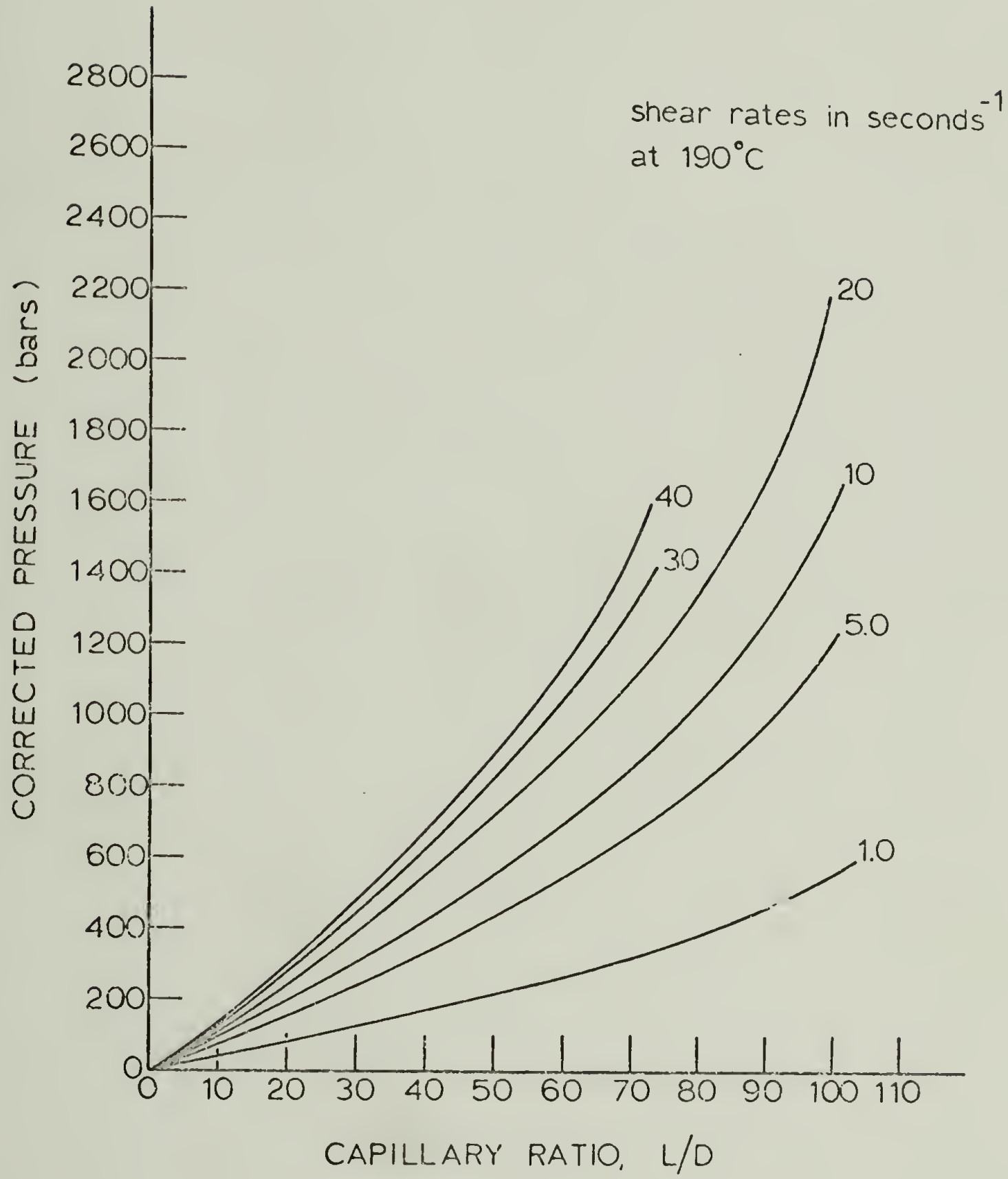

FIGURE D-2

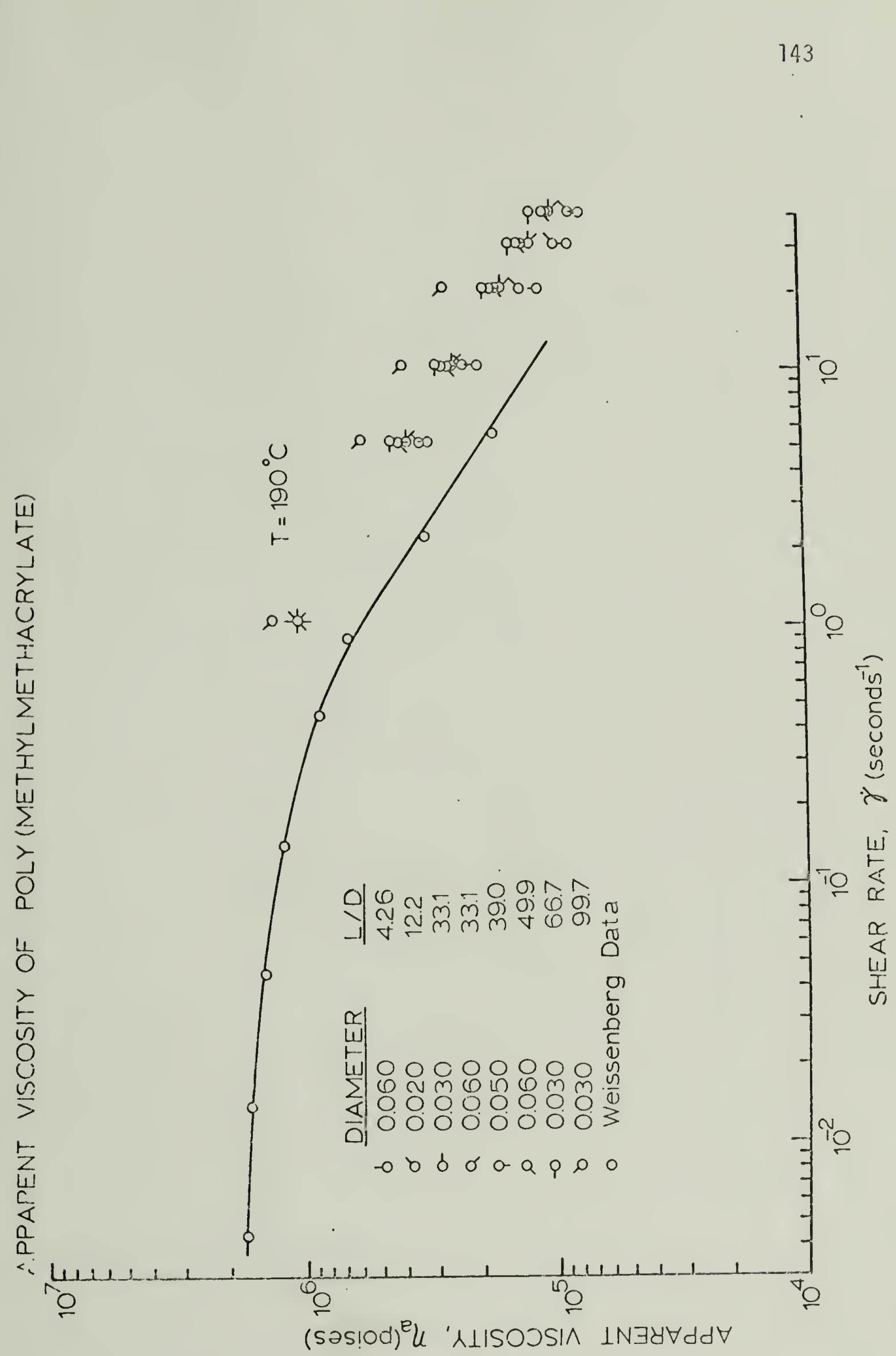
APPARENT VISCOSITY OF POLY (METHYLMETHACRYLATE)
T = 190°C
DIAMETER L/D
0.060 4.26
0.020 12.2
0.030 33.1
0.060 33.1
0.050 39.0
0.060 49.9
0.030 66.7
0.030 99.7
Weissenberg Data
APPARENT VISCOSITY, η_a (poises)
SHEAR RATE, $\dot{\gamma}$ (seconds^{-1})
10^7
10^6
10^5
10^4
10^0
10^1
10^{-1}
10^{-2}

FIGURE D-3

CAPTIONS FOR FIGURES

I-1. Comparison of experimental data from Weissenberg Rheogoniometer and calculated apparent viscosities for narrow distribution low molecular weight polystyrene.

I-2. Capillary flow data compared with calculated apparent viscosities for narrow distribution high molecular weight polystyrene at 180 and 200°C.

I-3. Capillary flow data compared with calculated apparent viscosities for narrow distribution high molecular weight polystyrene at 150 and 165°C.

I-4. Comparison of Weissenberg Rheogoniometer and capillary flow data with calculated results for narrow distribution low molecular weight polystyrene.

I-5. Pressure correction of the apparent viscosity of the narrow distribution high molecular weight polystyrene.

A-1. Frequency dependence of the glass transition for polystyrene.

A-2. Comparisons of the complex viscosity to the viscosity calculated considering the frequency dependence of the glass transition for low molecular weight polystyrene.

A-3. Comparison similar to Figure A-2 for high molecular weight polystyrene.

A-4. The glass transition of polystyrene plotted as a function of pressure.

A-5. Plot of log zero shear viscosity vs. 1/T for low molecular weight polystyrene.

A-6. Plot of the activation energy vs. 1/T for low molecular weight polystyrene.

II-1. Comparison of calculated and measured flow rates for narrow distribution low molecular weight polystyrene at 140°C.

II-2. Comparison of calculated and measured flow rates for narrow distribution low molecular weight polystyrene at 160°C.

LIST OF TABLES